



**Dottorato di Ricerca in Neuroscienze
Curriculum Neuroscienze e Neurotecnologie
Ciclo XXXVI**

Coordinatore Prof. Lino Nobili

Functional dissection of the piRNA pathway
in adult neurogenesis and neuroinflammation

Author: Silvia Beatini

Supervisor: Davide De Pietri Tonelli

Abstract

Piwi proteins and the small non-coding RNAs interacting with them (piRNAs), collectively referred to as the piRNA pathway, are best known in gonads where they safeguard genomic integrity and male fertility. The piRNA pathway is also present in various somatic tissues, especially in the central nervous system (CNS), and altered piRNAs expression has been implicated in pathological and inflammatory conditions such as neurodegenerative diseases [1]–[4]. However, little is known about the underlying mechanisms, and the potential functions of PIWI-piRNAs in brain cells remain unclear.

This thesis extends our prior research presenting the initial evidence of the functional role of piRNA pathway in neurogenesis and neuroinflammation [5], which are critical processes for maintaining central nervous system (CNS) homeostasis and cognitive function. Piwil2 and piRNAs were discovered in adult neural progenitor cells (aNPCs) to support neurogenesis by reducing cellular senescence and neuroinflammation [5]. In this thesis, a constitutive Mili knockout mouse model was used to validate and expand these findings. *In vivo* proliferation disturbances and *in vitro* impaired differentiation of aNPCs with mutated Mili were observed. Concerning neuroinflammation, our investigation demonstrated that Piwil2 depletion in the postnatal hippocampus leads to the generation of reactive astrocytes [5]. This thesis extends these findings by illustrating that Mili knockdown results in microgliosis. Additionally, the presence of the piRNA pathway was uncovered in microglia. Microglial Piwil2 and piRNAs were shown to be responsive to both acute (LPS-induced) and chronic (inflammaging) inflammation. Moreover, inflammation-responsive piRNAs are Mili-dependent and are predicted to target, and therefore potentially regulate, several gene transcripts involved in inflammatory processes.

The work reported in this thesis provides an initial characterization of the piRNA pathway's role in adult neurogenesis and neuroinflammation, suggesting a broader function of the piRNA pathway as a guardian of brain homeostasis. This offers potential therapeutic avenues for age-related central nervous system (CNS) disorders, contributing to the promotion of successful brain aging.

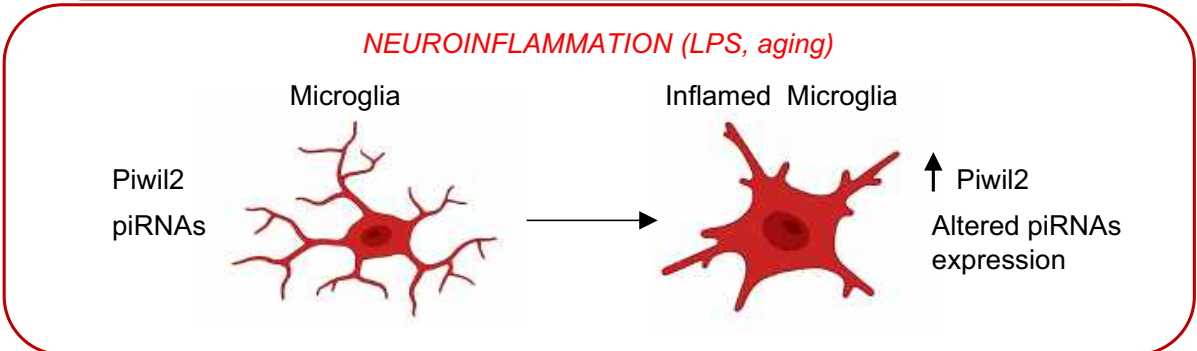
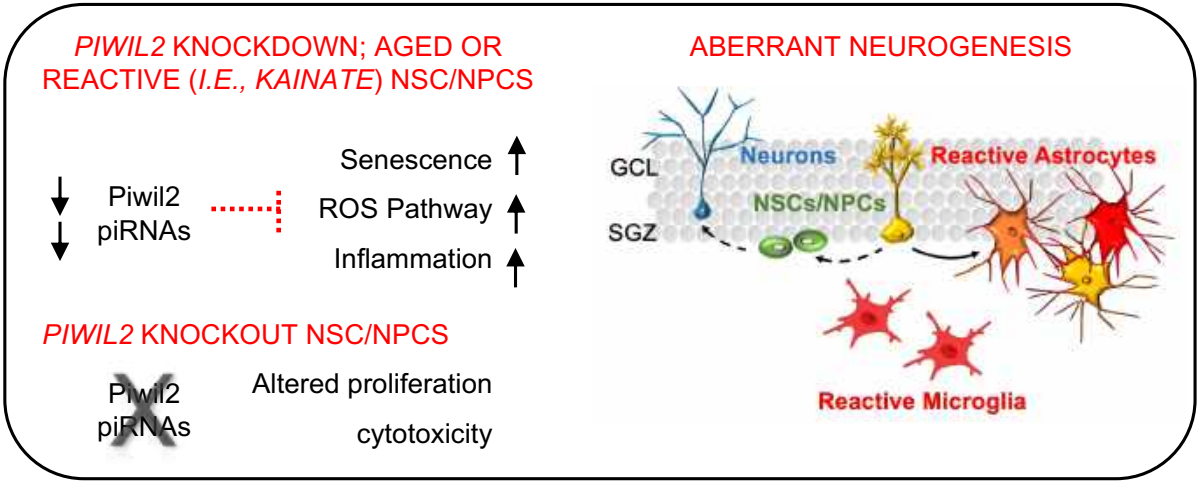
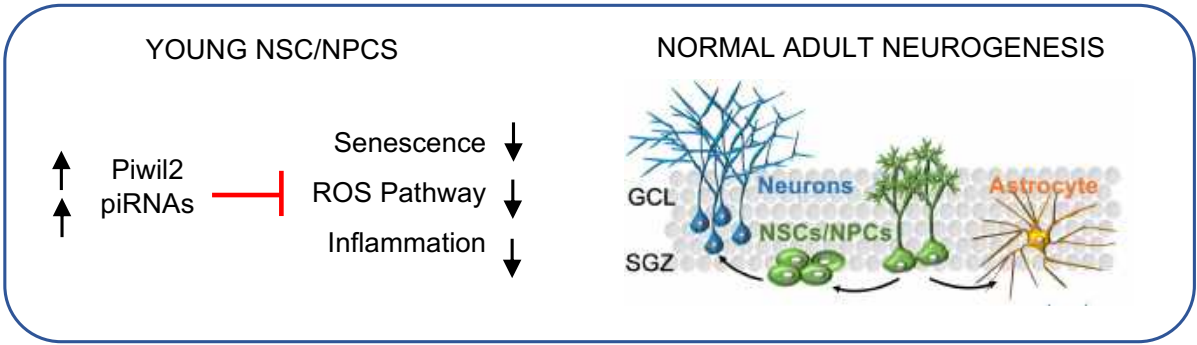


Table of Contents

| | | |
|------------|---|-----------|
| 1 | Introduction | 1 |
| 1.1 | <i>The piRNA pathway</i> | 1 |
| 1.1.1 | PIWI-interacting RNAs (piRNAs) | 1 |
| 1.1.2 | PIWI proteins | 2 |
| 1.1.3 | piRNAs biogenesis and mechanism of action | 3 |
| 1.1.4 | piRNAs in Central Nervous System | 5 |
| 1.1.5 | piRNAs in inflammation | 7 |
| 1.2 | <i>Adult neurogenesis</i> | 9 |
| 1.2.1 | The hippocampal neurogenic niche | 10 |
| 1.2.2 | Regulation of adult hippocampal neurogenesis | 11 |
| 1.3 | <i>Microglia functions in neurogenesis and neuroinflammation</i> | 14 |
| 1.3.1 | Microglia functions in neurogenesis | 16 |
| 1.3.2 | Microglia functions in neuroinflammation | 17 |
| 1.3.3 | Regulation of microglial inflammatory responses | 18 |
| 2 | Rationale and aims | 22 |
| 3 | Results | 24 |
| 3.1 | <i>Piwil2 (Mili) sustains neurogenesis and prevents cellular senescence in the postnatal hippocampus</i> | 24 |
| 3.2 | <i>Characterization of the hippocampal stem cell niche in constitutive Mili KO and Mili HET mice</i> | 25 |
| 3.2.1 | Validation of the constitutive Mili KO mouse model | 25 |
| 3.2.2 | Altered cell proliferation in the hippocampal neurogenic niche of Mili KO and Mili HET mice | 26 |
| 3.2.3 | Stemness and proliferation of Mili KO and Mili HET aNPCs is not impaired <i>in vitro</i> in proliferative culture medium | 27 |
| 3.2.4 | Induction of aNPCs differentiation results in higher cytotoxicity in Mili KO and Mili HET cells <i>in vitro</i> | 28 |
| 3.3 | <i>The piRNA pathway in microglia and neuroinflammation</i> | 30 |
| 3.3.1 | Acute Mili KD in adult mouse hippocampus results in microgliosis | 30 |
| 3.3.2 | The key piRNA pathway genes Mili and Mov10 are expressed in CX ₃ CR1 ^{GFP+} microglia and increase upon LPS-induced inflammation <i>in vivo</i> | 31 |
| 3.3.3 | Mili and Mov10 increase their expression in inflamed primary microglia | 33 |
| 3.3.4 | Piwil2 (Hili, in human) responsiveness to acute LPS-induced inflammation is conserved in human microglia | 34 |
| 3.3.5 | Ageing-induced neuroinflammation (inflammaging) increases Mili expression in microglia | 35 |

| | | |
|------------|---|-----------|
| 3.3.6 | Acute inflammation alters the expression of (Mili-dependent) piRNAs in murine microglia ----- | 36 |
| 3.3.7 | <i>In silico</i> piRNAs' target prediction in microglia ----- | 38 |
| 4 | Discussion----- | 40 |
| 5 | Procedures and References ----- | 45 |
| 5.1 | <i>Experimental procedures</i> ----- | 45 |
| 5.1.1 | Experimental mice ----- | 45 |
| 5.1.2 | Primary aNPCs isolation and culture----- | 45 |
| 5.1.3 | Primary microglia isolation and culture ----- | 46 |
| 5.1.4 | Human microglial cell line HMC3 culture----- | 46 |
| 5.1.5 | GapmeR injection----- | 46 |
| 5.1.6 | BrdU and LPS treatments----- | 47 |
| 5.1.7 | Fluorescence-Activated Cell Sorting (FACS) for microglia isolation ----- | 47 |
| 5.1.8 | Histology Immunofluorescence and Imaging ----- | 48 |
| 5.1.9 | Cytotoxicity assay in aNPCs ----- | 49 |
| 5.1.10 | Protein extraction and Western Blot (WB) ----- | 50 |
| 5.1.11 | RNA extraction and real-time qPCR ----- | 50 |
| 5.1.12 | PCR-based genotyping----- | 51 |
| 5.1.13 | Small RNA library preparation----- | 52 |
| 5.1.14 | Small RNA sequencing and data processing----- | 52 |
| 5.1.15 | Quantification and statistical analysis ----- | 53 |
| 5.2 | <i>References</i> ----- | 54 |
| 6 | Appendix ----- | 90 |

1 Introduction

1.1 The piRNA pathway

PIWI-interacting RNAs (piRNAs) are a relatively novel class of small non-coding RNAs (sncRNAs). They consist of single-stranded RNA sequences in the range of ~23-35 nucleotides in length, modified by a 2'-O-methylation at the 3' end and with a Uridine bias at their 5' end. These small non-coding RNAs (sncRNAs) work in association with P-element-induced wimpy testis (PIWI) proteins, forming the piRNA-induced silencing complexes (piRISCs), in which the piRNA, by sequence complementarity, guides the PIWI proteins to silence RNA targets and regulate gene expression [3], [6]–[8].

1.1.1 PIWI-interacting RNAs (piRNAs)

PiRNAs were first discovered in the *Drosophila melanogaster* germline [9], [10], where they have been shown to repress transposons, repetitive element transcripts, and even certain genes through transcriptional, post-transcriptional, and epigenetic mechanisms, thus preserving genomic integrity and male fertility [1], [11]–[14]. Indeed, the piRNA pathway has predominantly been investigated within the germline, where piRNAs primarily target transposable elements (TEs), i.e., mobile genetic entities capable of relocating and integrating into diverse genomic locations. Consequently, piRNAs are recognized as frontline defenders of genomic integrity, safeguarding against the intrusion of these genomic parasites. As a result, they are critical for germline stem cell maintenance [1]. Although first described in *Drosophila* gonads, their protective role is notably conserved across different animal species, including mammals [1], [15]–[23]. Furthermore, emerging evidence indicates that piRNAs are also abundant in somatic tissues, particularly in somatic stem cells, where they are involved in a broad spectrum of functions, including cell proliferation, differentiation and survival, during physiological as well as pathological events [11], [13], [20], [23]–[25].

PiRNAs sequences exhibit remarkable diversity, with most animal genomes harboring more than 1 million unique piRNAs [26]. In contrast to other sncRNAs, such as microRNAs (miRNAs), which tend to have limited sequence diversity and are typically conserved across species, piRNAs are poorly conserved [27], [28]. Finally, another distinctive feature of piRNAs is that their primary sequences are transcribed from genomic regions typically found within

clusters spanning a length range of 20 to 100 kilobases in the genome. These clusters are often enriched in transposons, repetitive elements, and other spurious transcripts or pseudogenes and can be transcribed mono- or bi-directionally. Importantly, also protein-coding genes, specific intergenic loci, and long non-coding RNAs (lncRNAs) can serve as piRNAs sources [11], [12], [17], [18], [29].

1.1.2 PIWI proteins

PIWI proteins are highly conserved proteins belonging to the Piwi subclade of Argonaute (Ago) proteins, the other subclade being the Ago family of proteins which bind miRNAs and small-interfering RNAs (siRNAs) [30], [31]. They exhibit the canonical structural organization characteristic of Ago proteins, which is a bilobated structure with four domains connected by three linker regions (*Figure 1*) [32]. The variable N-terminal domain is linked to a conserved PAZ (standing for Piwi/Argonaute/Zwille) domain which, in conjunction with the MID (middle) domain, binds piRNAs, while at the C-terminal, these proteins feature the PIWI endonuclease domain, an RNase-H-like domain with slicer activity responsible for the catalytic cleavage of the target RNA [24], [33].

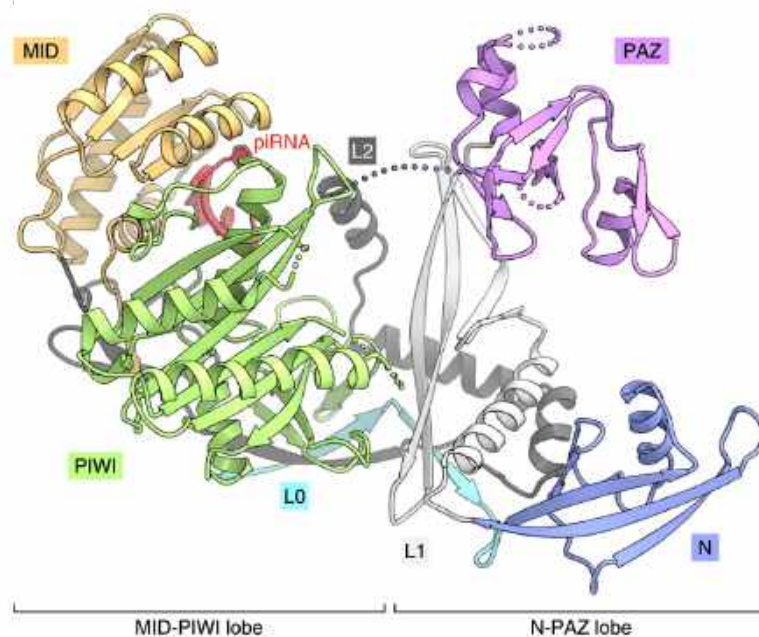


Figure 1: Crystal structure of the PIWI-piRNA complex. Modified from [25].

Most mammals possess four Piwi genes. In humans, Hiwi (Piwil1), Hili (Piwil2), Piwil3, and Hiwi2 (Piwil4) are encoded in the genome [34]. In mice, three main PIWI genes can be found: Piwil1 (Miwi), Piwil2 (Mili) and Piwil4 (Miwi2), lacking the mouse genome of one of the four Piwi paralogs [13]. Several cofactors are commonly associated with the PIWI proteins in the

piRISC complex. Among those helicases, such as MOV10, are crucial for facilitating PIWI's binding and catalytic functions by unwinding RNA secondary structures [35]. Interestingly, PIWI proteins can perform functions independent of their endonuclease activity. In this alternative mode, PIWI is implicated in the epigenetic silencing of target genes through piRNA-directed recruitment of epigenetic factors to chromatin [1], [11], [36].

1.1.3 piRNAs biogenesis and mechanism of action

The biogenetic process of piRNAs production has historically been divided into three pathways: primary, secondary and phased piRNA pathways (*Figure 2*) [37]–[40]. In the primary biogenesis pathway, long precursors of piRNAs are transcribed in the nucleus from genomic clusters and exported to the cytoplasm for further processing [11], [41]–[44]. There, the precursors transcripts are fragmented by endonucleolytic cleavage. The intermediate products whose sequence starts with Uridine are preferentially loaded into PIWI proteins [11], [45]. This preference is inherently determined by the structure of the MID domain of PIWI, and results in the generation of the 5' Uridine bias characteristic of primary piRNAs [46]. Upon loading of these sequences in the PIWI proteins, maturation of the piRNA is completed by trimming at the 3' end and subsequent 2'-O-methylation [47], [48]. The length of the mature piRNA depends on the specific PIWI protein it binds, which determines how many nucleotides are protected and inaccessible during the last step of maturation [45], [48]. The secondary biogenesis pathway consists of a self-amplification mechanism, termed the ping-pong cycle, through which the piRNA target becomes itself a piRNA once it is cleaved [37], [49]. Indeed, this pathway is highly efficient in selectively amplifying piRNAs that target active transposons. The process begins with piRNA-directed PIWI cleavage of the target transcript, in correspondence of the tenth position of the piRNA [37], [49]–[51]. This determines a partial overlap between secondary-generated piRNAs and the primary piRNAs that produce them. The newly generated secondary piRNAs then undergo maturation as described above and continue to be further amplified by repeating this cycle [52], [53]. Complementary to secondary piRNA biogenesis is the production of phased piRNAs: during the ping-pong cycle the target transcript is cleaved and gives rise to a secondary piRNA from the portion that is partially paired with the primary piRNA. The remaining 3' fragment of the transcript undergoes a process of stepwise fragmentation that ultimately leads to the generation of new adjacent piRNAs, with their sequences phased approximately by the length of a mature piRNA [38]–[40]. Secondary piRNAs biogenesis, along with the phasing process,

is particularly effective in silencing the target transcript by consuming its RNA to generate new piRNAs, which, in turn, can be amplified in the ping-pong process [38], [54].

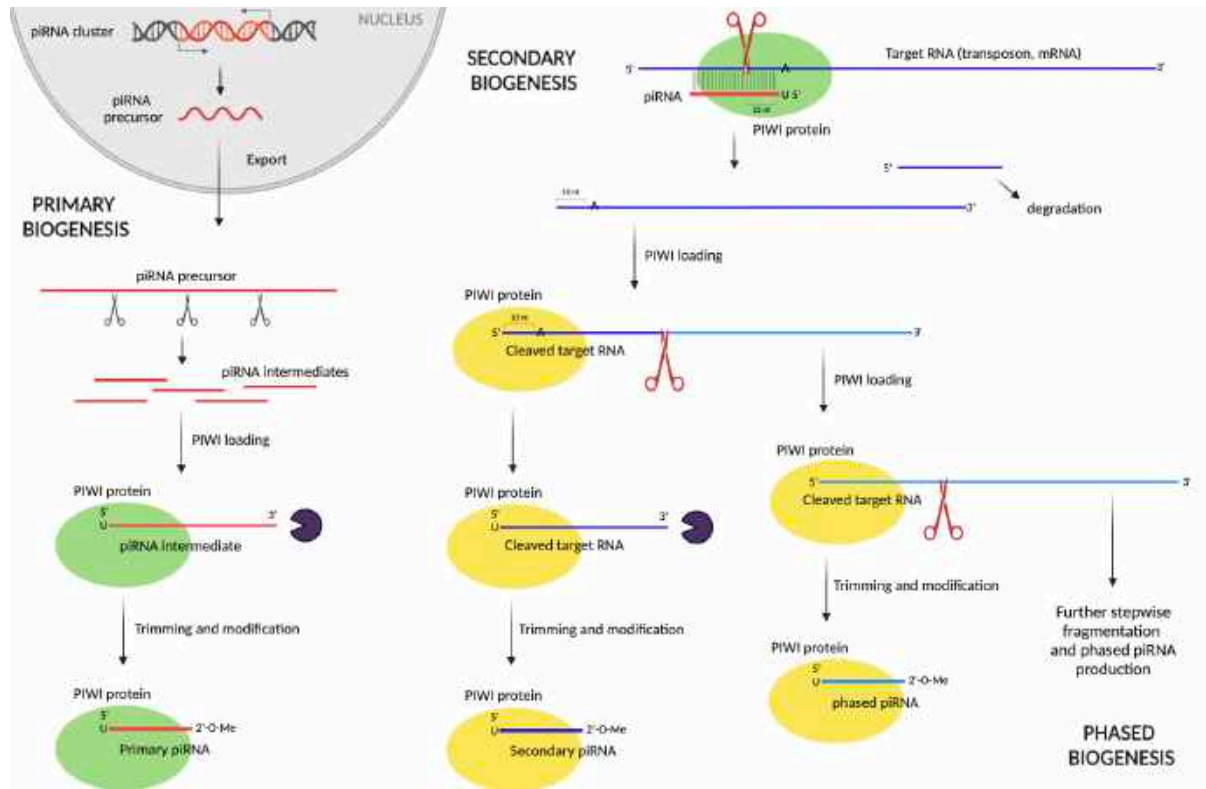


Figure 2: piRNAs biogenesis. In primary piRNA biogenesis, piRNA precursors transcribed from clusters are exported, processed into intermediates, and those having a Uridine at the 5' end are preferentially loaded onto PIWI proteins. Subsequent 3' end trimming and 2'-O-methylation generate mature primary piRNAs. Secondary biogenesis involves PIWI-piRNA complex cleavage of target mRNA, integrating the 3' cleaved RNA into PIWI. The 10th position, enriched in Adenine, is complementary to the 1st position of Uridine-enriched piRNA. Further trimming and modification give rise to a mature secondary piRNA. In phased biogenesis, the 3' cleaved RNA integrated into PIWI undergoes a stepwise fragmentation downstream of the future secondary piRNA, giving rise to phased piRNAs.

Recent findings suggest that the processes of biogenesis might not be distinctly separated as historically described. Instead, new models are proposed to unify these biogenetic mechanisms [20]. However, it should be remarked that numerous dynamics and molecular players remain to be elucidated. Particularly, the biogenetic process and all the involved factors have been extensively studied primarily in the germline [1], therefore it cannot be excluded that in somatic tissues other proteins and mechanisms may be involved.

At the functional level PIWI-piRNA complexes carry out their gene repressive functions through two primary mechanisms: transcriptional gene silencing (TGS) and post-transcriptional gene silencing (PTGS) [1], [11], [12]. Canonical PTGS relies on the endonuclease activity of PIWI proteins, which, guided by piRNAs, perform sequence-specific suppression by cleaving the target transcript [41], [55], [56]. In recent years, evidence has

emerged suggesting that this cleavage depends on the level of base-pairing between the guide piRNA and the target mRNA, requiring a high degree of complementarity [57]. In the other cases where the catalytic activity of PIWI is not involved, it is possible that it acts solely as an RNA-binding protein, recruiting other factors to regulate the target mRNA. This would explain why, surprisingly, it has been observed that piRNA-guided binding of PIWI proteins can also result in the positive regulation of target mRNAs [1]. Whereas, in the case of TGS, the catalytic activity of PIWI is not necessary because gene silencing is achieved indirectly through interactions with histone modifying enzymes and DNA methyltransferases [58]. As a result, this second mechanism enables precise regulation not only of transposons but also extends to broader functions, such as the control of heterochromatin formation [1], [12].

1.1.4 piRNAs in Central Nervous System

As anticipated above, piRNAs and PIWI proteins are found in numerous somatic tissues across diverse animal species, with a significant presence in the central nervous system (CNS) [1]. Notably, the brain, specifically the hippocampus followed by the cortex, has been identified as the second tissue with the highest piRNAs abundance after gonads [3]. Moreover, it has been proposed that there is a stronger correlation between piRNAs targeting and binding energy compared to piRNAs abundance [59], suggesting that somatic piRNAs may operate in a concentration-independent manner, allowing for functional efficacy at lower expression levels. Since the first report of piRNAs in the CNS, particularly in the mouse hippocampus, by Kosik and Vemuganti labs in 2011 [60], [61], a growing body of evidence suggested that CNS piRNAs play a functional role in processes such as neuronal development, learning, and memory [62]–[65]. Just a year later, the Kandel lab uncovered a functional role for piRNAs in CNS, demonstrating their contribution to the epigenetic control of memory related plasticity in *Aplysia* [66]. Subsequently, a parallel role was acknowledged in mammals by the Bredy lab. Indeed, disruption of the hippocampal piRNA pathway in mice enhances contextual fear memory, possibly by regulating the expression of genes associated with plasticity [65]. Additionally, Piwil2 mutant mice display behavioral deficits, including hyperactivity and reduced anxiety, indicating a piRNA pathway-dependent behavioral regulation. Moreover Piwil2/piRNA deficient mice exhibit significant altered methylation in LINE1 retransposons promoters and intergenic areas thus suggesting that piRNAs in CNS are involved in transposable elements suppression, akin to their germline counterparts [64], [67]. This is in line with the fact that transposon mobilization, in particular LINE1 elements activity, generates somatic mosaicism within hippocampal neurons - a mechanism associated

with learning and memory [68], [69]. Importantly, transposition events caused by mis-regulated mobile elements are linked to various neurological disorders, including Alzheimer's, and Parkinson's disease. In these pathological conditions, evidence suggests that the dysregulation of transposable elements coincides with alterations in PIWI-piRNAs, emphasizing a potential role for CNS piRNAs in regulating mobile elements [70]–[73].

In sum, piRNAs exhibit a wide-ranging regulatory capacity, functioning both post-transcriptionally and transcriptionally through interactions with epigenetic effectors [1]. Indeed, the involvement of piRNAs and PIWI proteins has been observed in various pathologies of the CNS (*Table 1*) [62], [71]–[81].

Table 1: piRNA pathway involvement in CNS pathologies.

| DISEASE | MODEL | PIRNA PATHWAY | Ref. |
|--|--|---|-----------------------------|
| Rett Syndrome | Cerebellum, Mecp2 KO mice | ↑ piRNAs | Saxena et al., 2012 |
| Autism | Newborn cortical neurons, Piwil1 KD mice/rats | Impaired neuronal polarization/migration | Zhao et al., 2015 |
| Autism Spectrum Disorder (ASD) | Gene association study on 2500 individuals with familial ASD | Gene variations in Piwil2 and Piwil4 | Iossifov et al., 2014 |
| Alzheimer's Disease (AD) | Prefrontal cortex tissue, patients | Deregulated piRNAs | Qiu et al., 2017 |
| | Postmortem human brain samples | ↑ piRNAs ↓ TEs | Sun et al., 2018 |
| | Postmortem human brain samples | Deregulated piRNAs | Roy et al., 2017 |
| | Human cerebrospinal fluid (CSF) | Deregulated miRNAs/piRNAs | Jain et al., 2019 |
| Sporadic Amyotrophic Lateral Sclerosis (ALS) | Postmortem human brain samples | Deregulated piRNAs, Piwil1, Piwil4 | Abdelhamid et al., 2022 |
| Parkinson's Disease (PD) | Fibroblasts, iPSCs and neurons from patients | ↓ SINE- and TE-derived piRNAs | Schulze et al., 2018 |
| | Genetic model (Enrailed), mouse | ↑ Piwil1 is neuroprotective against oxidative stress induced by LINE1 | Blaudin de Thé et al., 2018 |
| | Prefrontal cortex, amygdala, from patients | Deregulated piRNAs | Zhang et al., 2022 |
| Transient Global Cerebral Ischemia (tGCI) | Wistar rats | ↓ Piwil2 is neuroprotective | Zhan et al., 2023 |
| Progressive Supranuclear Palsy (PSP) | Human CSF | Deregulated miRNAs/piRNAs | Simoes et al., 2022 |

Moreover, as also observed in the germline and gonads where piRNAs targets extend beyond transposable elements, it is plausible that piRNAs similarly modulate coding genes in the CNS. Especially, given that somatic tissues exhibit more extensive epigenetic markers compared to germ cells [82]. Thereby, it is conceivable that the repression of transposable elements

may not be the primary function of somatic piRNAs. Hence, piRNAs in the CNS likely harbor a diverse array of functions [83], [84].

These evidences encourage further investigations that hold the potential to understand the roles of CNS PIWI proteins and piRNAs, offering a promising opportunity to uncover possible diagnostic and therapeutic applications within the landscape of neurological disorders [2].

1.1.5 piRNAs in inflammation

Inflammation constitutes a fundamental process underlying both the aging phenomenon and pathological conditions within the CNS, including neurodegenerative diseases [85]. Hence, it raises intriguing questions regarding the potential involvement of piRNAs in inflammatory states and responses. Despite limited knowledge about piRNAs and PIWI proteins in inflammation, the available evidence is highly interesting as it highlights a connection between the piRNA pathway and inflammatory states in various somatic tissues.

PiRNA pathway in peripheral inflammatory pathologies: PIWI proteins, specifically Piwil2 and Piwil4, have been observed to exhibit responsiveness and increased expression in reaction to inflammatory cytokines in the pathogenesis of rheumatoid arthritis [86]. Within the same pathology, a differential expression of piRNAs related to immunoregulation was identified [87]. PIWI-piRNAs are also involved in respiratory tract diseases [88]. Piwil4 is expressed in a subset of airway epithelial cells, and its deletion results in a higher magnitude immune response upon infection [89].

PiRNA pathway direct regulation of inflammatory mediators: A PIWI-piRNAs direct regulation on inflammatory mediators has been reported in human cell lines. Hili (human Piwil2) has been shown to suppress Transforming growth factor β (TGF- β) signaling, a potent regulator of inflammatory activity, in human embryonic kidney (HEK) cells [90]. Moreover, in human primary T- lymphocytes, a specific piRNA mediates the degradation of the interleukin-4 pre-mRNA, thus regulating a crucial cytokine involved in inflammation [91].

PiRNAs in immune cells: In addition to the report of a role for specific piRNAs in human primary T- lymphocytes [91], piRNAs presence in immune cells have also been reported in a study that identified the changes in small non-coding RNAome during macrophage inflammatory activation. In this work it was also identified a specific piRNA that overexpressed promotes the pro-inflammatory macrophages' antitumor activity [92].

Furthermore, in a recent pre-print work, Santiago and colleagues characterized state-specific proteomic and transcriptomic signatures of microglia derived extracellular vesicles, and showed that they include specific piRNAs populations [93].

PiRNAs in aging: Interestingly, a correlation between aging and the expression of specific piRNAs has been identified through transcriptome-wide piRNAs profiling analysis in human brains [94], [95]. This suggests that piRNAs might play a role in influencing successful brain aging, possibly through the regulation of genomic integrity and aging-associated processes such as neuroinflammation, although this hypothesis awaits formal confirmation. This holds particular significance because inflammatory processes are implicated not only in well-established diseases but also during aging. In fact, aging and age-related pathologies have common underlying mechanisms, primarily centered around inflammation. As individuals age, a persistent, sterile, low-grade inflammation known as inflammaging develops [96], [97]. In addition to peripheral changes, age-associated inflammatory responses extend to the brain, where microglia drive neuroinflammation thus contributing to the pathogenesis of age-related diseases [98]. Moreover, aging, neuroinflammation, and neurodegeneration are closely intertwined with the process of adult neurogenesis, which in turn is influenced by and influences microglia responses [99].

Altogether, the current knowledge supported by a surge of recent studies strongly suggests that the piRNA pathway may play important functions in somatic tissue, particularly in stem cells. As related to the CNS, it is plausible to hypothesize that the piRNA pathway plays a role in neural stem cells (NSCs) and neuroinflammation, opening interesting perspectives towards the maintenance of lifelong plasticity and successful aging. Given the growing interest in the emerging roles of PIWI proteins and piRNAs as biomarkers of human diseases [100], the integration of piRNAs research with neurogenesis and neuroinflammation becomes a crucial and promising avenue for further exploration. In this context deciphering the regulatory functions of the piRNA pathway holds the potential to unveil the intricate regulatory mechanisms governing brain function and pathology, with implications for diagnostic and therapeutic applications in aging and neurological disorders.

1.2 Adult neurogenesis

Neurogenesis is the process of de novo neuronal and glial cell formation within the brain, primarily driven by the division of NSCs [101], [102]. In mammals, neurogenesis was thought to be exclusive to brain development, with limited regenerative capacities in the adult brain [103]. However, groundbreaking experiments by Joseph Altman in the 60s challenged this dogma by revealing mitotically active NSCs capable of giving rise to new neurons in the brains of adult rats [104]. These NSCs can remain quiescent, or they may undergo division to self-renew and produce committed offspring in a tightly regulated manner [101], [105]. The revelation of persistent neurogenesis in the adult mammalian brain challenged a century-old scientific dogma and set the stage for extensive investigations [106], offering a new perspective on the plasticity of the mature nervous system. Current research affirms the continuous presence of adult neurogenesis throughout the lifespan of various primates, humans included [107]–[119]. However, numerous unresolved questions fuel an ongoing debate [120]–[126]. The existence of adult neurogenesis in humans is surrounded by conflicting evidence: employing thymidine analogue labeling, carbon dating, and protein expression analyses, several studies reported the occurrence of neurogenesis in the human hippocampus, while others have failed to find evidence of neurogenic cell divisions [113]–[115], [123], [127]–[130]. Addressing this controversy is complicated by the scarcity of healthy human tissues, delays in post-mortem brain sample fixation, and inherent flaws and experimental errors in the techniques used to visualize newborn cells. Additionally, translating experimental data from rodents to human brain function poses a significant challenge. In light of these factors, ongoing debates question the relevance of neurogenesis for human physiology and disease [120]–[126]. Interestingly new hypothesis, like the possibility of de novo neurogenesis by non-newly generated “immature” neurons, are emerging [131]. These propositions hold the potential to bridge opposing views [132], [133] and add complexity to our understanding of this phenomenon.

1.2.1 The hippocampal neurogenic niche

Neurogenic niches are specialized areas of the adult brain where NSCs are maintained throughout life and new neurons are continuously generated. In the adult mammalian brain, two primary neurogenic niches stand out: the subventricular zone (SVZ) and the dentate gyrus (DG) of the hippocampus (*Figure 3*) [101], [134]. The SVZ, situated along the lateral walls of the lateral ventricles, contributes to olfaction and is particularly well-studied in rodents [135], [136]. Interestingly the other region, i.e., the subgranular zone (SGZ) of the hippocampal DG is the sole neurogenic niche conserved across mammalian species [137].

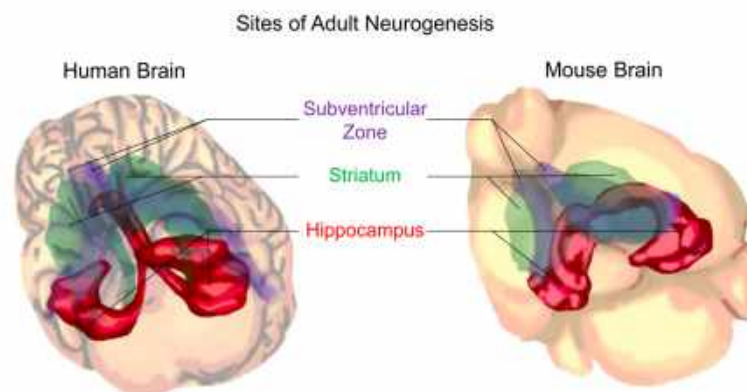


Figure 3: Adult neurogenic regions. (Left) Human adult neurogenesis occurs under basal conditions in the hippocampus (red) and the striatum (green). (Right) Murine adult neurogenesis occurs in the hippocampus (red) and the subventricular zone (purple). The hippocampus serves as the only brain region where adult neurogenesis is conserved across mammalian species [137].

Neurogenic niches are distinct microenvironments, which comprise NSCs, their progeny, immature neurons, endothelial cells, other glial cells, and immune cells such as macrophages and microglia. These niches offer a unique milieu, comprising elements such as extracellular matrix components, short and long-distance signaling molecules, and cellular interactions. All these factors and players intricately regulate neuronal development, adjusting and responding to external signals, while preserving a permissive setting for this process [138], [139].

Adult neurogenesis represents an impressive form of neural plasticity in the postnatal brain. The Regulation of this process is a topic of significant interest, primarily because the hippocampus is intimately involved in learning and memory. This has led to the hypothesis that adult neurogenesis could play a crucial role in cognitive functions and brain plasticity [101], [134], [140]–[152]. Moreover, the lifelong maintenance of adult neurogenesis in the DG plays a pivotal role in successful aging [153]. The ageing process of the niche attracts considerable interest for therapies aimed at preventing age-related brain diseases such as neurodegeneration. Indeed, the relevance of adult hippocampal neurogenesis extends to its

connections with neurodevelopmental and mood disorders, as well as neurodegenerative conditions. It is also noteworthy for its susceptibility to various insults, including epileptic seizures, strokes, and traumatic brain injuries [84], [154].

1.2.2 Regulation of adult hippocampal neurogenesis

Adult neurogenesis is a complex, multi-stage process subject to precise spatio-temporal regulation influenced by gene expression and environmental factors (*Figure 4*) [84], [124], [155]–[157]. At the cellular level, the regulation of adult neurogenesis influences several critical aspects: I) Preservation of the stem cell population, including their dynamics of division and survival. II) Lineage determination and cellular fate commitment of newly generated progeny originating from aNPCs. III) Migration of aNPCs to their ultimate brain locations. IV) Effective integration of newly generated neurons into pre-existing brain circuits [158], [159]. The process of adult neurogenesis originates from a population of radial-glia-like precursor cells, referred to as adult NSCs. These cells are located in the SGZ of the DG and possess radial branches that span the granule cell layer (GCL) of the hippocampus [101]. The DG of a young adult brain is known to harbor dozens of thousands of aNSCs. However, in a given moment, only about 1-2%, of these aNSCs are actively involved in the cell division process [160]. This activity can be quantified through the incorporation of the thymidine analog 5-bromo-2'-deoxyuridine (BrdU), specifically occurring during the S-phase of the cell cycle [104], [128], [161]–[163]. aNSCs are mostly found in a non-dividing, quiescent state, but upon activation, they have the capacity for symmetric division, expanding the neurogenic pool, or differentiation into neurons. While the majority of activated aNSCs undergo division to generate neurons, resulting in depletion over time, some aNSCs opt for remaining inactive for longer periods, prolonging their self-renewal and symmetric division capabilities or entering a deeper quiescent state, thus preserving the aNSC population in later stages of life. Upon activation, aNSCs re-enter a proliferative state, giving rise to transient amplifying adult neural progenitor cells (aNPCs) or astroglial cells [111], [153], [157], [164], [165]. The survival of newborn cells is a crucial step in the regulation of adult hippocampal neurogenesis and many aNPCs undergo apoptosis to prevent the excessive generation of new or unfit neurons [101], [166]–[171]. The surviving aNPCs mature into neuroblasts, which are lineage-committed cells that exit the cell cycle and enter a maturation stage [111], [157], [164], [165]. These neuroblasts undergo differentiation, migration, and maturation, ultimately forming a granule cell layer consisting of the principal excitatory neurons in the dentate gyrus, known as granule cells. Upon completing the neurogenic process, these

neurons become integrated into the hippocampal network: they receive input from the entorhinal cortex, send axonal projections to area CA3, and modulate the activity of CA3 pyramidal cells. These granule cells exhibit sparse firing activity and are subject to regulation by local interneurons within the dentate gyrus and hilus area [101], [149], [172]–[174]. Both extrinsic mechanisms and intrinsic genetic factors have been shown to regulate different aspects of hippocampal neurogenesis. Extrinsic factors, neurogenesis undergoes fine-tuning through a diverse array of environmental, physiological, and pharmacological stimuli [101]. Enriched environments positively impact adult neurogenesis, whereas stress, global ischemia, seizures, aging, and inflammation have detrimental effects on this process, thereby affecting cognition [146], [162], [175]–[184].

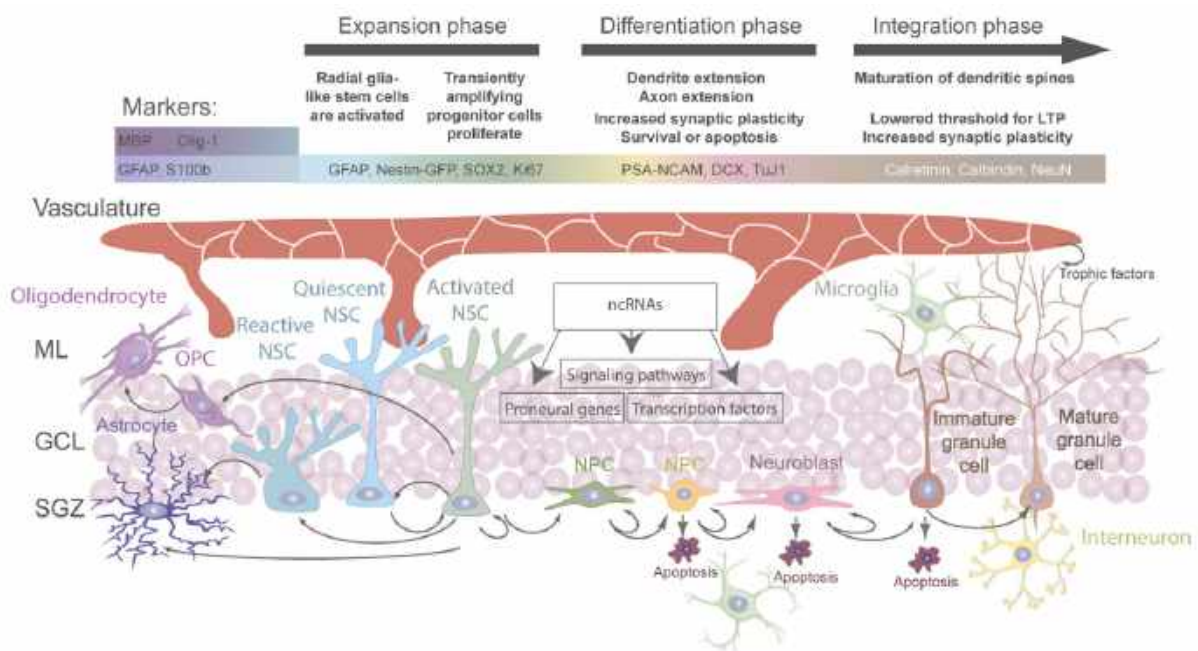


Figure 4: Adult hippocampal neurogenesis process and regulation. (Top) Overview of the neurogenic phases and of the principal markers used to define the stage and cell identity. (Bottom) Overview of all cell types involved directly or indirectly in the regulation of adult hippocampal neurogenesis, as well as of cell-intrinsic and extrinsic signals that govern the various phases of adult neural stem cells (aNSCs) quiescence, activation, neurogenesis, astrogliogenesis, and oligodendroglialogenesis in the adult DG. [78]

Intrinsic mechanisms regulating adult neurogenesis, especially cell differentiation, include both genetic and epigenetic mechanisms. While transcriptional cascades have been elucidated over the past two decades [185], epigenetic mechanisms, although less understood, are certainly involved in the regulation of adult neurogenesis and its maintenance lifelong. These epigenetic regulations occur by processes like histone

modification, DNA methylation, chromatin remodeling, and non-coding RNAs (ncRNAs) action. These controls may serve as potential bridges between the environment and the intrinsic signaling [186], [187]. Indeed, epigenetic controls on identical genomes have been shown to govern postnatal neurogenesis through temporal and spatial regulation of gene activity [188], [189]. The dynamic nature of these epigenetic mechanisms allows them to play a pivotal role in gene regulation, controlling adult neurogenesis in response to external world, life experience and various environmental signals [190], [191]. Specifically, sncRNAs such as miRNAs, endo-siRNAs, lncRNAs and other are an essential layer of control of the gene regulatory network involved in adult neurogenesis, finely tuning gene expression and cellular differentiation [84].

This control is of paramount importance, considering that adult neurogenesis can have both beneficial and detrimental effects on disease outcomes [101], [137]. For instance, neurogenesis plays a crucial role in promoting efficient repair and regeneration following stroke and traumatic brain injury. Furthermore, it exhibits a beneficial influence on the treatment and amelioration of symptoms in depression. Conversely, impaired adult neurogenesis is linked to a range of pathological conditions, including mood disorders, epilepsy, ischemic insults, and neurodegenerative diseases [84], [137], [154]. Significantly, age also impacts neurogenesis: during the aging process, there is the development of the so called inflammaging [96], [97] that is associated with a decline in neurogenesis and coincides with an increased incidence of neurodegenerative pathologies and reduced regenerative capacities following injury [99], [134], [192]–[194]. Although aNSCs decline sharply with age, some of them remain quiescent in aged brains [105], [113], [153], [162]. These findings suggest the potential for leveraging adult hippocampal neurogenesis for therapeutic applications, particularly in addressing conditions such as depression, stroke, traumatic brain injury and neurodegenerative diseases, for a successful brain aging.

1.3 Microglia functions in neurogenesis and neuroinflammation

Inflammation is a fundamental pathological mechanism through which biological tissues react to external triggers, including infections, trauma, and various forms of injury. The distinctive, intricate, and dynamic inflammatory process occurring within the CNS is referred to as neuroinflammation. Triggered by infection, trauma, toxins, or autoimmune reactions, neuroinflammation is a fundamental defense mechanism for restoring tissue balance. It is characterized by the inflammatory and immunomodulatory responses of glial cells, primarily microglia and astrocytes, mainly through the release of inflammatory mediators, such as cytokines, chemokines, and reactive oxygen species [195]–[198]. Neuroinflammation has gained significant attention in recent years, as accumulating evidence suggests its involvement in the pathogenesis of various neurological disorders and neurodegenerative diseases, such as Alzheimer's disease, Parkinson's disease, and multiple sclerosis [199]–[207].

In the context of neuroinflammation, microglia, the resident immune cells of the CNS, emerge as central players [196], [208]–[210]. Comprising roughly 10-15% of the adult brain's glial cell population, microglia are the vanguard of the CNS's immune defense system and perform multifaceted roles critical to the preservation of brain homeostasis [211]. These immune cells originate from a transient hematopoietic wave of erythromyeloid precursors in the embryonic yolk sac, and subsequently populate the CNS parenchyma through the circulatory system. They are long-lived and persist in adulthood thanks to their self-renewing capabilities [212]–[221]. Microglia, once considered primarily as immune sentinels, have gained prominence due to their newly uncovered roles in synaptic plasticity, tissue repair, and neurodevelopment. This recognition has positioned microglia as central figures in neuroimmunology, offering valuable insights into brain health, the pathogenesis of neurological disorders, and the development of potential therapeutic strategies [98], [196], [222]. Microglia serve as the specialized macrophages of the CNS innate immune system, residing within the brain parenchyma in close proximity with neurons. Notably, other extra-parenchymal CNS-resident myeloid cells known as Border-associated macrophages (BAMs) also contribute to CNS homeostasis. BAMs include leptomeningeal, perivascular, and choroid plexus macrophages, collectively exhibit distinct phenotypic and functional characteristics and are located at CNS interfaces such as the meninges, perivascular spaces, and choroid

plexus, where they coexist with various other immune cell types. With their phagocytic and migratory abilities, BAMs serve as regulators of immune responses at CNS borders and have garnered attention for their potential involvement in neurodegenerative diseases. However, compared to microglia, BAMs remain relatively less understood, necessitating further research to fully elucidate their origin, identity, and functions [223]–[225].

Microglia play a pivotal role in the preservation of CNS homeostasis through a varied array of functions aimed at safeguarding the integrity of neural circuits while protecting the brain from potential threats [226]. These immune cells actively engage in a perpetual state of surveillance: in the healthy tissue they have a highly ramified morphology and patrol the brain parenchyma dynamically moving their processes and sensing the microenvironment for any indications of injury, infection, or aberrant cellular activity [215], [227]–[229]. Microglia promptly detect and respond to any deviations from homeostasis adopting a wide range of complex phenotypes [230]–[234]. These responses entail significant alterations in their molecular profile, morphology and ultrastructure and are concomitant with the release of various molecules, encompassing pro-inflammatory cytokines, reactive oxygen species, excitotoxins such as glutamate, as well as neuroprotective and neurotrophic factors, anti-inflammatory cytokines and molecules that promote tissue repair, extracellular matrix deposition, and suppression of the inflammatory state [209], [222], [235]. This extreme versatility allows them to exert both detrimental and protective effects, engaging in cytotoxic responses, immune regulation, or injury resolution, depending on the context and local microenvironment. Therefore, it is crucial that these responses are tightly controlled thus protecting the CNS and minimizing tissue damage [211], [236].

The core properties that characterize microglia, i.e. surveillance, phagocytosis, and capability of releasing soluble factor, underlie their various biological functions. Indeed, microglia is involved in the regulation of: inflammation, tissue repair, blood brain barrier (BBB) permeability, vasculogenesis, synapse remodeling, myelination, neuronal function and neurogenesis (*Figure 5*) [237].

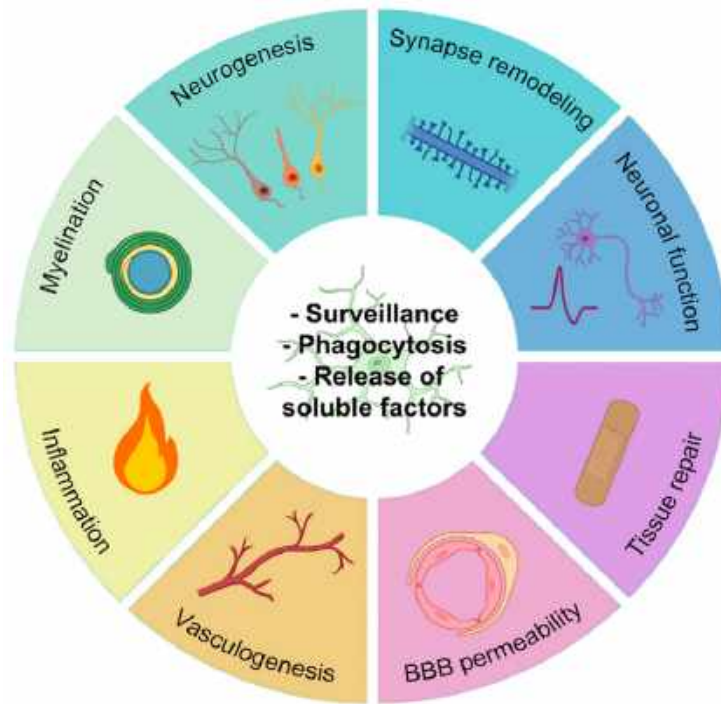


Figure 5: Microglia core properties and functions. Phagocytosis, surveillance, and capacity for releasing soluble factors (inner circle) are core properties through which microglia contribute to key biological functions (outer circle). [224]

1.3.1 Microglia functions in neurogenesis

During both developmental and adult stages microglia contribute to NSCs proliferation and differentiation, synapse formation and remodeling, myelination, and neural circuits refinement [237]. In particular, they participate in the programmed cell death of immature or defective neurons, facilitating the removal of cellular debris through phagocytosis [171], [238], [239]. Their involvement in synaptic pruning, the selective elimination of surplus synapses, results in the optimization of neural networks by removing weak or redundant connections: a process that is integral in enhancing cognitive function and information processing [229], [240]–[244]. Furthermore, microglia regulates myelinogenesis and oligodendrocyte progenitors maintenance [245]–[247]. In the adult brain microglia regulate neuronal activity [248] both directly, through mechanisms such as ATP-dependent negative feedback loops [249], and indirectly, acting on adult neural stem and progenitor cells (aNSPCs) [101]. Specifically, in the adult neurogenic niche microglia participates not only in the removal of unfit neural cells but also in a mutual crosstalk with NSPCs, which involves release of soluble factors, cell-cell interactions, and the modulation of the local microenvironment [194], [250], [251]. ANSPCs release granulocyte-macrophage colony-

stimulating factor (GM-CSF) and interleukin 4 (IL 4), which influence microglia phenotypes. Conversely, microglia enhance aNSPCs' proliferation, differentiation, and fate decisions through various factors, including but not limited to brain-derived neurotrophic factor (BDNF), interleukin 6 (IL 6), insulin-like growth factor-1 (IGF-1), and transforming growth factor-beta (TGF- β) [252]–[255]. Finally, when inflammation occurs, microglia can exhibit both neuroprotective and neuroinflammatory effects, depending on the prevailing microenvironment [84], [182], [183], [251], [254], [256], [257]. Their neuroprotective functions consist in the support tissue regeneration by releasing trophic factors that, on one hand, stimulate aNSPCs mobilization and local generation of neurons and glia and, on the other hand, result in aNSPCs' responses through immunomodulatory, neuroprotective, and remyelinating mechanisms [258]–[262]. Microglia also play a role in preserving the integrity of the blood-brain barrier (BBB) and participating in vasculogenesis. However, even though under normal conditions microglia exert a protective role in maintaining BBB integrity, in sustained inflammatory conditions they increase the barrier's permeability through phagocytic actions on the astrocytic end-feet that compose the BBB [263], [264]. Similarly, microglia contribute significantly to the maintenance of vascular integrity, sustaining angiogenic processes and supporting the maturation of blood vessels, which is vital for providing oxygen and nutrients to neural tissues and to NSPCs in the neurogenic niche [237], [265]–[267].

1.3.2 Microglia functions in neuroinflammation

Microglial cells are constantly sensing their surrounding microenvironment ready to properly react to a plethora of different trigger signals, therefore a significant portion of microglial functions and responses are reliant on the expression and signaling through specific receptors [268]. Because of this, microglia exhibit a diverse array of receptors, including pattern recognition receptors (PRRs), immunomodulatory receptors, neurotransmitter receptors, and distinctive signaling receptors such as the C-X₃-C motif chemokine receptor 1 (CX₃CR1) [269], [270]. CX₃CR1, also known as fractalkine receptor, is primarily associated with maintaining neuronal health, regulating microglial surveillance and responses [271]–[276]. Its ligand fractalkine can serve as chemoattractant guiding microglia to sites of injury or neuroinflammation [277], [278]. Pattern recognition receptors (PRRs), such as Toll-like receptors (TLRs), NOD-like receptors (NLRs), RIG-I-like receptors (RLRs) and C-type lectin receptor (CLRs), allow the detection of pathogens and damage-associated molecular patterns (PAMPs and DAMPs)[279]–[289] and are master initiators of

the microglial immune response [290]–[293]. Triggered by this signaling, microglia activate an inflammatory response marked by the synthesis and release of nitric oxide (NO), chemokines, and inflammatory cytokines. Pro-inflammatory cytokines, including interleukin 1 β (IL 1 β), IL6, and tumor necrosis factor alpha (TNF α), are central to microglial inflammatory responses, inducing a pro-inflammatory state and amplifying immune responses. Production of reactive oxygen species (ROS) and phagocytosis of pathogens, as well as clearing of dead neurons and cellular debris are other integral parts of microglia inflammatory response [211], [294], [295]. While essential for tissue repair, they can also cause damage to neighboring cells and exacerbate neuroinflammation. Additionally, microglia act as intermediaries between the immune system and the brain, exerting influence over both local and systemic neuroinflammatory responses [234], [293], [296]–[299]. A common tool employed to study microglia in the inflammatory context is stimulation with lipopolysaccharide (LPS) exposure [300]–[303]. LPS is a component of gram-negative bacteria that triggers TLR4-mediated pro-inflammatory responses [304]–[307]. Indeed, TLR4 signaling is a key neuroinflammatory mechanism and it is involved in various pathological and neurodegenerative conditions [308]–[310]. Finally, immunomodulatory receptors enable microglia to detect cytokines, chemokines, and immunomodulatory factors, and play a crucial role in the regulation of the inflammatory response and phagocytosis. In the same fashion, neurotransmitter receptors, that are fundamental to allow the crosstalk between microglia and other neural or glial cells, can lead to neuroprotection or the facilitation of inflammatory responses, depending on the context [270], [311].

1.3.3 Regulation of microglial inflammatory responses

Microglial functions are shaped by intrinsic and extrinsic determinants, spatiotemporal context, and different levels of complexity (*Figure 6*) [237]. As a result, the regulation of microglial functions, in particular in neuroinflammation, involves multiple types and levels of control ensuring a finely tuned and context-dependent immune response.

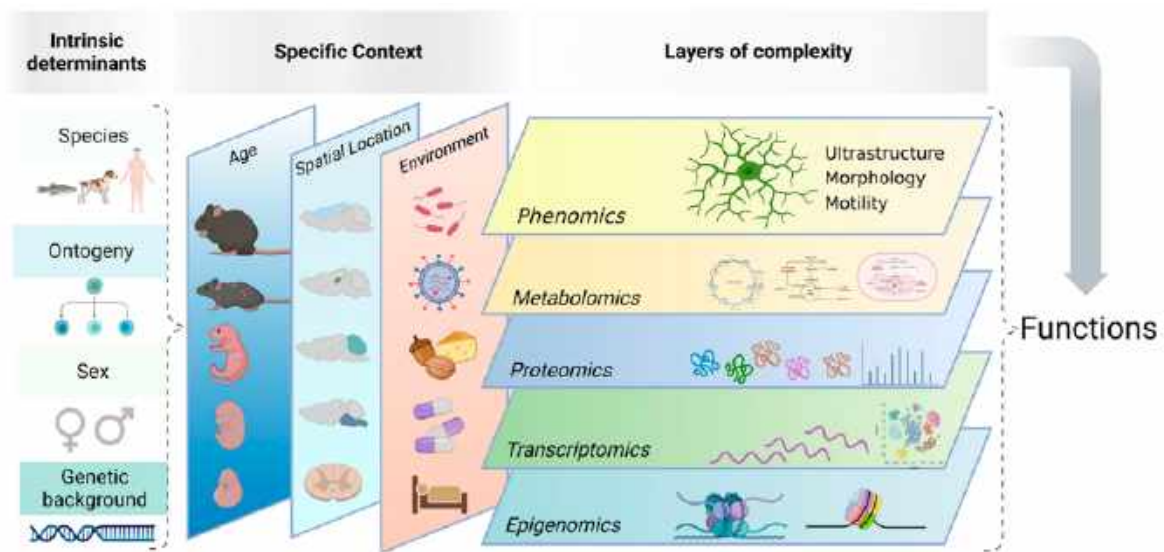


Figure 6: Microglia functions are the results of intrinsic and extrinsic determinants, spatiotemporal context, and layers of complexity. Microglial states are defined by intrinsic factors (such as species, ontogeny, sex, genetic background) in addition to the context they exist in, including age, spatial location, and environmental factors (such as nutrition, microbiota, pathogens, drugs, etc.). Collectively, these factors impact microglia at multiple levels (i.e., epigenomic, transcriptomic, proteomic, metabolomics, ultrastructural, and phenomic), ultimately contributing to the determination of microglial functions. [224]

Intrinsic factors, including genetic background, ontogeny, and species-specific characteristics, contribute to the baseline reactivity and predisposition of microglia to inflammatory stimuli. Simultaneously, extrinsic elements such as age, spatial location within the CNS, and exposure to external stimuli like pathogens, microbiota, and drugs significantly influence microglial inflammatory responses [237], [312], [313]. Metabolic pathways also play a role, as the availability of nutrients and the metabolic state of microglia can influence their polarization towards pro-inflammatory or anti-inflammatory phenotypes [314], [315]. At the molecular level, transcriptional regulation orchestrates the synthesis of pro-inflammatory or anti-inflammatory mediators, dictated by various signaling pathways, gene expression patterns, and transcription factors [316]. Key transcription factors, such as NF- κ B, an integral components of the TLR signaling pathway, actively contribute to inducing the release of a spectrum of inflammatory cytokines and immune modulators [317]–[319]. Epigenetic regulation stands out as a crucial level of control, given its dynamic nature that allows responsiveness to external stimuli. Epigenetic modifications, such as DNA methylation and histone acetylation, contribute to the long-term regulation of microglial inflammatory responses, influencing the accessibility of genes associated with inflammatory pathways [320]. At the post-transcriptional and post-translational levels, regulatory elements like

ncRNAs fine-tune gene expression, while post-translational modifications of proteins regulate their activity, stability, and function [321]–[323]. Notably, recent evidence highlights the ability of microglia to form memories of environmental stimuli. This phenomenon, referred to as innate immune memory or microglia priming, relies in epigenetic reprogramming, and determines microglial enhanced or attenuated responses to secondary stressors. While this mechanism enables rapid adaptation to environmental challenges, it can also lead to chronic hyperinflammatory states if the adaptive response becomes overly reactive, posing potential risks to brain health [236], [324]–[326].

The central role of microglia in maintaining CNS homeostasis highlights the potential repercussions of disruptions in their function. In fact, dysregulated microglia and neuroinflammation can lead to pathological conditions marked by neuronal damage and cognitive decline [85], [198], [222]. Inflammaging significantly influences age-related diseases, particularly neurodegenerative disorders [96]. Cellular senescence, a hallmark of aging, has been implicated in microglial dysfunction: senescent microglia display impaired phagocytic activity and an altered secretome and this phenotypic change contributes to the persistence of neuroinflammation in the aged brain [327]. Microglia exists in many diverse and context dependent states [237], among which are the disease-associated microglia states (DAMs). DAM states were identified through in-depth single-cell RNA sequencing analyses of microglia in models of CNS diseases, revealing specific microglial genes that define core signatures associated with pathology. These microglial states may arise from common trigger signals present in the diverse pathological conditions, and influence the nature of microglia responses [233], [328]–[335]. Thus, it's crucial to understand the functional roles underlying microglial states and their regulation, in the perspective of targeting them therapeutically. Indeed, microglia active involvement in neuroinflammatory responses designates them as crucial therapeutic targets, presenting opportunities to mitigate neuroinflammation and inflammaging thereby retarding the progression of neurodegenerative pathologies [336].

Whereas the role of some ncRNAs, such as miRNAs, is actively investigated in the framework of epigenetic regulation of microglial functions [337]–[341], little is known about the potential role of piRNAs in the regulation of microglial inflammatory responses. Exploring the role of the piRNA pathway in microglia and neuroinflammation promises to advance our comprehension of the nervous system. Additionally, it provides avenues for devising innovative therapeutic strategies to address neurodegenerative and neuroinflammatory diseases, promoting successful brain aging.

2 Rationale and aims

Adult neurogenesis and neuroinflammation are interrelated processes that are crucial for maintaining CNS homeostasis and supporting cognitive functions throughout life.

The brain has multiple defense mechanisms against potential threats, one of which is neuroinflammation where microglia play a central role. In this respect, the neuroprotective role of NSCs and the generation of new neurons in the mature brain are regarded as forms of plasticity essential for cognition and play a fundamental role in resolving damage. Disruption or alteration of the stringent regulations governing these processes results in pathological situations. This is notably significant given the association of inflammaging with increased occurrence of age-related diseases and neurodegenerative pathologies, such as Alzheimer's and Parkinson's disease. Nonetheless, numerous cellular and molecular mechanisms underlying the regulation of adult neurogenesis and neuroinflammation remain elusive.

Non-coding RNAs are involved in this regulatory control. Altered piRNAs expression has been implicated in pathological and inflammatory conditions underlying neurodevelopmental and neurodegenerative diseases. However, the potential functions of PIWI and piRNAs in brain cells remain unclear.

In this thesis, I have investigated the presence and potential functions of the piRNA pathway in aNSCs and microglia.

The first aim of this thesis is to determine whether the piRNA pathway is present in aNSCs and has a role in neurogenesis in the adult hippocampus. This investigation is grounded in evidence associating the piRNA pathway with hippocampal-dependent behaviors and neuronal functions, along with the reported significance of this pathway in stem cell maintenance. To address this question first, I contributed to the research led by a former PhD student in the lab (Gasperini C, Tuntevski K, Beatini S, et al., 2023 - *see Appendix*). Then, I employed a constitutive Mili knock-out (KO) mouse model to confirm and further dissect the role of the piRNA pathway in the adult hippocampal neurogenesis context.

The second aim of this thesis is to explore the potential involvement of the piRNA pathway in neuroinflammation, specifically within the context of microglial inflammatory responses. This investigation builds upon the insights derived from addressing the first question, as detailed in Gasperini C, Tuntevski K, Beatini S, et al., 2023 (*see Appendix*), wherein the

manipulation of Mili in the adult hippocampus led to neuroinflammation and gliosis. Additionally, the exploration is underpinned by limited yet suggestive evidence pointing towards a potential connection between the piRNA pathway and its possible role in the regulation of inflammatory processes.

Understanding the involvement of the piRNA pathway in neurogenesis and neuroinflammation will not only enhance our understanding of CNS processes but will also open avenues for the use of piRNAs as biomarkers, as well as therapeutic agents or targets. This advancement holds promise for the development of targeted interventions for age-related diseases and neurodegenerative pathologies.

3 Results

3.1 Piwil2 (Mili) sustains neurogenesis and prevents cellular senescence in the postnatal hippocampus

To explore the potential role of the piRNA pathway in adult neurogenesis, I collaborated on the project published in Gasperini C, Tuntevski K, Beatini S, et al., 2023 (*see Appendix*). This study uncovered the presence of Piwil2 and piRNAs in both mouse and human aNPCs, with their expression diminishing in their differentiated progenies, and demonstrated that Mili plays a crucial role in safeguarding the fitness of aNPCs, ensuring proper neurogenesis, and contrasting senescence and neuroinflammation in the postnatal mouse hippocampus. Specifically, knock-down (KD) of Piwil2 (Mili) in aNPCs induced senescence and impaired neurogenesis, leading to an increased generation of reactive glia both *in vivo* and *in vitro*. Moreover, depletion of Mili was also observed in aged aNPCs and upon the induction of aNPCs reactivity (by kainic acid). Interestingly, the piRNA pathway in neurogenesis was found to selectively target transcripts from repetitive elements and genes encoding regulators associated with senescence, neuroinflammation and oxidative stress.

I contributed to this study performing experiments necessary to prove the piRNA identity of the sncRNAs identified in aNPCs as *bona fide* piRNAs. In particular, I optimized and performed the co-immunoprecipitation of Mili and Mili-bound RNAs, i.e. the gold standard experiment that validates the piRNA identity of putative piRNAs sequences (*Figure 7*) [342].

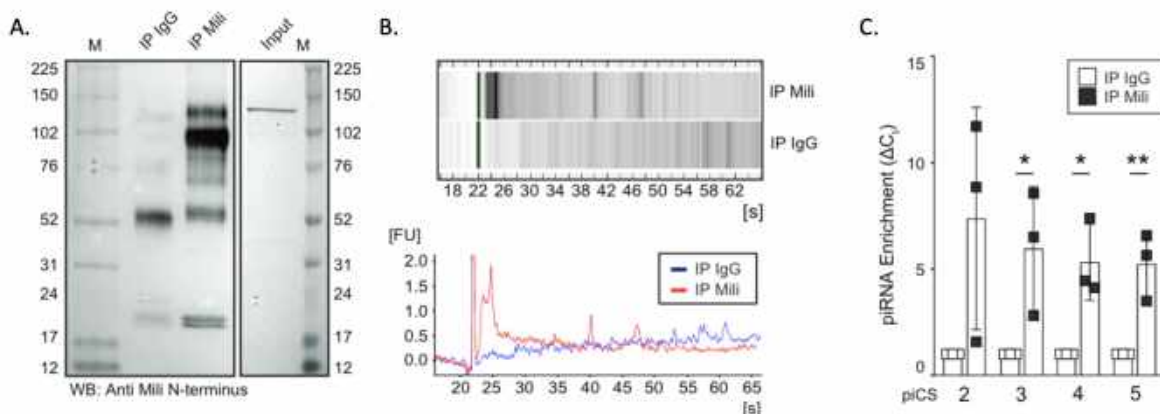


Figure 7: Validation of piRNAs identified in murine aNPCs. (A) Western blot of Mili, (B) analysis by capillary electrophoresis or (C) quantification via qPCR of the endogenous PiRNA consensus sequences (piCS) after co-immunoprecipitation (IP) with endogenous Mili (IP Mili) or control IgG (IP IgG) in lysates of DIF4 aNPCs. Data are expressed as mean \pm SD. N=3 independent experiments. *P < 0.05, **p < 0.01 as assessed by the two-tailed Student's t-test.

3.2 Characterization of the hippocampal stem cell niche in constitutive Mili KO and Mili HET mice

To confirm the role of the piRNA pathway in adult hippocampal neurogenesis I employed constitutive Mili KO mice. In the sections below, I will provide an initial characterization of how *in vivo* the adult hippocampal neurogenic niche, and *in vitro* aNPCs of Mili KO and Mili heterozygous (HET) mice are affected by the piRNA pathway's constitutive loss of function.

3.2.1 Validation of the constitutive Mili KO mouse model

The constitutive KO of Piwil2 (Mili) was previously published by O'Carroll lab [343], and was obtained through the CRE-LoxP system-mediated excision of exon 21 of the Mili gene, which encodes the functional endonuclease PIWI domain. This deletion results in an out-of-frame mutation, generating a premature STOP codon that directs the transcript for degradation via non-sense mediated decay (*Figure 8 A*). Mili KO mice have no reported phenotypes other than male sterility [343] but have never been investigated adequately outside gonads. To confirm the deletion of the exon 21 of the Mili gene and to exclude possible mosaicism in the brain, I extracted DNA from different tissues of Mili KO and Mili HET animals and performed PCR genotyping (*Figure 8 B*). Deletion of exon 21 was shown to result in Mili transcript degradation. To confirm this observation, I performed WB analysis for Mili protein, and found that it was completely absent in Mili KO animals and reduced in Mili HET animals (*Figure 8 C*).

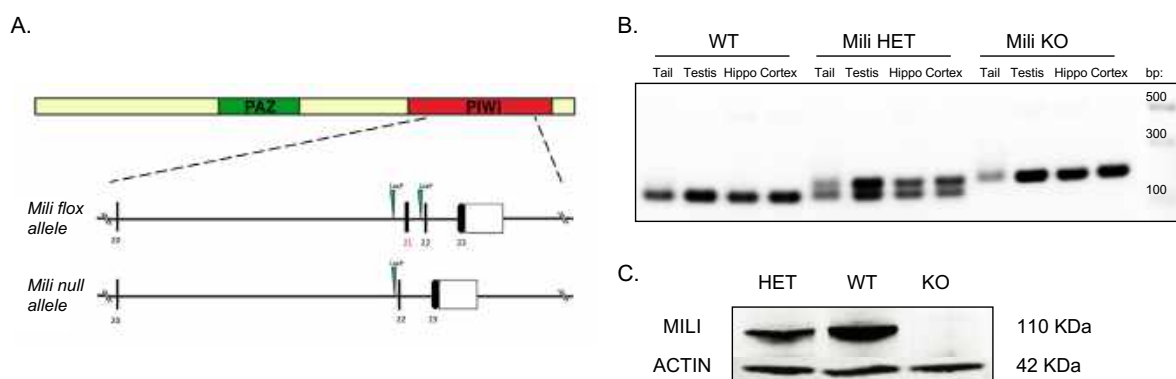


Figure 8: Validation of the constitutive Mili KO mouse model. (A) Schematic representation of Mili KO generation. Modified from [330]. (B) Analysis of genomic DNA performed on tails, testes, hippocampi and cortices showed that the tissues present an amplified band in correspondence of the 0.2 kb, confirming the presence of the Mili null allele only in Mili KO and Mili HET, as expected. (C) Mili protein abundance in lysates from postnatal WT, Mili KO and MILI HET mouse testes.

3.2.2 Altered cell proliferation in the hippocampal neurogenic niche of Mili KO and Mili HET mice

Next, I evaluated the effect of the absence (KO) or depletion (HET) of Mili on the proliferation of aNPCs in the adult hippocampus. To this end, I employed BrdU labeling. BrdU (100mg/kg, three injections every 2 h) was administered to 11 weeks old WT, HET and KO mice, which were then sacrificed 24 h after the first BrdU administration (*Figure 9 A*). More than 90% of the BrdU-positive cells in the DG labeled with this protocol are *bona fide* aNPCs [344]. BrdU incorporation was quantified in the SGZ of the postnatal hippocampi, according to previously published methodologies [161], [344], and plotted as number of BrdU positive cells per DG volume (mm^3).

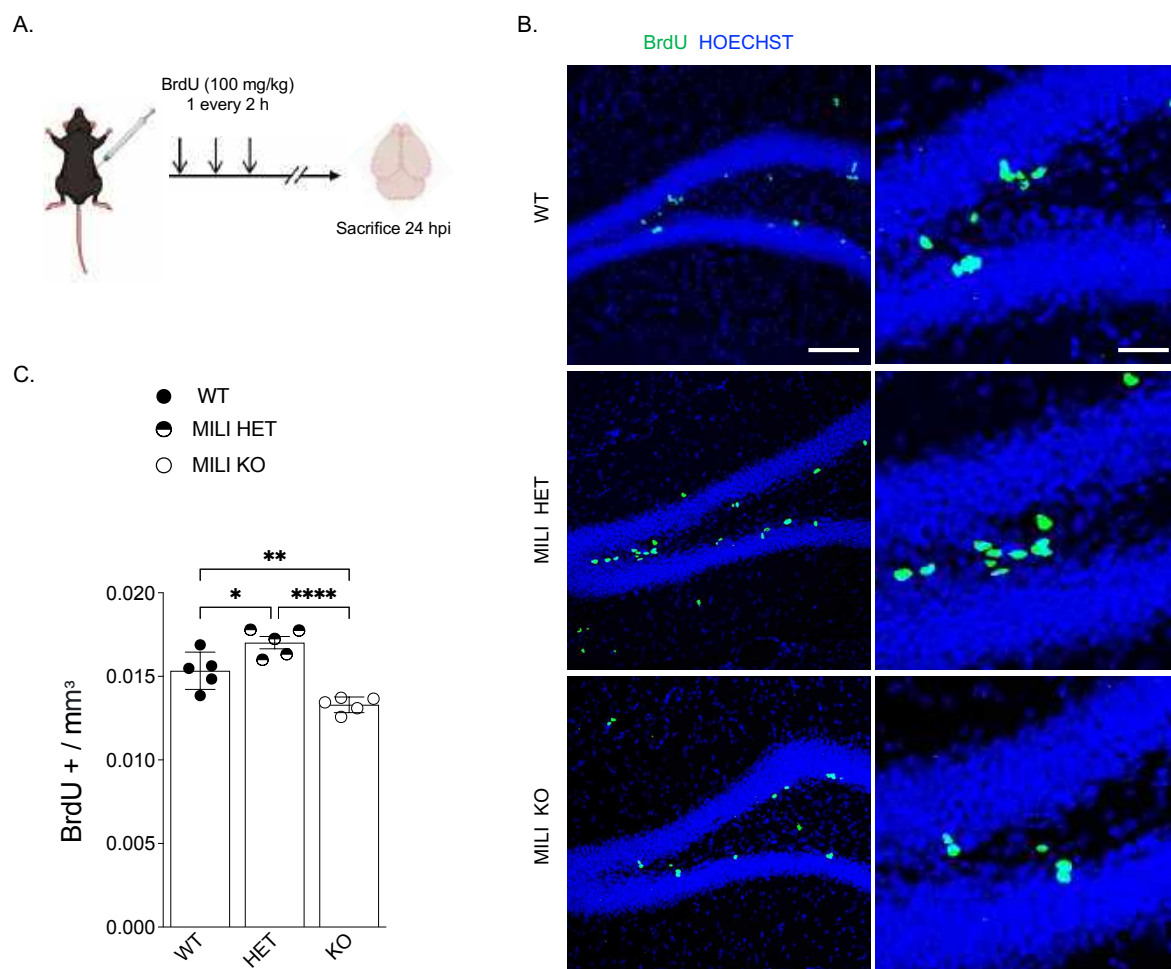


Figure 9: Altered cell proliferation in the hippocampal neurogenic niche of Mili KO and Mili HET mice. (A) Schematic representation of the experiment. (B) Representative confocal micrographs showing BrdU positive cells (green) in the hippocampus of 11 weeks old WT, Mili KO and Mili HET mice, subjected to three injections of BrdU 24 h before sacrifice. (C) Number of BrdU positive cells per DG volume (mm^3). Data are expressed as mean \pm SD, n = 5 mice per group. One-way ANOVA, Bonferroni as post hoc * $p < 0.05$, ** $p < 0.01$, **** $p < 0.0001$. The scale bars represent 100 μm (left), 25 μm (right).

This analysis indicated a reduction in the proliferation in the DG of Mili KO mice, compared to WT mice. In contrast an increase in cell proliferation in the DG of Mili HET mice compared to WT mice was observed (*Figure 9 B,C*). The opposite results in cell proliferation in the DG of Mili HET and Mili KO mice could be due to possible compensatory mechanisms induced by the constitutive absence of Mili, leading to divergent outcomes compared to the presence of a single functional allele.

This result substantiates our earlier observations (*see Appendix*), highlighting that the absence or depletion of Mili influence proliferation in the postnatal DG, opening possible implications for the maintenance of the stem cell pools in the adult hippocampus. An increase/decrease in proliferation of aNPCs in the DG is not necessarily indicative of a positive/negative correlation with neurogenic activity [137]. Thereby, further analyses are in progress to determine the fate of the proliferating cells and ascertain whether they will differentiate into neurons. In fact, an alternative scenario is that akin to what was observed in the case of Mili KD, the proliferation process may be altered and skewed towards the generation of reactive astrocytes.

3.2.3 Stemness and proliferation of Mili KO and Mili HET aNPCs is not impaired *in vitro* in proliferative culture medium

To further investigate the impact of Mili absence/depletion on aNPCs' proliferation and stemness I isolated primary hippocampal aNPCs from the DG of WT, Mili KO and Mili HET mice, and cultured them in monolayers as previously described [345], [346]. Cultured cells were maintained under proliferative conditions in a medium supplemented with fibroblast growth factor 2 (FGF2/bFGF) and epidermal growth factor (EGF) [347]. In order to evaluate whether the stemness of Mili KO and Mili HET aNPCs was altered *in vitro*, I performed immunostaining for Nestin, which is a marker of stemness, and observed no significant differences between the three genotypes (*Figure 10*). I then examined the impact of Mili KO and Mili depletion on aNPCs proliferation, quantifying BrdU incorporation and positivity for the proliferation marker Ki67 through immunofluorescence staining. To this end, BrdU was added to the culture medium 48 hours before cell fixation. Quantification of the proportion of BrdU positive or Ki67 positive aNPCs over total cells did not reveal any significant difference between the three genotypes (*Figure 10*). The discrepancy between the *in vitro* and *in vivo* proliferation of Mili KO/HET aNPCs are likely due to the presence of growth factors in the culture medium which might result in an active stimulation of proliferation.

Such conditions may mask subtle differences which, in a highly regulated process like neurogenesis, can be of significant relevance. Moreover, the *in vitro* environment lacks all the supporting factors and physiological cellular interactions found *in vivo* in the neurogenic niche.

These results are consistent with our earlier findings where Mili KD did not alter the stemness and proliferation of cultured aNPCs (see Appendix, Figure EV3A).

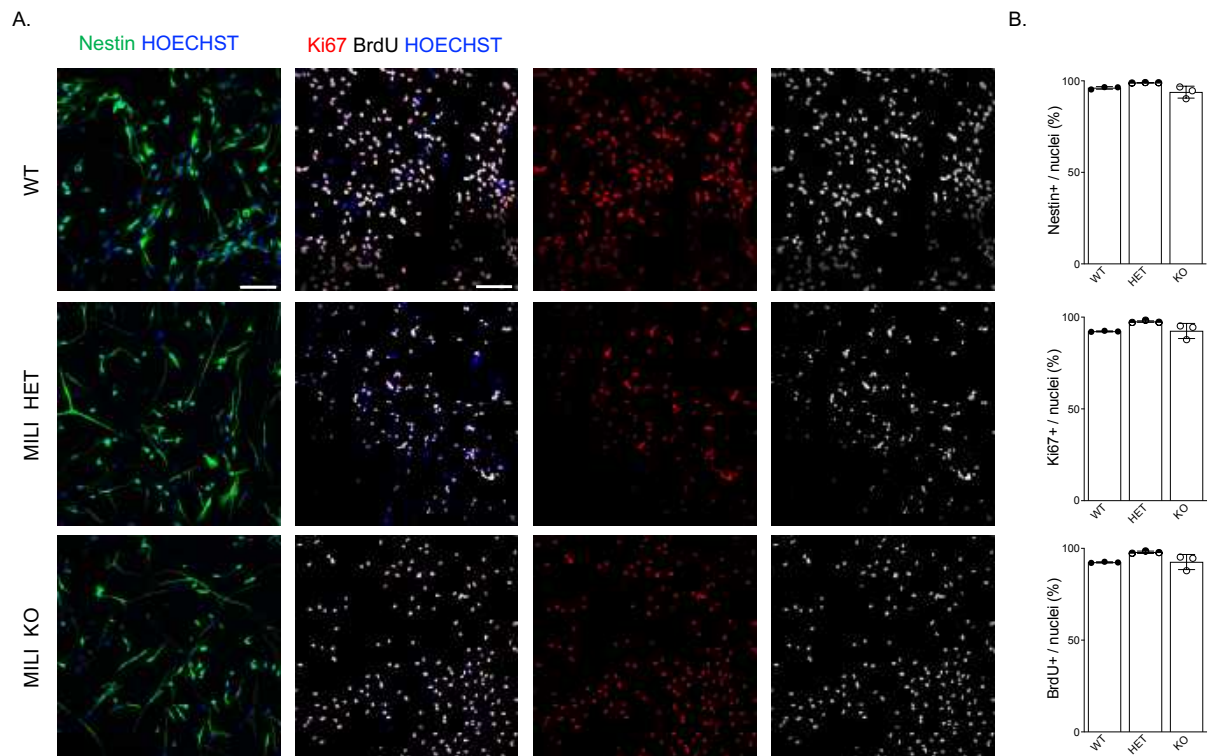


Figure 10: Stemness and proliferation of Mili KO and Mili HET aNPCs is not impaired *in vitro* in proliferative culture medium. (A) Representative confocal micrographs of WT, Mili KO and Mili HET primary hippocampal aNPCs, cultured in proliferative medium and incubated with BrdU 48h before fixation, and immunostained for Nestin (green), Ki67 (red), BrdU (grey). (B) Quantification of the percentage of Nestin (left), BrdU or Ki67 (right) positive cells over total cells. Data are expressed as mean \pm SD, n=3 biological replicates. The scale bars represent 100 μ m.

3.2.4 Induction of aNPCs differentiation results in higher cytotoxicity in Mili KO and Mili HET cells *in vitro*

As reported in Gasperini C, Tuntevski K, Beatini S, et al., 2023 (see Appendix), Mili and piRNAs show an increased expression 4 days after the induction of aNPCs differentiation, and depletion of the piRNA pathway impaired neurogenesis *in vitro* and *in vivo*. To confirm this result in the Mili KO and Mili HET aNPCs, I induced their spontaneous differentiation by the withdrawal of growth factors from the culture medium. During differentiation, programmed cell death of immature or defective neurons is part of the normal neurogenic process [105],

and in this context, I examined whether Mili absence/depletion affected cytotoxicity – a hallmark of cell death. Cytotoxicity, in terms of disruption of cell membrane integrity, was assessed by measuring the incorporation of “cytotox green”, a membrane-impermeable dye. Both Mili KO and Mili HET aNPCs displayed a more pronounced cytotoxicity compared to WT aNPCs, noticeable as early as 42 hours following the induction of differentiation (*Figure 11*). This result indicates that Mili prevents cytotoxicity of aNPCs, upon induction of their spontaneous differentiation *in vitro*.

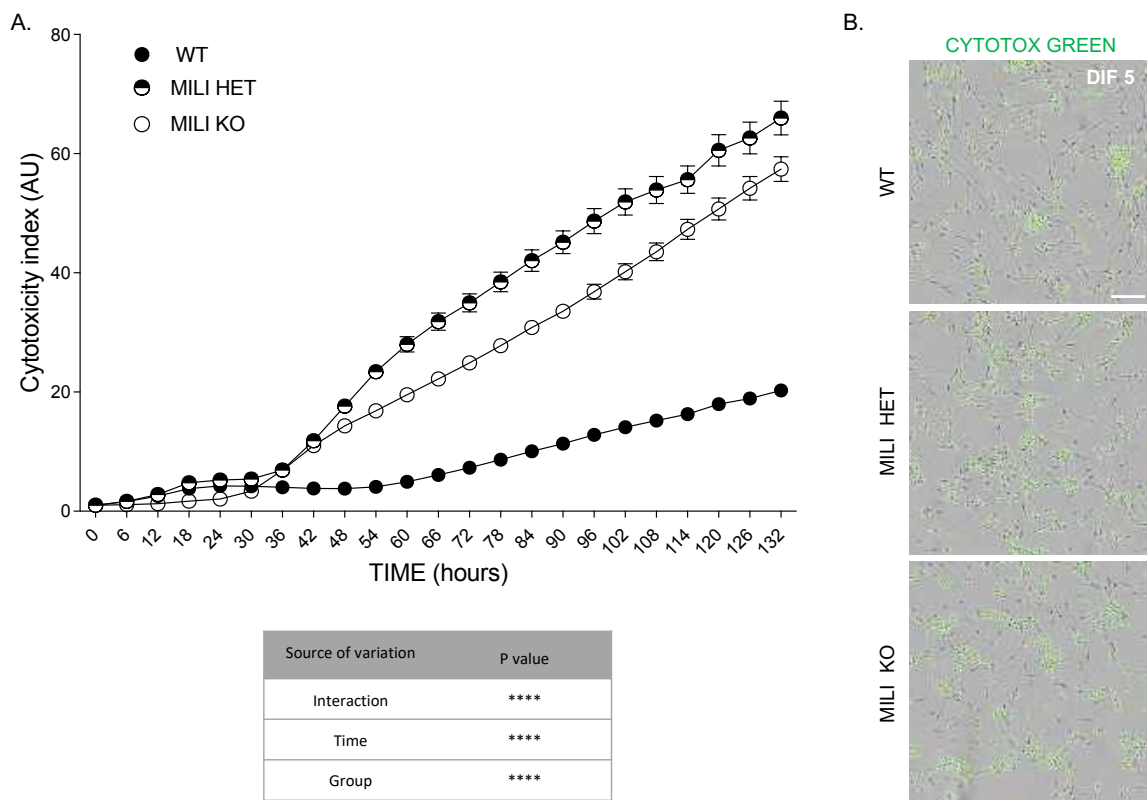


Figure 11: Induction of aNPCs differentiation results in higher cytotoxicity in Mili KO and Mili HET cells *in vitro*. (A) Cytotoxicity measure in differentiative culture conditions of WT, Mili KO, Mili HET aNPCs (top). Cells were incubated with membrane impermeable CYTOTOX GREEN dye for detection of cell membrane integrity disruption. Cytotoxicity index is defined as green object count per image, divided per phase area confluence -calculated by IncuCyte® software- and normalized to time zero. Two-way ANOVA main effects analysis results (bottom). (B) Representative micrographs of WT, Mili KO, Mili HET aNPCs at differentiation day (DIF) 5, in green: IncuCyte® signal reconstruction of green fluorescent CYTOTOX GREEN dye signal. Data are expressed as mean \pm SEM, n=4 biological replicates. Two-way ANOVA, ****P < 0.0001. The scale bars represent 100 μ m.

3.3 The piRNA pathway in microglia and neuroinflammation

In the previous work (Gasperini C, Tuntevski K, Beatini S, et al., 2023 - *see Appendix*) we observed that the KD of Mili in the adult hippocampus induced the expression of senescence-associated secretory phenotype (SASP) and reactive oxygen pathway genes and gliosis. This observation, coupled with existing evidence implicating the piRNA pathway in the polarization of macrophages upon inflammation [92], led us to hypothesize that the piRNA pathway could be present in microglia and play a role in neuroinflammation.

3.3.1 Acute Mili KD in adult mouse hippocampus results in microgliosis

To ascertain whether Mili is involved in the maintenance of microglial cells homeostasis, I inspected brain sections spanning across the hippocampus of mice I injected with a control scrambled GapmeR (Control) or a GapmeR targeting Mili (GapmeR1, Mili KD), as described and validated in Gasperini C, Tuntevski K, Beatini S, et al., 2023 (*see Appendix, Figure 4 A, C*).

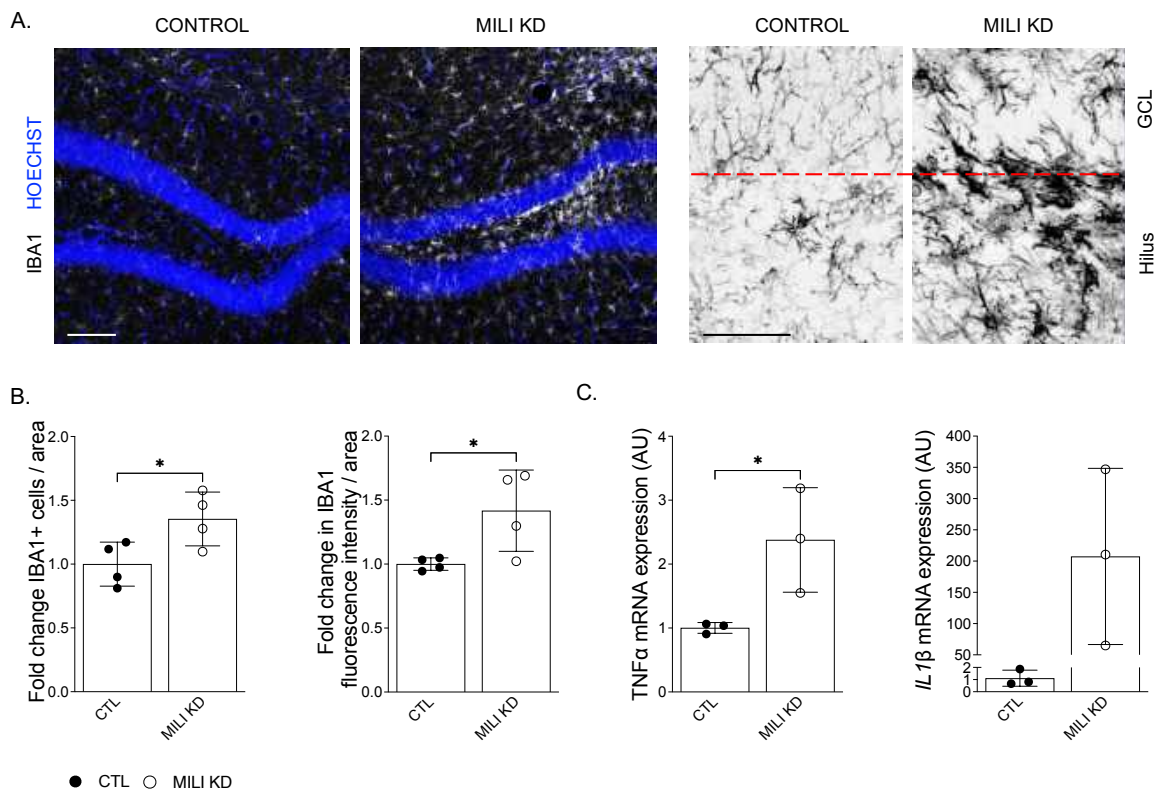


Figure 12: Acute Mili KD in adult mouse hippocampus results in microgliosis. Caption on following page.

Figure 12: Previous page - (A) Representative confocal micrographs of postnatal hippocampal sections, immunostained for IBA1 30 days post injection (dpi) of scrambled GapmeR (CTL, left hemisphere) and GapmeR against Mili (MILI KD, right hemisphere). (B) Fold change in number of IBA1 positive cells (left), fold change in IBA1 fluorescence intensity level (right) normalized over the area of a region of interest (ROI) corresponding to hippocampal GCL and hilus in brain slices, upon Mili KD compared with Control. (C) Inflammatory markers (TNF α left, IL1 β right) expression analysis in the DG from postnatal mouse hippocampi 48 hours after the injection of scrambled GapmeR (CTL) or GapmeR against Mili (MILI KD). Data are expressed as mean \pm SD, n = 4 (A, B) n=3 (C) biological replicates. *P < 0.05 as assessed by the two-tailed Student's t-test. GCL, granular cell layer. The scale bars represent 100 μ m (A, left), 50 μ m (A, right).

Inspection of brain sections 30 days after bilateral injections of GapmeRs indicated an increase in Iba1 positive cells, which were also characterized by hypertrophic cell bodies, in the ipsilateral hippocampus injected with GapmeR antisense to Mili, compared with the contralateral side injected with control GapmeR (Figure 12 A, B). In agreement, we observed an increase in the levels of the inflammatory markers TNF α and IL1 β upon Mili KD in the postnatal hippocampus (Figure 12 C).

This result indicates that Mili prevents microgliosis in the postnatal mouse hippocampus, either directly or indirectly via aNSCs-mediated functions.

3.3.2 The key piRNA pathway genes Mili and Mov10 are expressed in CX₃CR1^{GFP+} microglia and increase upon LPS-induced inflammation *in vivo*

As an entry point to explore the potential involvement of the piRNA pathway in microglial inflammatory responses, I evaluated the expression of key piRNA pathway genes in microglia isolated from the brain of mice subject to acute inflammation. To this end, I took advantage of the knock-in/ knock-out CX₃CR1^{GFP} mice model, which express the enhanced green fluorescent protein (EGFP) under the control of the endogenous Cx3cr1 locus in monocytes, dendritic cells, NK cells, and brain microglia [348]. Microglial inflammatory response in the brain was induced by the intraperitoneal (i.p.) injection of LPS at the concentration of 5mg/kg in P20-P30 CX₃CR1^{GFP} mice (LPS) [300]. As control, CX₃CR1^{GFP} mice were injected with saline (CTL). 48 hours after i.p. injection, brains were dissociated and GFP+ cells isolated via Fluorescent Activated Cell Sorter (FACS). Sorted cells were then processed for RNA extraction (Figure 13 A). As expected, LPS injection induced inflammatory response in the brain, as confirmed by the increased expression of the pro-inflammatory markers TNF α and IL1 β (Figure 13 B), and by the increased size and complexity detected by forward and side scatter flow cytometry measures in sorted GFP+ cells, compared to GFP+ cells sorted from the brains of control mice (Figure 13 C). Acute (LPS-induced) inflammation significantly increased the expression of Mili, as well as that of one of the essential cofactors for piRNA biogenesis, the

helicase Mov10, in GFP+ cells compared to GFP+ cells sorted from the brains of control mice (Figure 13 D). In contrast, Miwi expression was unaltered and Miwi2 expression undetectable in GFP+ cells sorted from LPS treated or control mice.

These results indicate that *bona fide* microglia cells express the key piRNA pathway genes Miwi, Mili and Mov10 and that the latter two increase their expression in inflammatory (LPS) conditions, *in vivo*.

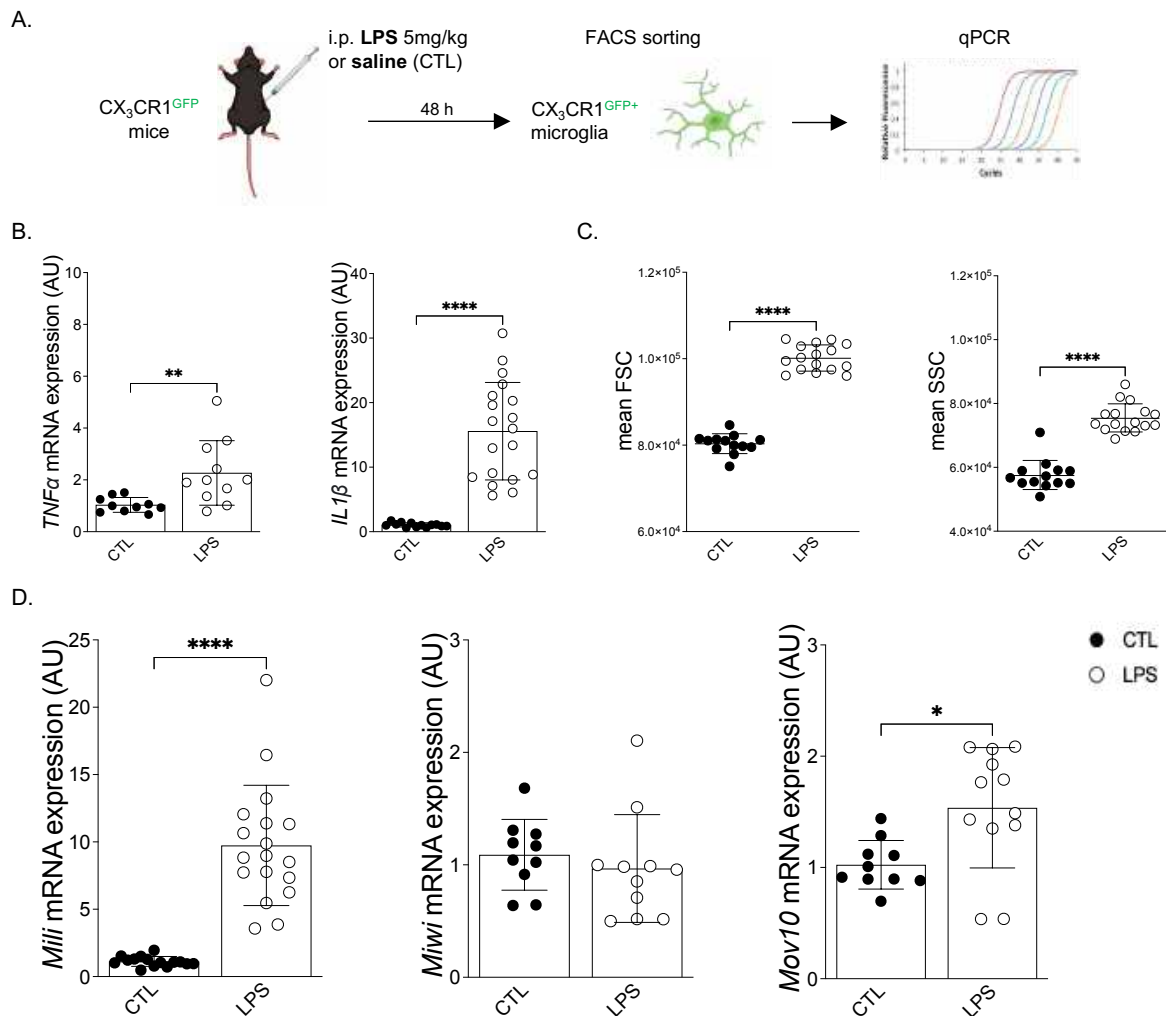


Figure 13: The key piRNA pathway genes Mili and Mov10 are expressed in CX₃CR1^{GFP+} microglia and increase upon LPS-induced inflammation *in vivo*. (A) Schematic representation of the experiment. (B) Inflammatory markers (TNF α left, IL1 β right) expression analysis. (C) Mean forward scatter (left) and mean side scatter (right) measured with flow cytometry. (D) PiRNA pathway genes (from left to right: Mili, Miwi, Mov10) expression analysis in GFP+ microglia sorted from CX₃CR1^{GFP} mice injected with LPS or saline (CTL). Data are expressed as mean \pm SD, n = 10-13 (CTL) 12-16 (LPS) mice per group. *p < 0.05, **p < 0.01 as assessed by the two-tailed Student's t-test.

3.3.3 Mili and Mov10 increase their expression in inflamed primary microglia

Acute (LPS-induced) inflammation may lead to immune cells infiltration in the CNS, among which are monocytes that also express CX₃CR1 [348], [349]. To validate my observations *in vitro*, I established primary microglia cell cultures, following previously published protocols [350], and I induced their acute inflammation treating them with LPS at increasing concentrations (10ng/ml, 0.1µg/ml). Microglial cells were harvested at the indicated time points after treatment, and RNA and proteins extracted to monitor inflammatory markers expression and levels of Mili and Mov10 (Figure 14 A). As expected, LPS treatment successfully inflamed microglia as indicated by the increase of TNFα and IL1β (Figure 14 B). Again, I observed a significant (and dose dependent) increase in the levels of Mili and Mov10 transcripts (Figure 14 C). In agreement, protein levels of MILI and MOV10 increased significantly in inflammatory conditions (Figure 14 C).

Together, these results demonstrate that the essential Piwi proteins Miwi, Mili and Mov10 are expressed in microglia, and the latter two are responsive to acute (LPS-induced) inflammation *in vivo* and *in vitro*.

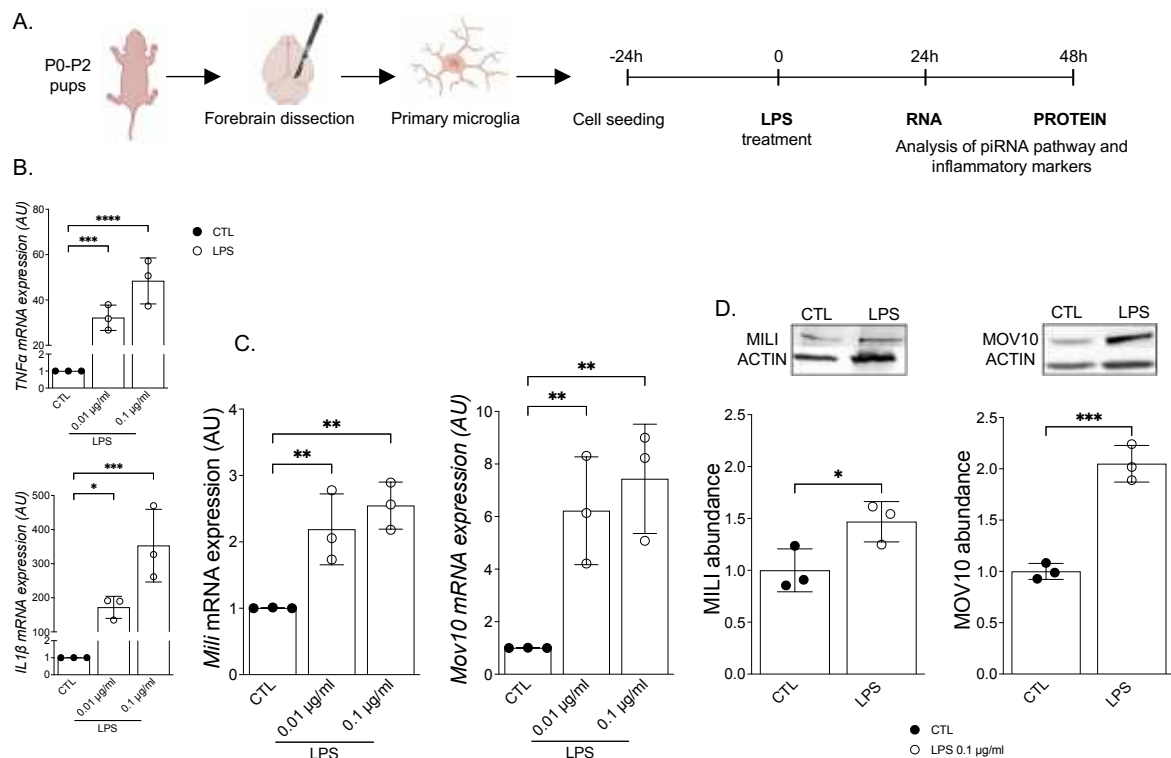


Figure 14: Mili and Mov10 increase their expression in inflamed primary microglia. (A) Schematic representation of the experiment. (B) Inflammatory markers (TNFα up, IL1β down) and (C) PiRNA pathway genes (Mili left, Mov10 right) expression analysis in untreated (CTL) or inflamed (LPS) primary microglia. (D) MILI (left) and MOV10 (right) levels in untreated (CTL) or inflamed (LPS) primary microglia. Data are expressed as mean ± SD, n = 3 biological replicates. One-way ANOVA, Bonferroni as post hoc (B, C), two-tailed Student's t-test (D) *p < 0.05, **p < 0.01, ***p < 0.001, ****p < 0.0001.

3.3.4 Piwil2 (Hili, in human) responsiveness to acute LPS-induced inflammation is conserved in human microglia

To investigate whether piRNA pathway genes' responsiveness to acute LPS-induced inflammation was occurring also in human, I employed HMC3 cells, a well characterized human microglial cell line (Figure 15 A) [351]. HMC3 cells expressed three of the four human Piwi paralogs, i.e., Hiwi (Piwil1), Hili (Piwil2) and Piwil3. Hiwi2 (Piwil4) transcript was undetectable (Figure 15 C), in agreement with our data in murine microglia (Figure 13, 14). To induce inflammation, cells were treated with LPS (0.1µg/ml) for 24h. TNFα, IL1β and IL6 higher expression in LPS treated cells compared to untreated control confirmed the successful induction of inflammation (Figure 15 B). Remarkably, Hili expression significantly increased in the inflamed condition. HILI increase was confirmed at the protein level (Figure 15 D).

This evidence indicates that Piwil2 increase, previously observed in murine microglia in response to inflammation, is conserved also in human microglia. The conserved nature of Piwil2 responsiveness to inflammation further suggests a potential underlying function, possibly in the regulation of microglial inflammatory response.

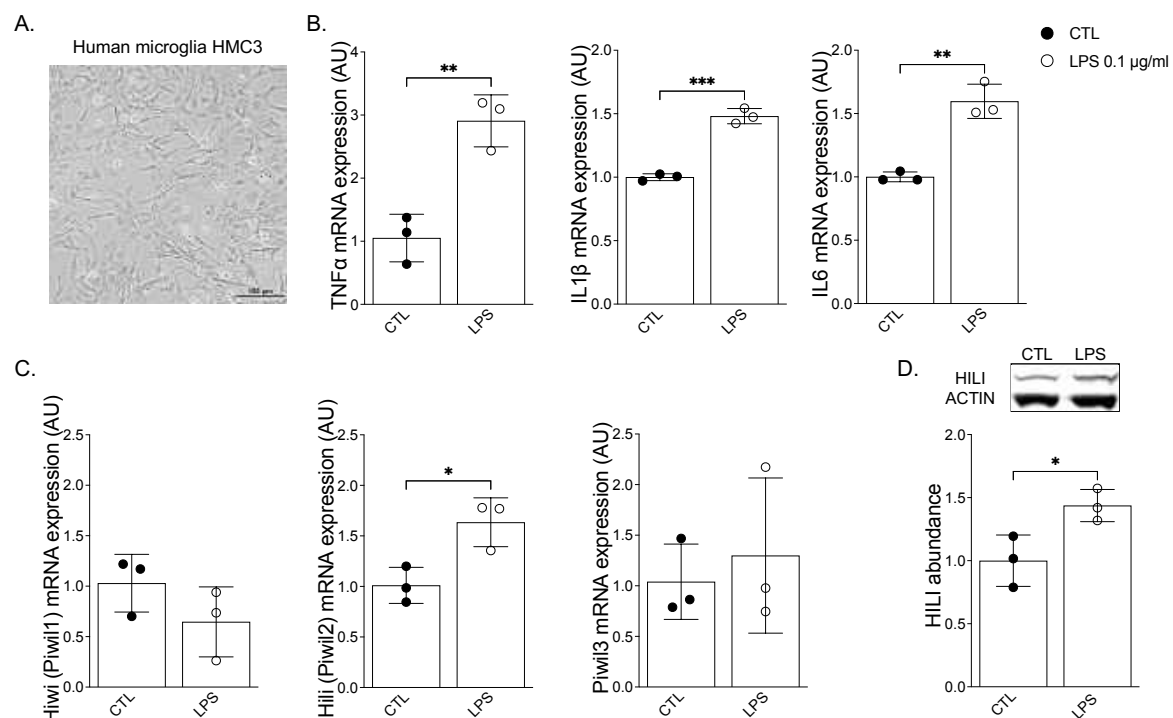


Figure 15: Piwil2 (Hili, in human) responsiveness to acute LPS-induced inflammation is conserved in human microglia. (A) Representative phase contrast micrographs of 2D cultured HMC3 cell line. (B) Inflammatory marker (TNFα, IL1β, IL6) and (C) PiRNA pathway genes (Hili, Hiwi, Piwil3) expression analysis, and (D) HILI levels in untreated (CTL) or inflamed (LPS) human microglia, 24h (RNA) or 48h (protein) after treatment. Data are expressed as mean ± SD, n = 3 biological replicates. *p < 0.05, **p < 0.01 as assessed by the two-tailed Student's t-test. The scale bars represent 100 µm.

3.3.5 Aging-induced neuroinflammation (inflammaging) increases Mili expression in microglia

Physiological aging is associated with the development of chronic, sterile, low grade inflammation (inflammaging) [96], [97]. Therefore, I wanted to check whether Mili expression in microglia is also responsive to this physiological inflammatory context. To this end, I isolated microglia from adult (12-24 weeks old, CTL) or physiologically aged (96-97 weeks old, OLD) mice. Specifically, I dissociated the brain tissue and performed immunostaining for microglial markers CD45 and CD11b on the obtained single cell suspension. Cells positive for CD45^{dim} and CD11b^{bright} were isolated via FACS (*Figure 16 A*) [352]. The observed increase in IL1 β expression in old mice, compared to young ones, confirmed the inflamed status of the elderly animals. Moreover, this was paralleled by Mili increase in aged mice (*Figure 16 B*).

This result corroborates and extends the responsiveness of the piRNA pathway to different acute (LPS) and chronic (ageing) inflammatory contexts.

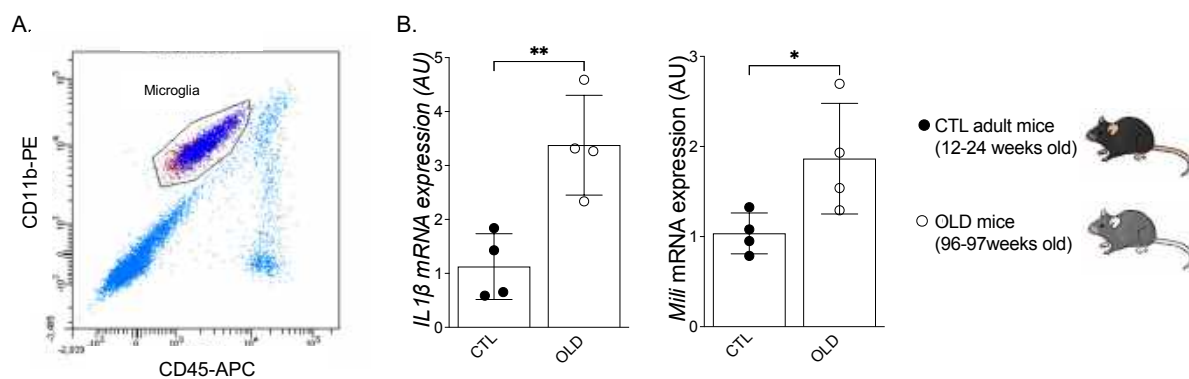


Figure 16: Aging-induced neuroinflammation (inflammaging) increases Mili expression in microglia. (A) Microglia isolation via FACS, spectrum of APC and PE fluorescence intensity. Microglia cells are double positive for CD11b-PE, at high intensity, and CD45-APC, at medium intensity. (B) IL1 β (left) and Mili (right) expression analysis in CD45⁺ CD11b⁺ microglia sorted from adult 12-24 weeks old (CTL) or physiologically aged and inflamed 96-97 weeks old (OLD) mice. Data are expressed as mean \pm SD, n = 4 mice per group. *p < 0.05, **p < 0.01 as assessed by the two-tailed Student's t-test.

3.3.6 Acute inflammation alters the expression of (Mili-dependent) piRNAs in murine microglia

Next, to investigate the presence of endogenous piRNAs in microglia, small-RNA sequencing was performed on primary and sorted microglia, in CTL and inflamed conditions. Primary microglia acute inflammation was induced in vitro using 0.1µg/ml LPS, and cells were harvested 24 hours post-treatment. In vivo inflammation was induced by i.p. injection of 5mg/kg LPS or saline (CTL) in CX₃CR1^{GFP} mice aged between P20-P30. 48 hours after the injection, GFP⁺ cells were FACS sorted. Subsequently, RNA was extracted from primary and sorted microglia cells and processed for small-RNA sequencing. Following a previously published analysis pipeline (*see Appendix*, [63]) putative piRNAs were identified in CX₃CR1^{GFP+} and primary microglia, and using stringent criteria, subsequent analyses were restricted on the small non-coding RNAs that perfectly aligned (i.e., no mismatch) with mouse piRNAs previously annotated in the piRNA database piRBase [6]. Putative microglial piRNAs exhibit a peak length of 23 nt (*Figure 17 A*) and a 5' Uridine (U) bias (*Figure 17 B*), consistent with earlier findings in the brain of adult mice [3], [4]. Additionally, the probability distribution of nucleotide- pair distance between the 5' termini of putative primary and secondary piRNAs closely resembled that of other animals [20], showing asymptotic convergence around the "0" mark on the x-axis (*Figure 17 C*). Given that Mili increases in inflammation, we checked whether a parallel increase in piRNAs content happens in inflamed microglia. Total piRNA content, normalized in transcript per kilobase in a million (TPM), did not evidence significant differences in piRNAs abundance in basal conditions (CTL) and upon LPS-induced inflammation (LPS), both in sorted (CX₃CR1^{GFP+}) and primary microglia (*Figure 17 D*), indicating that inflammation didn't alter piRNA abundance in these cells. Interestingly, we could distinguish two subsets of piRNAs in inflamed microglia, one that was upregulated and the other downregulated upon LPS treatment (*Figure 17 E,F*), consistent with the reports of altered expression of piRNAs populations in macrophage polarization [92]. In particular, LPS-responder piRNAs in sorted microglia were identified as outliers larger (LPS-upregulated), or smaller (LPS-downregulated) than 3 standard deviations from the mean of a linear 20% noise identity model, based on the piRNA levels in control CX₃CR1^{GFP+} sorted cells. Identification of the responder-piRNAs from sorted microglia in primary microglia demonstrated a similar response trend. Then, considering that Mili exhibited an LPS-responsive increase, we asked whether the LPS-responsive piRNAs subset we identified could be Mili-dependent. To check our hypothesis, we looked at the expression of this piRNAs

subset in WT and Mili KO mice, and we observed that LPS-upregulated piRNAs exhibit a higher trend of expression in WT versus Mili KO hippocampi, by the two-sample Kolmogorov-Smirnov test (Figure 17 G).

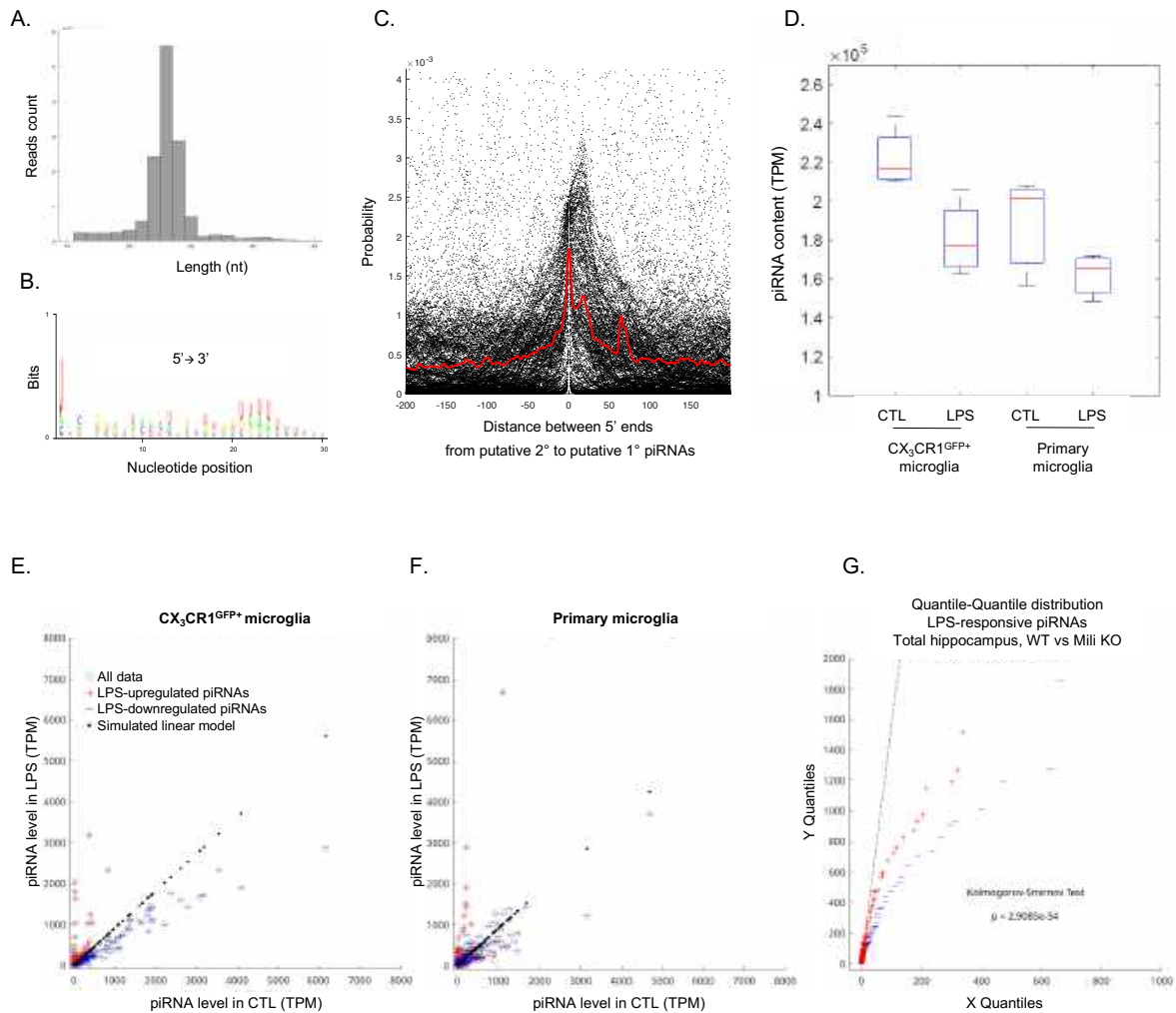


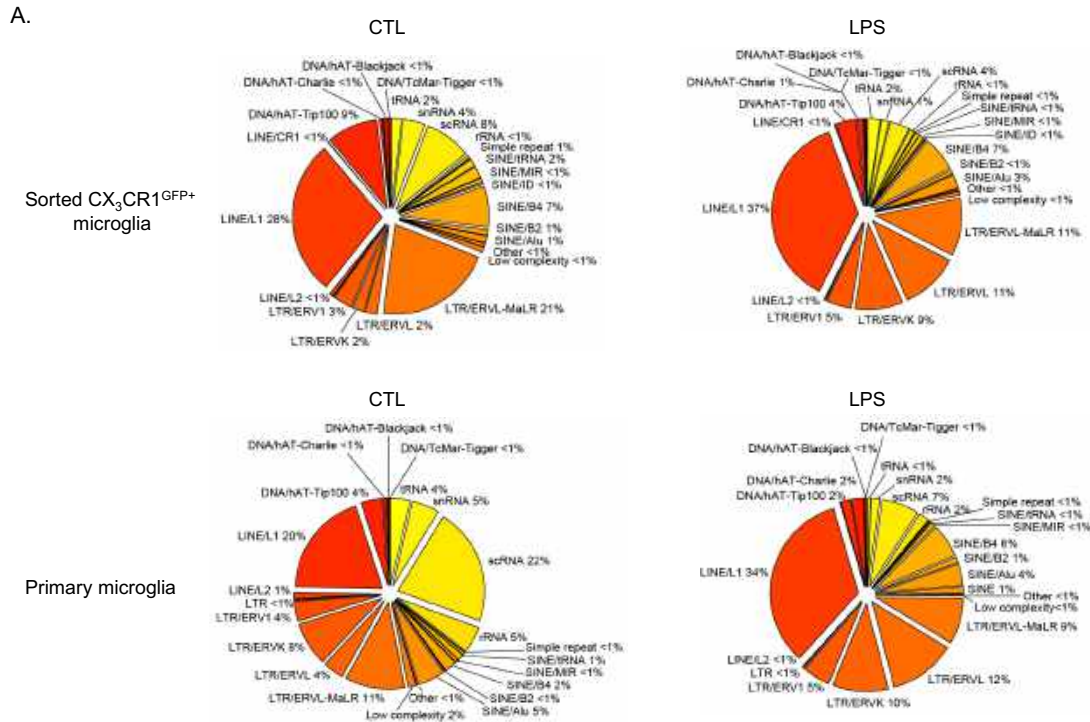
Figure 17: Acute inflammation alters the expression of (Mili-dependent) piRNAs in murine microglia. (A) Size distribution of the piRNA reads showing (B) Uridine bias at piRNA 5' ends and (C) probability of distances from the 5' ends of putative secondary piRNAs to the 5' ends of putative primary piRNAs. Distance probability was assayed for unique piRNAs (length between 15–35 nucleotides), without taking into account abundance, by locally weighted smoothing linear regression (LOWESS). (D) Total piRNA content in transcript per kilobase in a million (TPM) normalisation for sorted (CX_3CR1^{GFP+}) and primary microglia, in saline-treated (CTL) or LPS-treated animals (LPS), and in primary saline-treated (CTL) or LPS-treated (LPS) cells. (E) LPS responder-piRNAs in sorted microglia are identified as outliers larger (LPS-upregulated, red plus), or smaller (LPS-downregulated, blue minus) than 3 standard deviations from the mean of a linear 20% noise identity model, based on the piRNA levels in control CX_3CR1^{GFP+} sorted cells. (F) Identification of the responder-piRNAs from sorted microglia in a primary microglia culture model demonstrates a similar response trend. (G) LPS responder-piRNA levels in WT (y-axis) versus Mili KO (x-axis) whole hippocampi from transgenic animals demonstrate that LPS-upregulated piRNA in sorted microglia exhibit a higher trend of expression in WT versus Mili KO hippocampi by the two-sample Kolmogorov-Smirnov test, p-value 2.909e-34.

Altogether, these results indicate that *bona fide* piRNAs are expressed in microglia, and acute inflammation alters the expression of specific piRNAs subsets. Moreover, the piRNAs that are upregulated in inflammation exhibit Mili-dependency. This suggests that the piRNA pathway is involved in microglial inflammatory responses. In fact, upon inflammation microglia exhibits profound phenotypic and molecular changes, in particular at the gene expression level. Thus, the concomitant change in the expression of piRNAs subpopulations, could reflect their involvement in regulating the molecular changes that characterize microglia inflammatory response.

3.3.7 *In silico* piRNAs' target prediction in microglia

In order to identify possible targets of microglial piRNAs in inflammation, an *in silico* prediction of the piRNAs' targets expressed in CTL and upon LPS treatment was performed. Considering the wide variety of possible piRNAs' targets [1], [11], [353], piRNAs were aligned to both non-coding repetitive elements and mRNAs. Notably, amongst the non-coding RNA targets, the more prominently represented are LINE1 elements, with piRNAs targeting LINE1 being more abundant in inflamed microglia (*Figure 18 A*). Given that dysregulation of LINE1 and TEs in general has been reported in inflammatory and neuropathological conditions [71], [354]–[356], the observed increase in piRNAs, which are known repressors of LINE1, likely reflects an attempt to restrain the expression and mobilization of LINE1 in response to its dysregulation. Next, I sought to identify putative protein coding targets of piRNAs in CTL and inflamed microglia. To explore which of the predicted coding targets might be involved in inflammation, Gene Ontology (GO) analysis on piRNAs' targets shared by CX₃CR1^{GFP+} sorted and primary microglia in control or upon LPS treatment was performed. Interestingly, several piRNAs' predicted targets are involved in biological processes related to inflammatory responses, such as chromatin organization, immune system processes, proliferation, and cell migration (*Figure 18 B*). These results reveal possible downstream effects of the piRNAs, leading to the regulation of microglial inflammation. However, this preliminary analysis will be substantiated by matching piRNAs' predicted targets to differential gene expression data from transcriptomics of CTL, inflamed and Mili KO microglia, and the most relevant predicted targets will be validated by qPCR analysis.

In conclusion, this evidence revealed the presence of piRNAs and PIWI proteins in microglia and their differential expression in inflammation, therefore substantiating a potential regulatory role of the piRNA pathway in microglia's inflammatory processes.



B.

| GO biological process | CTL | LPS |
|------------------------|---|--|
| Terms: | Predicted targets involved in biological process: | Predicted targets involved in biological process: |
| Immune system process | Nlrp3, March1, Adam10, Ank1, Dock2, Sp100, Fgg, Xrcc6 | Hdac9, Trim26, Nr1h4, Camk2a, Bach2, Jarid2, Cyp7b1, Ebag9, Eif2ak2, L3mbtl3, Rab3c, Mbp, Dclre1c, C8b |
| Chromatin organization | Rbbp4 | Hdac8, Hdac9, Jarid2, Myocd, Cgd2, Cdan1, Smyd3, Arid1a, L3mbtl3, Rere |
| Proliferation | Sema5a, Itgb3, Fgfr2, Rad51l1, Adam10, Pkp2, Xrcc6, Rxfp2 | Jarid2, Cyp7b1, Gpc3, Prkx, Dazap1, Foxp2, Kank1, Adk, Ifitd1, Rere, Cdh13, Sox5 |
| Cell migration | Sema5a, Itgb3, Dock2, Nrg3 | Arsb, Large, Cyp7b1, Gpc3, Fut10, MRTFA, Grif1, Kank1, Fat3, Prkci, Rere, Cdh13, Adams12, Ttbk2 |

Figure 18: In silico piRNAs' target prediction in microglia. (A) Pie plots showing proportions of repetitive elements that are predicted piRNAs' targets in untreated (CTL) or inflamed (LPS) CX₃CR1^{GFP+} sorted (top) and primary (bottom) microglia. (B) Table summarizing relevant GO biological process analysis results: representative biological processes involved in microglia inflammation (left) and predicted piRNAs' targets involved in the process (right), in control (CTL) or upon induction of inflammation (LPS) in both sorted and primary microglia.

4 Discussion

This thesis builds on our work that provides the first evidence of the functional involvement of the piRNA pathway in neurogenesis and neuroinflammation (Gasperini C, Tuntevski K, Beatini S, et al., 2023 - *see Appendix*). Specifically, Mili has been shown to support the neurogenic differentiation of aNPCs and modulate the reactivity of glial cells. The depletion of Mili results in the aberrant generation of reactive astrocytes and perturbs the expression of various inflammatory, reactive oxygen, and circadian-related genes - recognized hallmarks of an aged hippocampal niche [160], [357]–[359]. Most of these observations resulted from acute *in vivo* Mili KD. Here, by utilizing a published Mili constitutive KO mouse model, that has never been characterized in the brain, we validated some of our previous findings. Specifically, by analyzing hippocampi of Mili mutant mice (Mili KO, Mili HET) we could confirm the disturbance of hippocampal aNPCs proliferation in the absence of Mili. Furthermore, *in vitro* experiments revealed that differentiation of aNPCs with mutated Mili was impaired, leading to increased cellular death.

We are currently conducting experiments to further investigate these phenotypes and to comprehend their implications. To discern whether the constitutive mutation of Mili has repercussions on effective aNPCs' differentiation and fate choice, we are carrying out *in vivo* lineage tracing experiments in Mili mutant animals. In parallel, to dissect the molecular regulation of the neurogenic process, we are exploiting the *in vitro* model of aNPCs differentiation, in particular, performing comprehensive long and short RNA sequencing at different stages of differentiation. These approaches will enable us to investigate the consequences of Mili absence/depletion, specifically focusing on the disruption of hippocampal balance. A potential scenario is that the constitutive absence/depletion of Mili could result in the conversion of aNPCs into reactive astrocytes, similar to that observed in acute Mili KD. Interestingly, aNPCs reduction through conversion in reactive astrocytes has been suggested to explain the age-related decline in adult neurogenesis, which is further accelerated by conditions such as epilepsy and neurodegeneration [114], [115], [193], [360]. Therefore, it is also conceivable that Mili mutant animals might exhibit an accelerated aging phenotype. To investigate this, we plan to characterize *in vivo* neurogenic processes in aged mice.

A key feature of the aging brain and age-related neurodegenerative disorders is the occurrence of gliosis. [208]. The heightened reactivity of astrocytes in this context triggers an inflammatory state, leading to a loss of their supportive functions to neurons which, as a

consequence, become vulnerable to hypo-metabolic states, excitotoxicity, and oxidative stress [358], [361]. Reactive microglia play a vital role in inflammaging, sustaining persistent sterile neuroinflammation and elevating the levels of Reactive Oxygen Species (ROS) and Reactive Nitrogen Species (RNS). Indeed, the oxidative stress theory of aging proposes that age-related functional declines result from the accumulation of damage induced by Reactive Oxygen and Nitrogen Species (RONS) [362]–[364].

As related to neuroinflammation, our research revealed that depletion of Mili in the postnatal hippocampus leads to astrocyte reactivity (Gasperini C, Tuntevski K, Beatini S, et al., 2023 - *see Appendix*). Here, we further extended this observation by showing that Mili KD leads to microgliosis. Moreover, investigating the presence and potential role of the piRNA pathway in microglia, we uncovered that PIWI proteins and piRNAs are indeed present in these cells. Strikingly, we observed that microglial Mili (Piwil2) and piRNAs were responsive to both acute (LPS-induced) and chronic (inflammaging) inflammation. Of note, the microglial piRNAs subset that we identified to be upregulated upon inflammation appears to be depleted in Mili KO animals, suggesting that Mili is necessary for the induction of certain piRNAs in response to inflammation. Our observations extended to human microglial cells, indicating a conserved response of Piwil2 to inflammation. Moreover, our preliminary data indicate that microglial inflammation-responsive piRNAs are predicted to target, and therefore potentially regulate, several gene transcripts involved in inflammatory processes. This evidence suggests a possible broader function for the piRNA pathway as a guardian of brain homeostasis.

The crucial open question is whether the piRNA pathway responsiveness to inflammation underlies possible pro- or anti-inflammatory functions in the regulation of microglial responses. To answer this question, we are employing Mili mutant mice to investigate the impact of Mili absence/depletion, in terms of microglial responses and neuroinflammation, comparing physiological and inflammatory contexts through small and long RNA-seq analyses, histological examinations and at the protein level. Given the constitutive nature of Mili absence/depletion, potential impairments in homeostatic conditions might not be clearly evident due to compensatory mechanisms occurring during development. However, by stressing the system with paradigms known to induce neuroinflammation, we expect to see some alterations in microglial inflammatory responses if the piRNA pathway is involved in the control of this process.

We are also studying the response of the piRNA pathway at different time points upon the induction of neuroinflammation to explore the dynamics of Mili and piRNAs increase.

Considering the evidence at hand, one potential scenario is that the piRNA pathway, observed to respond 24-48 hours post-inflammatory stimulus, might function as a downstream regulator of the inflammatory process. However, Mili and piRNAs might be altered already few hours after the stimulation, thus suggesting a potential involvement in the upstream regulation of inflammatory genes and responses. In that case, it would be particularly intriguing to explore the signals that induce and activate the piRNA pathway response. While master transcription factors such as A-MYB govern piRNAs and PIWI production in the gonads [365], the players and mechanisms that activate their production in the brain are currently unknown.

The primary focus of our ongoing investigations is on the piRNA pathway functions and targets that could be relevant for identifying novel therapeutic strategies for age-related diseases, such as neuroinflammatory and neurodegenerative pathologies. Our data indicate that among the predicted targets of inflammation-responsive piRNAs there are several genes involved in DNA repair, and chromatin accessibility. Moreover, microglial piRNAs selectively target multiple TEs, with LINE1 being the most prominent among them, and the abundance of piRNAs directed against it increasing in inflammatory conditions. This is interesting because an important aspect of aging is its direct connection to DNA damage, which is often caused by uncontrolled movement of TEs. Indeed, TEs dysregulation is involved in aging, neuroinflammation, and neurodegeneration [71], [354]–[356], [366]. Notably, the piRNA pathway can be regarded as a widespread strategy employed by most animals to efficiently suppress transposition [95]. In the absence of a functional piRNA pathway, aging somatic cells tend to undergo a gradual loss of heterochromatin, a critical element responsible for maintaining the transcriptional repression of TEs [367], [368].

Another point to be addressed is how TEs might be regulated by the piRNA pathway in our system—whether this occurs transcriptionally or post-transcriptionally. PIWI proteins and piRNAs, indeed, regulate targets at both transcriptional and post-transcriptional levels. However, these mechanisms are highly intricate, varying based on the cell type, specific Piwi proteins involved, effectors, and their subcellular localization. Furthermore, they do not necessarily require piRNAs or cleavage-competent PIWI proteins [11], [353]. A key unresolved question in this study revolves around whether the functions of Mili in the brain are orchestrated through piRNAs. Further exploration is needed to determine whether the neurogenic functions of Mili and those potentially involved in inflammatory responses are piRNA-mediated.

In this study, we report a role for the piRNA pathway in the maintenance of proper neurogenesis and, therefore, brain plasticity. Existing evidence links piRNA pathway alterations to learning and memory impairments [64], [65]. In this context we are performing behavioral experiments on Mili mutant mice to characterize how the piRNA pathway mediated regulation of neurogenesis, and possibly neuroinflammation, impacts cognitive functions. Other future explorations include longitudinal investigations in Mili conditional KO mice, incorporating Lox-P sites to selectively restrict Mili deletion to distinct brain subpopulations. This would enable a more detailed characterization of the piRNA pathway regulatory role in individual brain cell populations and in their crosstalk. This experiment would be particularly relevant in our system to clarify aspects such as the apparent inconsistency observed within aNPCs and microglia, wherein inflammatory contexts correlate with a lower or higher expression of Mili, respectively.

Regarding the translational significance of our findings, it is crucial to note that the piRNA pathway has been linked to various CNS disorders [2], [369]. Understanding its role in CNS physiology and pathology could lead to the use of piRNAs as diagnostic markers, therapeutic targets, or even as potential drugs. Of interest, piRNAs have been previously proposed as biomarkers, in combination with miRNAs, to detect Alzheimer's disease [80]. For the same purpose of identifying possible piRNAs signatures of neurological pathologies, in our laboratory we are conducting RNA sequencing studies to examine the piRNAs repertoire in various neurodegenerative and neuroinflammatory conditions. Another intriguing avenue could be utilizing the piRNA pathway itself as a drug or therapeutic strategy. Indeed, a recent study suggested that the piRNA pathway could be harnessed as part of the RNA vaccine strategy. Ikhlas and colleagues showed that exposure to viral RNA fragments of SARS-CoV-2 can stimulate NSCs to produce extracellular vesicles and microvesicles containing piRNAs targeted against the exogenous viral RNA [370]–[372].

In conclusion, the work presented in this thesis provides an initial characterization of the role of the piRNA pathway in maintaining brain homeostasis. Understanding the regulatory influence of the piRNA pathway on both neuroinflammation and neurogenesis paves the way to elucidate the functions and potential applications of these small RNAs in conditions associated with CNS dysregulation. This includes neurodegenerative diseases and age-related pathologies, contributing to the promotion of successful brain aging. Nonetheless, further investigations are necessary to elucidate the precise molecular mechanisms and downstream effectors through which the piRNA pathway exerts its influence.

5 Procedures and References

5.1 Experimental procedures

5.1.1 Experimental mice

Experimental mice C57BL6, CX₃CR1^{GFP} mice [348], and Mili null mice [343] were housed at Istituto Italiano di Tecnologia (IIT). All animal procedures were approved by the IIT animal use committee and the Italian Ministry of health and conducted in accordance with the Guide for the Care and Use of Laboratory Animals of the European Community Council Directives. All mice were group-housed under a 12-h light–dark cycle in a temperature and humidity-controlled environment with ad libitum access to food and water.

5.1.2 Primary aNPCs isolation and culture

Hippocampal NPCs were prepared and expanded as described previously [344], [347]. Briefly, DG was isolated from 8-10 C57BL6 mice at the age of 6-8 weeks. After dissection in Hanks Balanced Salt Solution (Hank's Balanced Salt Solution -HBSS, Gibco) medium, the tissue was enzymatically dissociated with papain (2.5 U/ml), dispase (2.5 U/ml) and DNase I (250 U/ml) for 20 min at 37°C. During incubation, the tissue was repeatedly triturated with a fire polished Pasteur pipette. The cell suspension was centrifuged at 130 g for 5 min and the pellet was re-suspended in buffer solution (1x HBSS, 30mM Glucose, 2mM HEPES pH 7.4, 26mM NaHCO₃) followed by a centrifugation at 130 g for 5 min. aNSCs were isolated using 22 % Percoll gradient solution. After further centrifugation for 5 min at 130 g the cell pellet was re-suspended in 2 ml of culture medium containing Neurobasal (Invitrogen), Glutamax (Invitrogen), 1% penicillin and streptomycin (Invitrogen), B27 without retinoic acid (Invitrogen), FGF (20 ng/ml; PeproTech) and EGF (20 ng/ml; PeproTech). The dissociated DG tissue was plated into PDL/Laminin (Sigma/Roche) coated wells and incubated at 37°C with 5% CO₂. To further remove excess debris, the growth medium was exchanged 24 hours later. Every 2 days half of the growth medium was exchanged with fresh medium to replenish the growth factors. aNSCs were passaged once they reached 80 % confluence. induction of spontaneous differentiation by growth factor removal was done as previously described [344], [347].

5.1.3 Primary microglia isolation and culture

Primary microglia were prepared and expanded as described previously [373].

In brief, forebrain was isolated from P0-P2 C57BL6 mice. After dissection and removal of meninges in cold Hanks Balanced Salt Solution (HBSS, Gibco) medium, the tissue was enzymatically dissociated with 1mg/ml of DNase I 0.05% (Sigma) in Trypsin without EDTA 0.25% (Gibco), for 30 min at 37°C. Following incubation, the digestion was stopped adding 10% FBS (Sigma) supplemented culture media. Then, the tissue was repeatedly mechanically triturated with a fire polished Pasteur pipette, followed by filtering through 40µm filters.

The obtained cell suspension was centrifuged at 1300 rcf for 10 min and the pellet was resuspended in culture medium, consisting of DMEM(1x) + GlutaMAX™-I (Gibco), supplemented with 10% FBS (Sigma) and 1% penicillin and streptomycin (Invitrogen). The dissociated tissue was plated into PDL (Sigma) coated flasks and incubated at 37°C with 5% CO₂. To further remove excess debris, the growth medium was exchanged 24 hours later. Every 4 days half of the growth medium was exchanged with fresh medium. After 1-2 weeks microglia were detached with the shaking method and seeded for experiments in PDL coated wells.

5.1.4 Human microglial cell line HMC3 culture

Human HMC3 microglia were cultured, according to ATCC instructions, in complete medium consisting of EMEM (ATCC® 30- 2003™) supplemented with 10% FBS (Sigma) and 1% penicillin and streptomycin (Invitrogen). Cells were cultured in plastic flasks incubated at 37°C with 5% CO₂. Every 2 days the growth medium was exchanged with fresh medium, and HMC3 cells were passaged 1:5 to 1:8 once they reached 90 % confluence.

5.1.5 GapmeR injection

GapmeRs injection was done as previously published [344], briefly, 8 weeks-old WT C57BL6 mice were anesthetized with isoflurane and 1.5 µl of 50 µM antisense GapmeR targeting Mili or negative control (custom design probes, MILI 339512, Control 339516, Qiagen), were stereotaxically injected in the dentate gyrus. Bilateral injection of Control GapmeR in the left hemisphere and Mili KD GapmeR in the right hemisphere allowed the analysis of the phenotypes within the same brain. To assess the GapmeRs uptake and the efficacy of Mili KD, the first group of mice (n = 3 for each GapmeR) was sacrificed 48 h after the injection and the

DG and tissue processed for RNA or protein extraction. Animals were sacrificed 30 days after GapmeRs injection (n = 4 for each oligo) and tissue processed for histological analysis [344]. GapmeR sequences 5'-3': CTL AACACGTCTATACGC, GapmeR1 GAGTGCAGTGAAGTTG.

5.1.6 BrdU and LPS treatments

To labeled proliferating cells in the postnatal hippocampus, 11 weeks old mice received 3 i.p. injections, with 2 hours intervals, of 100mg/kg BrdU diluted in phosphate-buffered saline (PBS), as previously described [344]. Mice were sacrificed 24h after the first BrdU injection and brains processed for further analysis. To label proliferating aNPCs *in vitro*, 10 mM BrdU was added to the culture medium for 48 h, followed by fixation (4 % PFA).

To induce inflammation, p20-p30 CX₃CR1^{GFP} mice received a single i.p. injection of phosphate-buffered saline (PBS; vehicle) or 5 mg/kg bacterial lipopolysaccharide (Escherichia coli 055:B5 LPS; Sigma) [300] and were sacrificed 48 h after the injection. Brains were then processed for microglia isolation.

To induce microglial cells inflammation *in vitro* the growth medium was exchanged with fresh medium, for control condition, or with culture medium containing 0.1 or 0.01 µg/ml of LPS diluted in PBS. Cells were then pelleted after 24h for RNA extraction, or 48h for protein extraction.

5.1.7 Fluorescence-Activated Cell Sorting (FACS) for microglia isolation

CX₃CR1^{GFP} mice were injected with LPS, as described above. CX₃CR1^{GFP+} Brains were dissociated to obtain a single-cell suspension using the Adult Brain Dissociation kit (Miltenyi Biotec), according to the manufacturer's protocol. GFP+ cells were sorted using a FACS Aria III system (BD). Cell duplets were removed based on forward and side scatters, and viable cells were selected based on PI negativity. GFP-positive (corrected for autofluorescence) cells were sorted and collected in PBS. Trizol LS (Thermo Scientific) was added and after resuspension samples were snap-frozen and stored at -20°C. Microglia isolation from adult (12-24 weeks old) and old (96-97 weeks old) WT animals was achieved by performing immunostaining on the single cell suspension obtained from brain dissociation, to allow FACS isolation. Briefly, the cell suspension was incubated for 15' with CD16/32 blocking antibody (BioLegend) followed by 30' incubation in the dark with primary fluorophore-conjugated antibodies against CD45 (CD45-APC, Biolegend) and CD11b (CD11b-PE, Invitrogen). Cells

double positive for PE (high intensity) and APC (medium intensity) were sorted [352]. Primary antibodies are listed in the Table 2.

5.1.8 Histology Immunofluorescence and Imaging

Mice were anesthetized and perfused transcardially with cold 4% paraformaldehyde in 1X PBS. Brains were removed and post-fixed in the same fixative for 24 hours at 4°C. Tissues were washed several times in 1X PBS prior to dehydration with 30% sucrose in 1X PBS, overnight (or until they sink) at 4°C and carefully dried before snap-freezing.

40 µm thick brain sections were generated using a sliding microtome and were stored in a -20°C freezer as floating sections in 48 well plates filled with cryoprotectant solution (glycerol, ethylene glycol, and 0.2 M phosphate buffer, pH 7.4, 1:1:2 by volume).

Immunofluorescence staining on brain slices:

After extensive washings with 0.1M PBS, sections were permeabilized with 0.3% PBS-T (PBS-Triton X-100) for 10 min followed with 20 min with 0.1% PBS-T. To detect Ki67 immunostaining, citrate buffer 10 mM pH = 6 treatment during 10 min at 95 °C was used. Pre-treatment with 2N HCL at 30,2°C for 20 min was used to detect BrdU incorporation. Sections were blocked during 1 h with 0.1% PBS-T and 5% normal goat serum (Vector laboratories), at room temperature (RT) followed by incubation with primary antibodies in blocking solution overnight at 4°C. The next day, after washing extensively with 0.1% PBS-T, sections were incubated for 2 h with the corresponding secondary fluorescent antibodies, diluted 1:1000 (Goat Alexa 488, 568, and 647 nm, Invitrogen) at room temperature. Sections were counterstained with Hoechst (1:300), mounted and cover slipped with Vectashield reagent (VECTOR Labs).

Immunofluorescence staining on cell cultures:

After fixing aNPCs for 15 min with 4% paraformaldehyde (PFA) followed by extensive washings with PBS, cells were washed three times with PBS 0,1% Triton X-100 (PBS-T) and blocked during 1 h with PBS-T containing 5% Normal Goat Serum (NGS) (Vector laboratories), followed by overnight incubation at 4°C with primary antibodies. The next day, after washing extensively with PBS-T, cells were incubated 2h at room temperature with secondary antibodies. Cells were mounted in mounting medium and counterstained with fluorescent nuclear dye DAPI (Invitrogen). Images were obtained using the microscope Confocal A1 Nikon Inverted SFC with 10x and 20× objectives (Nikon Instruments, Yokohama, Japan), and quantification was performed using a Cell-counter plugin in Fiji. For the

quantification analysis, five fields were analyzed from each coverslip, and the mean of the measures was used for that experimental replica.

Iba1 intensity fluorescence analysis:

Iba1 intensity fluorescence analysis was performed on fluorescence microscopy images acquired by the Confocal A1 Nikon Inverted SFC with 20× objective (Nikon Instruments), with the same parameters for all the sections. Quantification of fluorescence intensity was performed using ImageJ measuring the integrated density of a region of interest (ROI) corresponding to GCL and hilus. Fold change in fluorescence intensity, normalized to ROI area, of Mili KD compared with control one has been plotted in the graph.

Stereological sampling for the quantification of BrdU positive cells in adult mouse hippocampus (GCL of DG):

Mouse hippocampal brain slices of 40 µm were cut with a sliding microtome and collected as free-floating sections in plates' wells filled with cryoprotectant solution. Coronal sections starting from bregma -1.40 were moved in separate 48 wells plates. Following immunostaining for BrdU, a stereological sampling for the quantification of BrdU positive cells in adult mouse hippocampus (GCL of DG) was performed. First sampling: one in five sections (for a total of 12 slices) per animal were analyzed. Second sampling: 15 µm confocal stack images of brain slices were obtained with the Confocal A1 Nikon Inverted SFC with 10x objective. To obtain the number of positive cells in the volume a ROI of the DG area was drawn using the maximum projection of the Hoechst channel as a reference, and measured using FIJI software. The volume was calculated multiplying the ROI area for 15 µm (the stack sampled in the acquisition). BrdU positive cells in the granule cell layer of the DG (inclusion cut-off: 2 nuclei from granule cell layer) were counted. Counting was performed on the 2-channel image (Hoechst, BrdU), browsing along the Z axis to ensure the correct count of overlapping cells. For each animal, the value of total BrdU positive cell per DG volume was obtained as the average of the values of BrdU positive cells normalized to the DG volume, calculated per single acquisition. Cell quantification and analysis were performed using NIS-Elements software (Nikon) and Fiji (Fiji is just ImageJ).

Primary antibodies are listed in the Table 2.

5.1.9 Cytotoxicity assay in aNPCs

To monitor cytotoxicity upon induction of differentiation, aNPCs' culture medium was exchanged, 24h after cell seeding, with differentiation medium supplemented with 250nM CYTOTOX GREEN fluorescent reagent for IncuCyte® (Europa biosite). Green fluorescence

acquisition and cell confluence calculations were performed by IncuCyte® S3 (Essen Bioscience) software. The measured cytotoxicity index was defined as follow: green object count per image, divided per phase area confluence and normalized to time zero.

5.1.10 Protein extraction and Western Blot (WB)

For total protein extraction, adult testes or cell pellets were homogenized in RIPA buffer and the protein concentration was determined using a Bradford Assay kit (Bio-Rad). For blot analysis, equal amounts of protein (25 µg) were run on homemade 10% polyacrylamide gels and transferred on nitrocellulose membranes (GE Healthcare). Membranes were probed with the primary antibodies, followed by HRP-conjugated secondary antibody anti-rabbit or mouse (Invitrogen, A16104, A16072; 1:2,000). LAS 4000 Mini Imaging System (GE Healthcare) was used to digitally acquire chemiluminescence signals, and the band intensities were quantified using Fiji software. Primary antibodies are listed in the Table 2.

Table 2: List of primary antibodies

| Antibody | Host | Company | Catalog | Dilution |
|----------|------|---------------|----------------------|----------|
| MILI | Ms | Santa Cruz | sc-377347 | 1:100 |
| MILI | Ms | Santa Cruz | sc-377258 | 1:100 |
| HILI | Rb | Abcam | Ab85084 | 1:250 |
| MOV10 | Rb | Abcam | ab80613 | 1:1000 |
| ACTIN | Rb | Sigma | A2066 | 1:5000 |
| IBA1 | Rb | Fujifilm Wako | 019-19741 | 1:1000 |
| NESTIN | Ms | BD Pharmingen | 556309 | 1:250 |
| BrdU | Rat | Abcam | ab6326 | 1:75 |
| Ki67 | Rb | Abcam | ab15580 | 1:250 |
| CD16/32 | Rat | BioLegend | 101320 TruStain FcX™ | |
| CD45-APC | Rat | BioLegend | 103112 | |
| CD11b-PE | Rat | Invitrogen | 12-0112-82 | |

5.1.11 RNA extraction and real-time qPCR

Total RNA was extracted from primary microglia, HMC3 cells, microglia sorted from C57BL6 and CX₃CR1^{GFP} mice, and DG dissected from adult C57BL6 mice with QIAzol protocol (Qiagen) according to the manufacturer's instructions. One microgram of total RNA was treated with DNase I (Sigma) and cDNA was synthesized using ImProm-II reverse transcriptase (Promega). Real-time qPCR was performed in a duplex with Actin or Hprt as a reference gene,

with QuantiFast SYBR Green PCR Kit (Qiagen) on ABI-7500 Real-Time PCR System (Applied Biosystems). Expression levels were determined relative to Actin, using the delta-delta Ct method. Primers were designed using NCBI/UCSC Genome Browser and Primer3 software tools and then checked in PrimerBLAST for their specificity to amplify the desired genes. Oligonucleotide sequences are listed in the Table 3.

Table 3: List of primers

| Primer name | Sequence (5'-3') |
|--------------------|---------------------------|
| Actin Fw | GGCTGTATTCCCCTCCATCG |
| Actin Rv | CCAGTTGGTAACAATGCCATGT |
| Hprt Fw | CTCATGGACTGATTATGGACAGGAC |
| Hprt Rv | GCAGGTCAGCAAAGAACTTATAGCC |
| Mili Fw | GGCCAGCATAAATCTCACAC |
| Mili Rv | TAGCTGGCCATCAGACACTC |
| Miwi Fw | TAATTGGCCTGGAGTCATCC |
| Miwi Rv | GAGGTAGTAGAGGGCGGTTGG |
| Miwi2 Fw | TGACCTAAATCAGCCAGTGC |
| Miwi2 Rv | GCTCAGGCCTGTGAGAAAG |
| Mov10 Fw | GAGGTTTCGAGAGTTTTCTG |
| Mov10 Rv | GCGATCTTCATTCCATACAGCAT |
| TNF α Fw | CCCTCACACTCAGATCATCTTCT |
| TNF α Rv | GCTACGACGTGGGCTACAG |
| IL1 β Fw | GAAATGCCACCTTTTGACAGTG |
| IL1 β Rv | TGGATGCTCTCATCAGGACAG |
| Hili Fw | ATTCGAGGCCCGGCGCCGCG |
| Hili Rv | GAGACAGAGTCTTGCTTTGT |
| Hiwi Fw | TTACTGGGCGTATGGCGTAC |
| Hiwi Rv | CAAATAAGGTGACAATCACA |
| Hiwi2 Fw | GTGCTCGCGCCAACCCCTAC |
| Hiwi2 Rv | GATGTTCTGAACTTTATTTT |
| Piwil3 Fw | GGATCAGCTACAACCCAGGAG |
| Piwil3 Rv | GTTCCCTTACCCCTTGAGACT |
| Hs TNF α Fw | GAGGCCAAGCCCTGGTATG |
| Hs TNF α Rv | CGGGCCGATTGATCTCAGC |
| Hs actin Fw | TCACCCACACTGTGCCATCTACG |
| Hs actin Rv | CAGCGGAACCGCTCATTGCCAATG |

5.1.12 PCR-based genotyping

Mice DNA was extracted from tail, testes, hippocampi, and cortices biopsies with Phire direct kit (F170L, Thermo Fisher) following the manufacturer's instructions, and amplified on a DNA engine dyad peltier thermal cycler (Bio-Rad). A 3-step PCR protocol (98°C

for 1 min, then 35 cycles of 98°C for 5 sec, 58°C for 5 sec and 72°C for 20 sec, followed by 72°C for 1 min) was used. The following primers were used: Mili Fw GATTGAACCTTGTGCCTCGTA, Mili Rv 1 GGTACATGAGACCCTCAAAG, Mili Rv 2 GCAGGTGTGTGCAACCAGATA; amplicon size: 153 base pairs for WT allele and 200 base pairs for mutated Mili null allele. DNA was analyzed on a 2% agarose gel (AgaPure™ Agarose LE, Canvax) with ethidium bromide (Sigma-Aldrich).

5.1.13 Small RNA library preparation

For small RNA libraries preparation, the quantity and quality of the total RNA isolated from hippocampi, primary and sorted microglia were measured by Nanodrop spectrophotometer (Thermo Fisher) and Bioanalyzer RNA nano 6000 chips (Agilent). 1 µg in the case of cell pellets and hippocampi, or 200 ng in the case of sorted microglia, of high-quality RNA for each sample was used for library preparation according to the PerkinElmer NEXTFLEX Small RNA-seq v3 library protocol (PerkinElmer). Briefly, 3' adapters were ligated to 3' end of small RNAs using an RNA ligase enzyme followed by 5' adaptor ligation using an RNA ligase enzyme. Reverse transcription followed by PCR was used to prepare cDNA using primers specific for the 3' and 5' adapters. The amplification of those fragments having adapter molecules on both ends was carried out with 18 PCR cycles, to allow a gel free size selection according to the manufacturer's instructions. The quality of the library was assessed by the Bioanalyzer DNA chips (Agilent).

5.1.14 Small RNA sequencing and data processing

Small RNA sequencing data processing was done essentially as previously published [63]. PiRNA cluster analysis was performed as previously described (*see Appendix*), and with minor modifications in the initial small RNA sequence identification as reported elsewhere [374]. Small RNA reads into mature miRNA, hairpin-miRNA, isomiR-miRNA, mature tRNA, primary tRNA, snoRNA, rRNA and mRNA fragments, and non-coding RNAs by expanding the NCBI release 67 (mm9) ncRNA database [375], [376] with the current version of piRbase 2.0 [8], [377] and supplementarily, potential piRNA reads mapping to other immature non-coding RNAs were removed from further analysis. All these potential piRNA sequences were aligned against the mm9 version of the mouse genome, with a maximum of 2 mismatches, and 10,000 permissible alignments. The alignments were analysed for continuity of at least 35 nucleotide gaps with the mergeBed tool, after which 1,319,609 potential clusters were identified. piRNA

reads, normalised in TPM, were assigned to each cluster irrespectively of directionality, to obtain cluster expression, and cluster expression was normalised to the length of the cluster. The top 1st percentile of clusters per condition (in TPM/nt) was selected as the representative cluster repertoire of each treatment group. In order to assess the clustering behavior of putative piRNAs, the 5' termini positions of each cluster-associated putative primary and putative secondary piRNA sequences were analyzed for distance, represented as probability, within a range of 200 nucleotides in the 5' direction and 200 nucleotides in the 3' direction of the putative primary piRNAs, as reported previously [20]. The positional distance between piRNAs for each cluster was sampled iteratively for each assigned piRNA and normalized by the total number of diverse piRNAs associated with each cluster. The distance probability distribution was assayed by the locally weighted smoothing linear regression method (LOWESS), by using the built-in MATLAB "fit" function (MathWorks, Natick, MA), with a span value of 0.1. For the two cell model (sorted and primary microglia), and the two treatment groups (control and LPS), a unique union repertoire of 320 clusters were identified that accounted for the majority of piRNA expression in 622,360 unique piRNA sequences. Supplementarily, these sequences were identified for their multiple mapping on coding, as well as non-coding genes, and a targetomic profile for all the known ENSEMBL RNA transcripts for the mm9 genome was established across all conditions.

5.1.15 Quantification and statistical analysis

Data are presented as mean \pm SEM in figure 11A, for better visual representation, and as mean \pm SD in all the other figures. Data were analyzed using Prism 9 (GraphPad). Statistical significance was assessed with a two-tailed unpaired Student's t-test for two experimental groups. For experiments with three or more groups, one-way ANOVA with the Bonferroni's multiple comparison test was used. For experiments with three groups and two variables (group, time) two-way ANOVA with the Bonferroni's multiple comparison test was used. Two-sample Kolmogorov-Smirnov test was used to compare piRNAs distributions. Results were considered significant when $P < 0.05$. The number of samples (N) in each group is reported in the figure legend.

5.2 References

- [1] X. Wang, A. Ramat, M. Simonelig, and M. F. Liu, “Emerging roles and functional mechanisms of PIWI-interacting RNAs,” *Nat. Rev. Mol. Cell Biol.* 2022 242, vol. 24, no. 2, pp. 123–141, Sep. 2022, doi: 10.1038/s41580-022-00528-0.
- [2] K. T. Wakisaka and Y. Imai, “The dawn of piRNA research in various neuronal disorders,” *Front. Biosci. (Landmark Ed.)*, vol. 24, pp. 1440–1451, 2019, Accessed: Nov. 14, 2019. [Online]. Available: <http://www.ncbi.nlm.nih.gov/pubmed/31136989>.
- [3] B. P. U. Perera *et al.*, “Somatic expression of piRNA and associated machinery in the mouse identifies short, tissue-specific piRNA,” *Epigenetics*, vol. 14, no. 5, pp. 504–521, May 2019, doi: 10.1080/15592294.2019.1600389.
- [4] Y. Ghosheh *et al.*, “Characterization of piRNAs across postnatal development in mouse brain,” *Sci. Rep.*, vol. 6, Apr. 2016, doi: 10.1038/srep25039.
- [5] C. Gasperini *et al.*, “Piwil2 (Mili) sustains neurogenesis and prevents cellular senescence in the postnatal hippocampus,” *EMBO Rep.*, vol. 24, no. 2, p. e53801, Feb. 2023, doi: 10.15252/EMBR.202153801.
- [6] J. Wang *et al.*, “piRBase: integrating piRNA annotation in all aspects,” *Nucleic Acids Res.*, vol. 50, no. D1, pp. D265–D272, Jan. 2022, doi: 10.1093/NAR/GKAB1012.
- [7] D. Stoyko, P. Genzor, and A. D. Haase, “Hierarchical length and sequence preferences establish a single major piRNA 3'-end,” *iScience*, vol. 25, no. 6, p. 104427, Jun. 2022, doi: 10.1016/J.ISCI.2022.104427.
- [8] J. Wang *et al.*, “piRBase: a comprehensive database of piRNA sequences,” *Nucleic Acids Res.*, vol. 47, no. D1, pp. D175–D180, Jan. 2019, doi: 10.1093/NAR/GKY1043.
- [9] A. A. Aravin, N. M. Naumova, A. V. Tulin, V. V. Vagin, Y. M. Rozovsky, and V. A. Gvozdev, “Double-stranded RNA-mediated silencing of genomic tandem repeats and transposable elements in the *D. melanogaster* germline,” *Curr. Biol.*, vol. 11, no. 13, pp. 1017–1027, Jul. 2001, doi: 10.1016/S0960-9822(01)00299-8.
- [10] A. A. Aravin *et al.*, “The Small RNA Profile during *Drosophila melanogaster* Development,” *Dev. Cell*, vol. 5, no. 2, pp. 337–350, Aug. 2003, doi: 10.1016/S1534-5807(03)00228-4.
- [11] D. M. Ozata, I. Gainetdinov, A. Zoch, D. O’Carroll, and P. D. Zamore, “PIWI-interacting RNAs: small RNAs with big functions,” *Nature Reviews Genetics*, vol. 20, no. 2.

- Nature Publishing Group, pp. 89–108, Feb. 01, 2019, doi: 10.1038/s41576-018-0073-3.
- [12] B. Czech *et al.*, “piRNA-Guided Genome Defense: From Biogenesis to Silencing,” *Annu. Rev. Genet.*, vol. 52, no. 1, pp. 131–157, 2018, doi: 10.1146/annurev-genet-120417-031441.
- [13] Y. W. Iwasaki, M. C. Siomi, and H. Siomi, “PIWI-Interacting RNA: Its Biogenesis and Functions,” *Annu. Rev. Biochem.*, vol. 84, no. 1, pp. 405–433, Jun. 2015, doi: 10.1146/annurev-biochem-060614-034258.
- [14] M. C. Siomi, K. Sato, D. Pezic, and A. A. Aravin, “PIWI-interacting small RNAs: The vanguard of genome defence,” *Nat. Rev. Mol. Cell Biol.*, vol. 12, no. 4, pp. 246–258, 2011, doi: 10.1038/nrm3089.
- [15] N. C. Lau *et al.*, “Characterization of the piRNA complex from rat testes,” *Science (80-.)*, vol. 313, no. 5785, pp. 363–367, Jul. 2006, doi: 10.1126/SCIENCE.1130164/SUPPL_FILE/LAU_SOM.PDF.
- [16] S. T. Grivna, E. Beyret, Z. Wang, and H. Lin, “A novel class of small RNAs in mouse spermatogenic cells,” *Genes Dev.*, vol. 20, no. 13, pp. 1709–1714, 2006, doi: 10.1101/gad.1434406.
- [17] A. Girard, R. Sachidanandam, G. J. Hannon, and M. A. Carmell, “A germline-specific class of small RNAs binds mammalian Piwi proteins,” *Nat. 2006 4427099*, vol. 442, no. 7099, pp. 199–202, Jun. 2006, doi: 10.1038/nature04917.
- [18] A. Aravin *et al.*, “A novel class of small RNAs bind to MILI protein in mouse testes,” *Nature*, vol. 442, no. 7099, pp. 203–207, Jul. 2006, doi: 10.1038/nature04916.
- [19] V. V. Vagin, A. Sigova, C. Li, H. Seitz, V. Gvozdev, and P. D. Zamore, “A distinct small RNA pathway silences selfish genetic elements in the germline,” *Science (80-.)*, vol. 313, no. 5785, pp. 320–324, Jul. 2006, doi: 10.1126/SCIENCE.1129333/SUPPL_FILE/VAGIN.SOM.REVISED.PDF.
- [20] I. Gainetdinov, C. Colpan, A. Arif, K. Cecchini, and P. D. Zamore, “A Single Mechanism of Biogenesis, Initiated and Directed by PIWI Proteins, Explains piRNA Production in Most Animals,” *Mol. Cell*, vol. 71, no. 5, pp. 775-790.e5, Sep. 2018, doi: 10.1016/j.molcel.2018.08.007.
- [21] A. Grimson *et al.*, “Early origins and evolution of microRNAs and Piwi-interacting RNAs in animals,” *Nature*, vol. 455, no. 7217, pp. 1193–1197, Oct. 2008, doi: 10.1038/NATURE07415.

- [22] M. S. Kumar and C. Kevin, "Evolution of animal Piwi-interacting RNAs and prokaryotic CRISPRs," *Brief. Funct. Genomics*, vol. 11, no. 4, p. 277, Jul. 2012, doi: 10.1093/BFGP/ELS016.
- [23] S. H. Lewis *et al.*, "Pan-arthropod analysis reveals somatic piRNAs as an ancestral defence against transposable elements," *Nat. Ecol. Evol.*, vol. 2, no. 1, pp. 174–181, Jan. 2018, doi: 10.1038/S41559-017-0403-4.
- [24] C. Juliano, J. Wang, and H. Lin, "Uniting Germline and Stem Cells: The Function of Piwi Proteins and the piRNA Pathway in Diverse Organisms," *Annu. Rev. Genet.*, vol. 45, no. 1, pp. 447–469, 2011, doi: 10.1146/annurev-genet-110410-132541.
- [25] M. Ponnusamy, K. W. Yan, C. Y. Liu, P. F. Li, and K. Wang, "PIWI family emerging as a decisive factor of cell fate: An overview," *Eur. J. Cell Biol.*, vol. 96, no. 8, pp. 746–757, Dec. 2017, doi: 10.1016/J.EJCB.2017.09.004.
- [26] Y. H. Sun, B. Lee, · Xin, and Z. Li, "The birth of piRNAs: how mammalian piRNAs are produced, originated, and evolved," *Mamm. Genome*, vol. 33, pp. 293–311, 2022, doi: 10.1007/s00335-021-09927-8.
- [27] S. R. Mani and C. E. Juliano, "Untangling the web: the diverse functions of the PIWI/piRNA pathway," *Mol. Reprod. Dev.*, vol. 80, no. 8, pp. 632–664, Aug. 2013, doi: 10.1002/MRD.22195.
- [28] D. M. Özata *et al.*, "Evolutionarily conserved pachytene piRNA loci are highly divergent among modern humans," *Nat. Ecol. Evol. 2019 41*, vol. 4, no. 1, pp. 156–168, Dec. 2019, doi: 10.1038/s41559-019-1065-1.
- [29] E. Beyret, N. Liu, and H. Lin, "piRNA biogenesis during adult spermatogenesis in mice is independent of the ping-pong mechanism," *Cell Res. 2012 2210*, vol. 22, no. 10, pp. 1429–1439, Aug. 2012, doi: 10.1038/cr.2012.120.
- [30] M. A. Carmell, Z. Xuan, M. Q. Zhang, and G. J. Hannon, "The Argonaute family: tentacles that reach into RNAi, developmental control, stem cell maintenance, and tumorigenesis," 2002, doi: 10.1101/gad.1026102.
- [31] L. Peters and G. Meister, "Argonaute proteins: mediators of RNA silencing," *Mol. Cell*, vol. 26, no. 5, pp. 611–623, Jun. 2007, doi: 10.1016/J.MOLCEL.2007.05.001.
- [32] S. Yamaguchi *et al.*, "Crystal structure of Drosophila Piwi," *Nat. Commun.*, vol. 11, no. 1, Dec. 2020, doi: 10.1038/S41467-020-14687-1.
- [33] G. Hutvagner and M. J. Simard, "Argonaute proteins: key players in RNA silencing," *Nat. Rev. Mol. Cell Biol. 2008 91*, vol. 9, no. 1, pp. 22–32, Jan. 2008, doi:

- 10.1038/nrm2321.
- [34] T. Sasaki, A. Shiohama, S. Minoshima, and N. Shimizu, "Identification of eight members of the Argonaute family in the human genome," *Genomics*, vol. 82, no. 3, pp. 323–330, Sep. 2003, doi: 10.1016/S0888-7543(03)00129-0.
- [35] A. Vourekas *et al.*, "The RNA helicase MOV10L1 binds piRNA precursors to initiate piRNA processing," *Genes Dev.*, vol. 29, no. 6, p. 617, Mar. 2015, doi: 10.1101/GAD.254631.114.
- [36] N. Darricarrère, N. Liu, T. Watanabe, and H. Lin, "Function of Piwi, a nuclear Piwi/Argonaute protein, is independent of its slicer activity," *Proc. Natl. Acad. Sci. U. S. A.*, vol. 110, no. 4, pp. 1297–1302, Jan. 2013, doi: 10.1073/PNAS.1213283110/-/DCSUPPLEMENTAL.
- [37] J. Brennecke *et al.*, "Discrete small RNA-generating loci as master regulators of transposon activity in *Drosophila*," *Cell*, vol. 128, no. 6, pp. 1089–1103, Mar. 2007, doi: 10.1016/J.CELL.2007.01.043.
- [38] H. Siomi and M. C. Siomi, "Phased piRNAs tackle transposons," *Science*, vol. 348, no. 6236. American Association for the Advancement of Science, pp. 756–757, May 15, 2015, doi: 10.1126/science.aab3004.
- [39] F. Mohn, D. Handler, and J. Brennecke, "Noncoding RNA. piRNA-guided slicing specifies transcripts for Zucchini-dependent, phased piRNA biogenesis," *Science*, vol. 348, no. 6236, pp. 812–817, May 2015, doi: 10.1126/SCIENCE.AAA1039.
- [40] B. W. Han, W. Wang, C. Li, Z. Weng, and P. D. Zamore, "PiRNA-guided transposon cleavage initiates Zucchini-dependent, phased piRNA production," *Science (80-.)*, vol. 348, no. 6236, pp. 817–821, May 2015, doi: 10.1126/science.aaa1264.
- [41] Z. Yang *et al.*, "PIWI Slicing and EXD1 Drive Biogenesis of Nuclear piRNAs from Cytosolic Targets of the Mouse piRNA Pathway," *Mol. Cell*, vol. 61, no. 1, pp. 138–152, Jan. 2016, doi: 10.1016/j.molcel.2015.11.009.
- [42] H. Ishizu *et al.*, "Somatic Primary piRNA Biogenesis Driven by cis-Acting RNA Elements and trans-Acting Yb," *Cell Rep.*, vol. 12, no. 3, pp. 429–440, Jul. 2015, doi: 10.1016/J.CELREP.2015.06.035.
- [43] D. Homolka *et al.*, "PIWI Slicing and RNA Elements in Precursors Instruct Directional Primary piRNA Biogenesis," *Cell Rep.*, vol. 12, no. 3, pp. 418–428, Jul. 2015, doi: 10.1016/J.CELREP.2015.06.030.
- [44] Y. H. Sun *et al.*, "Ribosomes guide pachytene piRNA formation on long intergenic

- piRNA precursors," *Nat. Cell Biol.*, vol. 22, no. 2, pp. 200–212, Feb. 2020, doi: 10.1038/s41556-019-0457-4.
- [45] T. Watanabe and H. Lin, "Posttranscriptional regulation of gene expression by Piwi proteins and piRNAs," *Mol. Cell*, vol. 56, no. 1, pp. 18–27, 2014, doi: 10.1016/J.MOLCEL.2014.09.012.
- [46] E. Cora *et al.*, "The MID-PIWI module of Piwi proteins specifies nucleotide- and strand-biases of piRNAs," *RNA*, vol. 20, no. 6, pp. 773–781, 2014, doi: 10.1261/RNA.044701.114.
- [47] I. Gainetdinov *et al.*, "Terminal modification, sequence, length, and PIWI-protein identity determine piRNA stability," *Mol. Cell*, vol. 81, no. 23, pp. 4826–4842.e8, Dec. 2021, doi: 10.1016/J.MOLCEL.2021.09.012.
- [48] Y. Kirino and Z. Mourelatos, "Mouse Piwi-interacting RNAs are 2'-O-methylated at their 3' termini," *Nat. Struct. Mol. Biol.*, vol. 14, no. 4, pp. 347–348, Apr. 2007, doi: 10.1038/NSMB1218.
- [49] L. S. Gunawardane *et al.*, "A slicer-mediated mechanism for repeat-associated siRNA 5' end formation in *Drosophila*," *Science*, vol. 315, no. 5818, pp. 1587–1590, Mar. 2007, doi: 10.1126/SCIENCE.1140494.
- [50] A. A. Aravin *et al.*, "A piRNA Pathway Primed by Individual Transposons Is Linked to De Novo DNA Methylation in Mice," *Mol. Cell*, vol. 31, no. 6, pp. 785–799, Sep. 2008, doi: 10.1016/j.molcel.2008.09.003.
- [51] S. Kuramochi-Miyagawa *et al.*, "DNA methylation of retrotransposon genes is regulated by Piwi family members MILI and MIWI2 in murine fetal testes," *Genes Dev.*, vol. 22, no. 7, pp. 908–917, Apr. 2008, doi: 10.1101/gad.1640708.
- [52] B. Czech and G. J. Hannon, "One Loop to Rule Them All: The Ping-Pong Cycle and piRNA-Guided Silencing," *Trends in Biochemical Sciences*, vol. 41, no. 4. Elsevier Ltd, pp. 324–337, Apr. 01, 2016, doi: 10.1016/j.tibs.2015.12.008.
- [53] J. Zhang, S. Chen, and K. Liu, "Structural insights into piRNA biogenesis," *Biochim. Biophys. Acta - Gene Regul. Mech.*, vol. 1865, no. 2, p. 194799, Feb. 2022, doi: 10.1016/J.BBAGRM.2022.194799.
- [54] D. T. Ge, W. Wang, C. Tipping, I. Gainetdinov, Z. Weng, and P. D. Zamore, "The RNA-Binding ATPase, Armitage, Couples piRNA Amplification in Nuage to Phased piRNA Production on Mitochondria," *Mol. Cell*, vol. 74, no. 5, pp. 982–995.e6, Oct. 2019, doi: 10.1016/j.molcel.2019.04.006.

- [55] S. De Fazio *et al.*, “The endonuclease activity of Mili fuels piRNA amplification that silences LINE1 elements,” *Nature*, vol. 480, no. 7376, pp. 259–263, Dec. 2011, doi: 10.1038/NATURE10547.
- [56] M. Reuter *et al.*, “Miwi catalysis is required for piRNA amplification-independent LINE1 transposon silencing,” *Nature*, vol. 480, no. 7376, pp. 264–267, Dec. 2011, doi: 10.1038/NATURE10672.
- [57] T. A. Anzelon, S. Chowdhury, S. M. Hughes, Y. Xiao, G. C. Lander, and I. J. MacRae, “Structural basis for piRNA targeting,” *Nature*, vol. 597, no. 7875, pp. 285–289, Sep. 2021, doi: 10.1038/S41586-021-03856-X.
- [58] G. Sienski, D. Dönertas, and J. Brennecke, “Transcriptional silencing of transposons by Piwi and maelstrom and its impact on chromatin state and gene expression,” *Cell*, vol. 151, no. 5, pp. 964–980, Nov. 2012, doi: 10.1016/J.CELL.2012.10.040.
- [59] E. Z. Shen *et al.*, “Identification of piRNA Binding Sites Reveals the Argonaute Regulatory Landscape of the *C. elegans* Germline,” *Cell*, vol. 172, no. 5, pp. 937–951.e18, Feb. 2018, doi: 10.1016/J.CELL.2018.02.002.
- [60] E. J. Lee *et al.*, “Identification of piRNAs in the central nervous system,” *Rna*, vol. 17, no. 6, pp. 1090–1099, 2011, doi: 10.1261/rna.2565011.
- [61] A. Dharap, V. P. Nakka, and R. Vemuganti, “Altered expression of PIWI RNA in the rat brain after transient focal ischemia,” *Stroke*, vol. 42, no. 4, pp. 1105–1109, Apr. 2011, doi: 10.1161/STROKEAHA.110.598391.
- [62] P. P. Zhao *et al.*, “Novel function of PIWIL1 in neuronal polarization and migration via regulation of microtubule-associated proteins,” *Mol. Brain*, vol. 8, no. 1, Jun. 2015, doi: 10.1186/s13041-015-0131-0.
- [63] Y. Ghosheh *et al.*, “Characterization of piRNAs across postnatal development in mouse brain,” *Sci. Rep.*, vol. 6, pp. 1–7, 2016, doi: 10.1038/srep25039.
- [64] S. Nandi *et al.*, “Roles for small noncoding RNAs in silencing of retrotransposons in the mammalian brain,” *Proc. Natl. Acad. Sci. U. S. A.*, vol. 113, no. 45, pp. 12697–12707, Nov. 2016, doi: 10.1073/pnas.1609287113.
- [65] L. J. Leighton *et al.*, “Disrupting the hippocampal Piwi pathway enhances contextual fear memory in mice,” *Neurobiol. Learn. Mem.*, vol. 161, pp. 202–209, May 2019, doi: 10.1016/j.nlm.2019.04.002.
- [66] P. Rajasethupathy *et al.*, “A role for neuronal piRNAs in the epigenetic control of memory-related synaptic plasticity,” *Cell*, vol. 149, no. 3, pp. 693–707, Apr. 2012,

- doi: 10.1016/j.cell.2012.02.057.
- [67] M. C. N. Marchetto *et al.*, “Differential L1 regulation in pluripotent stem cells of humans and apes,” *Nature*, vol. 503, no. 7477, pp. 525–529, 2013, doi: 10.1038/NATURE12686.
- [68] A. R. Muotri, V. T. Chu, M. C. N. Marchetto, W. Deng, J. V Moran, and F. H. Gage, “Somatic mosaicism in neuronal precursor cells mediated by L1 retrotransposition,” *Nature*, vol. 435, no. 7044, pp. 903–10, Jun. 2005, doi: 10.1038/nature03663.
- [69] S. Bachiller, Y. Del-Pozo-Martín, and Á. M. Carrión, “L1 retrotransposition alters the hippocampal genomic landscape enabling memory formation,” *Brain. Behav. Immun.*, vol. 64, pp. 65–70, Aug. 2017, doi: 10.1016/j.bbi.2016.12.018.
- [70] J. K. Baillie *et al.*, “Somatic retrotransposition alters the genetic landscape of the human brain,” *Nature*, vol. 479, no. 7374, pp. 534–537, Nov. 2011, doi: 10.1038/nature10531.
- [71] F. Blaudin de Thé *et al.*, “Engrailed homeoprotein blocks degeneration in adult dopaminergic neurons through LINE-1 repression,” *EMBO J.*, vol. 37, no. 15, Aug. 2018, doi: 10.15252/embj.201797374.
- [72] W. Sun, H. Samimi, M. Gamez, H. Zare, and B. Frost, “Pathogenic tau-induced piRNA depletion promotes neuronal death through transposable element dysregulation in neurodegenerative tauopathies,” *Nat. Neurosci.*, vol. 21, no. 8, pp. 1038–1048, Aug. 2018, doi: 10.1038/s41593-018-0194-1.
- [73] M. Schulze *et al.*, “Sporadic Parkinson’s disease derived neuronal cells show disease-specific mRNA and small RNA signatures with abundant deregulation of piRNAs,” *Acta Neuropathol. Commun.*, vol. 6, no. 1, p. 58, Jul. 2018, doi: 10.1186/S40478-018-0561-X.
- [74] L. Zhan *et al.*, “Attenuation of Piwil2 induced by hypoxic postconditioning prevents cerebral ischemic injury by inhibiting CREB2 promoter methylation,” *Brain Pathol.*, vol. 33, no. 1, Jan. 2023, doi: 10.1111/BPA.13109.
- [75] F. A. Simoes *et al.*, “Potential of Non-Coding RNA as Biomarkers for Progressive Supranuclear Palsy,” *Int. J. Mol. Sci.*, vol. 23, no. 23, Dec. 2022, doi: 10.3390/IJMS232314554.
- [76] A. Saxena, D. Tang, and P. Carninci, “PiRNAs warrant investigation in Rett Syndrome: An omics perspective,” *Disease Markers*, vol. 33, no. 5. Hindawi Limited,

- pp. 261–275, 2012, doi: 10.3233/DMA-2012-0932.
- [77] I. Iossifov *et al.*, “The contribution of de novo coding mutations to autism spectrum disorder,” *Nature*, vol. 515, no. 7526, p. 216, Nov. 2014, doi: 10.1038/NATURE13908.
- [78] W. Qiu *et al.*, “Transcriptome-wide piRNA profiling in human brains of Alzheimer’s disease,” *Neurobiol. Aging*, vol. 57, pp. 170–177, Sep. 2017, doi: 10.1016/j.neurobiolaging.2017.05.020.
- [79] J. Roy, A. Sarkar, S. Parida, Z. Ghosh, and B. Mallick, “Small RNA sequencing revealed dysregulated piRNAs in Alzheimer’s disease and their probable role in pathogenesis,” *Mol. Biosyst.*, vol. 13, no. 3, pp. 565–576, 2017, doi: 10.1039/c6mb00699j.
- [80] G. Jain *et al.*, “A combined miRNA–piRNA signature to detect Alzheimer’s disease,” *Transl. Psychiatry*, vol. 9, no. 1, p. 250, Dec. 2019, doi: 10.1038/s41398-019-0579-2.
- [81] R. F. Abdelhamid *et al.*, “piRNA/PIWI Protein Complex as a Potential Biomarker in Sporadic Amyotrophic Lateral Sclerosis,” *Mol. Neurobiol.*, vol. 59, no. 3, pp. 1693–1705, Mar. 2022, doi: 10.1007/S12035-021-02686-2.
- [82] W. Reik, “Stability and flexibility of epigenetic gene regulation in mammalian development,” *Nature*, vol. 447, no. 7143, pp. 425–432, May 2007, doi: 10.1038/NATURE05918.
- [83] K. Sato, K. I. Takayama, and S. Inoue, “Role of piRNA biogenesis and its neuronal function in the development of neurodegenerative diseases,” *Front. Aging Neurosci.*, vol. 15, p. 1157818, May 2023, doi: 10.3389/FNAGI.2023.1157818/BIBTEX.
- [84] A. Penning *et al.*, “Adult Neural Stem Cell Regulation by Small Non-coding RNAs: Physiological Significance and Pathological Implications,” *Front. Cell. Neurosci.*, vol. 15, p. 548, Jan. 2022, doi: 10.3389/FNCEL.2021.781434/BIBTEX.
- [85] W. Zhang, D. Xiao, Q. Mao, and H. Xia, “Role of neuroinflammation in neurodegeneration development,” *Signal Transduct. Target. Ther.* 2023 81, vol. 8, no. 1, pp. 1–32, Jul. 2023, doi: 10.1038/s41392-023-01486-5.
- [86] L. Pleštilová *et al.*, “Expression and regulation of PIWIL-proteins and PIWI-interacting RNAs in rheumatoid arthritis,” *PLoS One*, vol. 11, no. 11, Nov. 2016, doi: 10.1371/journal.pone.0166920.

- [87] R. Ren, H. Tan, Z. Huang, Y. Wang, and B. Yang, "Differential expression and correlation of immunoregulation related piRNA in rheumatoid arthritis," *Front. Immunol.*, vol. 14, p. 1175924, May 2023, doi: 10.3389/FIMMU.2023.1175924/BIBTEX.
- [88] Y. Yao *et al.*, "The emerging role of the piRNA/PIWI complex in respiratory tract diseases," *Respir. Res.*, vol. 24, no. 1, p. 76, Dec. 2023, doi: 10.1186/S12931-023-02367-9.
- [89] G. A. Wasserman *et al.*, "Expression of Piwi protein MIWI2 defines a distinct population of multiciliated cells," *J. Clin. Invest.*, vol. 127, no. 10, pp. 3866–3876, Oct. 2017, doi: 10.1172/JCI94639.
- [90] K. Zhang *et al.*, "HILI Inhibits TGF- β Signaling by Interacting with Hsp90 and Promoting T β R Degradation," *PLoS One*, vol. 7, no. 7, p. e41973, Jul. 2012, doi: 10.1371/JOURNAL.PONE.0041973.
- [91] F. Zhong *et al.*, "A SnoRNA-derived piRNA interacts with human interleukin-4 pre-mRNA and induces its decay in nuclear exosomes," *Nucleic Acids Res.*, vol. 43, no. 21, pp. 10474–10491, 2015, doi: 10.1093/NAR/GKV954.
- [92] D. Ma *et al.*, "Changes in the Small Noncoding RNAome During M1 and M2 Macrophage Polarization," *Front. Immunol.*, vol. 13, May 2022, doi: 10.3389/FIMMU.2022.799733.
- [93] J. V. Santiago *et al.*, "Identification of state-specific proteomic and transcriptomic signatures of microglia-derived extracellular vesicles," *Mol. Cell. Proteomics*, p. 100678, Nov. 2023, doi: 10.1016/J.MCPRO.2023.100678.
- [94] Q. Mao *et al.*, "Transcriptome-wide piRNA profiling in human brains for aging genetic factors," *Jacobs J. Genet.*, vol. 4, no. 1, 2019, Accessed: Nov. 09, 2023. [Online]. Available: /pmc/articles/PMC7059831/.
- [95] P. Lenart, J. Novak, and J. Bienertova-Vasku, "PIWI-piRNA pathway: Setting the pace of aging by reducing DNA damage," *Mech. Ageing Dev.*, vol. 173, pp. 29–38, Jul. 2018, doi: 10.1016/J.MAD.2018.03.009.
- [96] C. Franceschi, P. Garagnani, P. Parini, C. Giuliani, and A. Santoro, "Inflammaging: a new immune–metabolic viewpoint for age-related diseases," *Nat. Rev. Endocrinol.* 2018 1410, vol. 14, no. 10, pp. 576–590, Jul. 2018, doi: 10.1038/s41574-018-0059-4.
- [97] C. Franceschi *et al.*, "Inflamm-aging: An Evolutionary Perspective on

- Immunosenescence," *Ann. N. Y. Acad. Sci.*, vol. 908, no. 1, pp. 244–254, Jun. 2000, doi: 10.1111/J.1749-6632.2000.TB06651.X.
- [98] M. V. Guillot-Sestier and T. Town, "Let's make microglia great again in neurodegenerative disorders," *Journal of Neural Transmission*, vol. 125, no. 5. Springer-Verlag Wien, pp. 751–770, May 01, 2018, doi: 10.1007/s00702-017-1792-x.
- [99] M. Amanollahi, M. Jameie, A. Heidari, and N. Rezaei, "The Dialogue Between Neuroinflammation and Adult Neurogenesis: Mechanisms Involved and Alterations in Neurological Diseases," *Mol. Neurobiol.* 2022 602, vol. 60, no. 2, pp. 923–959, Nov. 2022, doi: 10.1007/S12035-022-03102-Z.
- [100] Z. Wu, X. Yu, S. Zhang, Y. He, and W. Guo, "Novel roles of PIWI proteins and PIWI-interacting RNAs in human health and diseases," *Cell Commun. Signal.* 2023 211, vol. 21, no. 1, pp. 1–37, Nov. 2023, doi: 10.1186/S12964-023-01368-X.
- [101] A. Denoth-Lippuner and S. Jessberger, "Formation and integration of new neurons in the adult hippocampus," *Nat. Rev. Neurosci.*, vol. 22, pp. 223–236, 2021, doi: 10.1038/s41583-021-00433-z.
- [102] J. T. Gonçalves, S. T. Schafer, and F. H. Gage, "Adult Neurogenesis in the Hippocampus: From Stem Cells to Behavior," *Cell*, vol. 167, no. 4, pp. 897–914, 2016, doi: 10.1016/j.cell.2016.10.021.
- [103] S. Ramón Y Cajal, J. DeFelipe, E. G. Jones, and R. M. May, *Cajal's Degeneration and Regeneration of the Nervous System*. Oxford University Press, 2012.
- [104] J. Altman and G. D. Das, "Autoradiographic and histological evidence of postnatal hippocampal neurogenesis in rats," *J. Comp. Neurol.*, vol. 124, no. 3, pp. 319–335, Jun. 1965, doi: 10.1002/cne.901240303.
- [105] C. Olpe and S. Jessberger, "Cell population dynamics in the course of adult hippocampal neurogenesis: Remaining unknowns," *Hippocampus*, vol. 33, no. 4, pp. 402–411, Apr. 2023, doi: 10.1002/HIPO.23475.
- [106] C. G. Gross, "Neurogenesis in the adult brain: death of a dogma," *Nat. Rev. Neurosci.* 2000 11, vol. 1, no. 1, pp. 67–73, 2000, doi: 10.1038/35036235.
- [107] P. Rakic and R. S. Nowakowski, "The time of origin of neurons in the hippocampal region of the rhesus monkey," *J. Comp. Neurol.*, vol. 196, no. 1, pp. 99–128, 1981, doi: 10.1002/cne.901960109.
- [108] K. L. Spalding, R. D. Bhardwaj, B. A. Buchholz, H. Druid, and J. Frisén, "Retrospective

- birth dating of cells in humans,” *Cell*, vol. 122, no. 1, pp. 133–143, Jul. 2005, doi: 10.1016/j.cell.2005.04.028.
- [109] T. D. Palmer, J. Takahashi, and F. H. Gage, “The Adult Rat Hippocampus Contains Primordial Neural Stem Cells,” *Mol. Cell. Neurosci.*, vol. 8, no. 6, pp. 389–404, Jan. 1997, doi: 10.1006/MCNE.1996.0595.
- [110] B. A. Reynolds and S. Weiss, “Generation of Neurons and Astrocytes from Isolated Cells of the Adult Mammalian Central Nervous System,” *Science (80-.)*, vol. 255, no. 5052, pp. 1707–1710, Mar. 1992, doi: 10.1126/SCIENCE.1553558.
- [111] S. Bottes *et al.*, “Long-term self-renewing stem cells in the adult mouse hippocampus identified by intravital imaging,” *Nat. Neurosci.*, 2020, doi: 10.1038/s41593-020-00759-4.
- [112] F. H. Gage and P. Taupin, “Adult neurogenesis in mammals,” *Current Opinion in Molecular Therapeutics*, vol. 8, no. 4, pp. 345–351, Aug. 2006, doi: 10.1126/science.aav6885.
- [113] M. Boldrini *et al.*, “Human Hippocampal Neurogenesis Persists throughout Aging,” *Cell Stem Cell*, vol. 22, no. 4, pp. 589–599.e5, Apr. 2018, doi: 10.1016/j.stem.2018.03.015.
- [114] E. P. Moreno-Jiménez *et al.*, “Adult hippocampal neurogenesis is abundant in neurologically healthy subjects and drops sharply in patients with Alzheimer’s disease,” *Nat. Med.*, vol. 25, no. 4, pp. 554–560, 2019, doi: 10.1038/s41591-019-0375-9.
- [115] M. K. Tobin *et al.*, “Human Hippocampal Neurogenesis Persists in Aged Adults and Alzheimer’s Disease Patients,” *Cell Stem Cell*, vol. 24, no. 6, pp. 974–982.e3, Jun. 2019, doi: 10.1016/j.stem.2019.05.003.
- [116] G. Kempermann, H. Song, and F. H. Gage, “Adult neurogenesis in the hippocampus,” *Hippocampus*, vol. 33, no. 4, pp. 269–270, Apr. 2023, doi: 10.1002/HIPO.23525.
- [117] Y. Li, N. N. Xu, Z. Z. Hao, and S. Liu, “Adult neurogenesis in the primate hippocampus,” *Zool. Res.*, vol. 44, no. 2, p. 315, Mar. 2023, doi: 10.24272/J.ISSN.2095-8137.2022.399.
- [118] E. Voukali and M. Vinkler, “Proteomic-based evidence for adult neurogenesis in birds and mammals as indicated from cerebrospinal fluid,” *Neural Regen. Res.*, vol. 17, no. 12, p. 2576, Dec. 2022, doi: 10.4103/1673-5374.329002.
- [119] T. D. Palmer, J. Ray, and F. H. Gage, “FGF-2-Responsive Neuronal Progenitors Reside

- in Proliferative and Quiescent Regions of the Adult Rodent Brain,” *Mol. Cell. Neurosci.*, vol. 6, no. 5, pp. 474–486, Oct. 1995, doi: 10.1006/MCNE.1995.1035.
- [120] G. Kempermann *et al.*, “Human Adult Neurogenesis: Evidence and Remaining Questions,” *Cell Stem Cell*, vol. 23, no. 1. Cell Press, pp. 25–30, Jul. 05, 2018, doi: 10.1016/j.stem.2018.04.004.
- [121] M. F. Paredes *et al.*, “Does Adult Neurogenesis Persist in the Human Hippocampus?,” *Cell Stem Cell*, vol. 23, no. 6, p. 780, Dec. 2018, doi: 10.1016/J.STEM.2018.11.006.
- [122] A. Duque, J. I. Arellano, and P. Rakic, “An assessment of the existence of adult neurogenesis in humans and value of its rodent models for neuropsychiatric diseases,” *Mol. Psychiatry* 2021 271, vol. 27, no. 1, pp. 377–382, Oct. 2021, doi: 10.1038/s41380-021-01314-8.
- [123] S. F. Sorrells *et al.*, “Human hippocampal neurogenesis drops sharply in children to undetectable levels in adults,” *Nature*, vol. 555, no. 7696, pp. 377–381, Mar. 2018, doi: 10.1038/nature25975.
- [124] H. G. Kuhn, T. Toda, and F. H. Gage, “Adult hippocampal neurogenesis: A coming-of-age story,” *J. Neurosci.*, vol. 38, no. 49, pp. 10401–10410, Dec. 2018, doi: 10.1523/JNEUROSCI.2144-18.2018.
- [125] A. Duque and R. Spector, “A balanced evaluation of the evidence for adult neurogenesis in humans: implication for neuropsychiatric disorders,” *Brain Struct. Funct.*, vol. 224, no. 7, pp. 2281–2295, Sep. 2019, doi: 10.1007/S00429-019-01917-6.
- [126] C. V. Dennis, L. S. Suh, M. L. Rodriguez, J. J. Kril, and G. T. Sutherland, “Human adult neurogenesis across the ages: An immunohistochemical study,” *Neuropathol. Appl. Neurobiol.*, vol. 42, no. 7, pp. 621–638, Dec. 2016, doi: 10.1111/NAN.12337.
- [127] K. L. Spalding *et al.*, “Dynamics of hippocampal neurogenesis in adult humans,” *Cell*, vol. 153, no. 6, p. 1219, Jun. 2013, doi: 10.1016/J.CELL.2013.05.002.
- [128] P. S. Eriksson *et al.*, “Neurogenesis in the adult human hippocampus,” *Nat. Med.*, vol. 4, no. 11, pp. 1313–1317, Nov. 1998, doi: 10.1038/3305.
- [129] R. Knoth *et al.*, “Murine Features of Neurogenesis in the Human Hippocampus across the Lifespan from 0 to 100 Years,” *PLoS One*, vol. 5, no. 1, p. e8809, Jan. 2010, doi: 10.1371/journal.pone.0008809.
- [130] S. Cipriani *et al.*, “Hippocampal Radial Glial Subtypes and Their Neurogenic Potential in Human Fetuses and Healthy and Alzheimer’s Disease Adults,” *Cereb.*

- Cortex*, vol. 28, no. 7, pp. 2458–2478, Jul. 2018, doi: 10.1093/CERCOR/BHY096.
- [131] L. Bonfanti, C. La Rosa, M. Ghibaudi, and C. C. Sherwood, “Adult neurogenesis and ‘immature’ neurons in mammals: an evolutionary trade-off in plasticity?,” *Brain Struct. Funct.* 2023, vol. 1, pp. 1–19, Oct. 2023, doi: 10.1007/S00429-023-02717-9.
- [132] P. J. Lucassen, N. Toni, G. Kempermann, J. Frisen, F. H. Gage, and D. F. Swaab, “Limits to human neurogenesis—really?,” *Mol. Psychiatry* 2019 2510, vol. 25, no. 10, pp. 2207–2209, Jan. 2019, doi: 10.1038/s41380-018-0337-5.
- [133] A. B. Nogueira, H. S. R. Hoshino, N. C. Ortega, B. G. S. dos Santos, and M. J. Teixeira, “Adult human neurogenesis: early studies clarify recent controversies and go further,” *Metab. Brain Dis.*, vol. 37, no. 1, pp. 153–172, Jan. 2022, doi: 10.1007/S11011-021-00864-8/TABLES/12.
- [134] T. Toda, S. L. Parylak, S. B. Linker, and F. H. Gage, “The role of adult hippocampal neurogenesis in brain health and disease,” *Molecular Psychiatry*, vol. 24, no. 1. Nature Publishing Group, pp. 67–87, Jan. 01, 2019, doi: 10.1038/s41380-018-0036-2.
- [135] D. A. Lim and A. Alvarez-Buylla, “The Adult Ventricular–Subventricular Zone (V-SVZ) and Olfactory Bulb (OB) Neurogenesis,” *Cold Spring Harb. Perspect. Biol.*, vol. 8, no. 5, p. a018820, May 2016, doi: 10.1101/CSHPERSPECT.A018820.
- [136] K. Obernier and A. Alvarez-Buylla, “Neural stem cells: origin, heterogeneity and regulation in the adult mammalian brain,” *Development*, vol. 146, no. 4, Feb. 2019, doi: 10.1242/DEV.156059.
- [137] L. Peng and M. A. Bonaguidi, “Function and Dysfunction of Adult Hippocampal Neurogenesis in Regeneration and Disease,” *American Journal of Pathology*, vol. 188, no. 1. Elsevier Inc., pp. 23–28, Jan. 01, 2018, doi: 10.1016/j.ajpath.2017.09.004.
- [138] G. Kempermann, H. Song, and F. H. Gage, “Neurogenesis in the adult hippocampus,” *Cold Spring Harb. Perspect. Biol.*, vol. 7, no. 9, p. a018812, Sep. 2015, doi: 10.1101/cshperspect.a018812.
- [139] Y. Li and W. Guo, “Neural Stem Cell Niche and Adult Neurogenesis,” *Neuroscientist*, vol. 27, no. 3, pp. 235–245, Jun. 2021, doi: 10.1177/1073858420939034.
- [140] A. Sahay *et al.*, “Increasing adult hippocampal neurogenesis is sufficient to improve pattern separation,” *Nature*, vol. 472, no. 7344, pp. 466–470, Apr. 2011, doi: 10.1038/NATURE09817.

- [141] A. Gao *et al.*, “Elevation of Hippocampal Neurogenesis Induces a Temporally Graded Pattern of Forgetting of Contextual Fear Memories,” *J. Neurosci.*, vol. 38, no. 13, pp. 3190–3198, Mar. 2018, doi: 10.1523/JNEUROSCI.3126-17.2018.
- [142] S. M. Miller and A. Sahay, “Functions of adult-born neurons in hippocampal memory interference and indexing,” *Nat. Neurosci.* 2019 2210, vol. 22, no. 10, pp. 1565–1575, Sep. 2019, doi: 10.1038/s41593-019-0484-2.
- [143] S. Y. Ko and P. W. Frankland, “Neurogenesis-dependent transformation of hippocampal engrams,” *Neurosci. Lett.*, vol. 762, Sep. 2021, doi: 10.1016/J.NEULET.2021.136176.
- [144] J. B. Aimone, J. Wiles, and F. H. Gage, “Computational Influence of Adult Neurogenesis on Memory Encoding,” *Neuron*, vol. 61, no. 2, pp. 187–202, Jan. 2009, doi: 10.1016/j.neuron.2008.11.026.
- [145] A. Barnea and F. Nottebohm, “Seasonal recruitment of hippocampal neurons in adult free-ranging black-capped chickadees,” *Proc. Natl. Acad. Sci. U. S. A.*, vol. 91, no. 23, pp. 11217–11221, Nov. 1994, doi: 10.1073/PNAS.91.23.11217.
- [146] G. Kempermann, H. G. Kuhn, and F. H. Gage, “More hippocampal neurons in adult mice living in an enriched environment,” *Nature*, vol. 386, no. 6624, pp. 493–495, Apr. 1997, doi: 10.1038/386493A0.
- [147] T. J. Shors, G. Miesegaes, A. Beylin, M. Zhao, T. Rydel, and E. Gould, “Neurogenesis in the adult is involved in the formation of trace memories,” *Nature*, vol. 410, no. 6826, pp. 372–376, Mar. 2001, doi: 10.1038/35066584.
- [148] G. Kempermann, “What Is Adult Hippocampal Neurogenesis Good for?,” *Front. Neurosci.*, vol. 16, Apr. 2022, doi: 10.3389/FNINS.2022.852680.
- [149] S. N. Tuncdemir, C. O. Lacefield, and R. Hen, “Contributions of adult neurogenesis to dentate gyrus network activity and computations,” *Behav. Brain Res.*, vol. 374, p. 112112, Nov. 2019, doi: 10.1016/J.BBR.2019.112112.
- [150] H. Van Praag, B. R. Christie, T. J. Sejnowski, and F. H. Gage, “Running enhances neurogenesis, learning, and long-term potentiation in mice,” *Proc. Natl. Acad. Sci. U. S. A.*, vol. 96, no. 23, pp. 13427–13431, Nov. 1999, doi: 10.1073/PNAS.96.23.13427.
- [151] K. G. Akers *et al.*, “Hippocampal neurogenesis regulates forgetting during adulthood and infancy,” *Science (80-.)*, vol. 344, no. 6184, pp. 598–602, 2014, doi: 10.1126/science.1248903.
- [152] W. Deng, J. B. Aimone, and F. H. Gage, “New neurons and new memories: How does

- adult hippocampal neurogenesis affect learning and memory?," *Nature Reviews Neuroscience*, vol. 11, no. 5. Nature Publishing Group, pp. 339–350, May 31, 2010, doi: 10.1038/nrn2822.
- [153] S. Martín-Suárez and J. M. Encinas, "The future belongs to those who prepare for it today," *Cell Stem Cell*, vol. 28, no. 5, pp. 783–785, May 2021, doi: 10.1016/j.stem.2021.04.014.
- [154] J. Terreros-Roncal *et al.*, "Impact of neurodegenerative diseases on human adult hippocampal neurogenesis," *Science*, vol. 374, no. 6571, pp. 1106–1113, Nov. 2021, doi: 10.1126/SCIENCE.ABL5163.
- [155] C. Vicidomini, N. Guo, and A. Sahay, "Communication, Cross Talk, and Signal Integration in the Adult Hippocampal Neurogenic Niche," *Neuron*, vol. 105, no. 2, pp. 220–235, Jan. 2020, doi: 10.1016/J.NEURON.2019.11.029.
- [156] H. Mira and J. Morante, "Neurogenesis From Embryo to Adult – Lessons From Flies and Mice," *Front. Cell Dev. Biol.*, vol. 8, p. 555674, Jun. 2020, doi: 10.3389/FCELL.2020.00533/BIBTEX.
- [157] N. Urbán, I. M. Blomfield, and F. Guillemot, "Quiescence of Adult Mammalian Neural Stem Cells: A Highly Regulated Rest," *Neuron*, vol. 104, no. 5, pp. 834–848, Dec. 2019, doi: 10.1016/J.NEURON.2019.09.026.
- [158] J. Hsieh, "Orchestrating transcriptional control of adult neurogenesis," *Genes and Development*, vol. 26, no. 10. Genes Dev, pp. 1010–1021, May 15, 2012, doi: 10.1101/gad.187336.112.
- [159] R. J. Oliver and C. D. Mandyam, "Regulation of adult neurogenesis by non-coding RNAs: Implications for substance use disorders," *Frontiers in Neuroscience*, vol. 12, no. NOV. Frontiers Media S.A., p. 849, Nov. 22, 2018, doi: 10.3389/fnins.2018.00849.
- [160] J. M. Encinas *et al.*, "Division-coupled astrocytic differentiation and age-related depletion of neural stem cells in the adult hippocampus," *Cell Stem Cell*, vol. 8, no. 5, pp. 566–579, May 2011, doi: 10.1016/j.stem.2011.03.010.
- [161] X. Zhao and H. van Praag, "Steps towards standardized quantification of adult neurogenesis," *Nat. Commun.*, vol. 11, no. 1, Dec. 2020, doi: 10.1038/S41467-020-18046-Y.
- [162] H. G. Kuhn, H. Dickinson-Anson, and F. H. Gage, "Neurogenesis in the dentate gyrus of the adult rat: age-related decrease of neuronal progenitor proliferation," *J.*

- Neurosci.*, vol. 16, no. 6, pp. 2027–2033, Mar. 1996, doi: 10.1523/JNEUROSCI.16-06-02027.1996.
- [163] D. R. Kornack and P. Rakic, “Continuation of neurogenesis in the hippocampus of the adult macaque monkey,” *Proc. Natl. Acad. Sci. U. S. A.*, vol. 96, no. 10, pp. 5768–5773, May 1999, doi: 10.1073/PNAS.96.10.5768.
- [164] Z. Nicola, K. Fabel, and G. Kempermann, “Development of the adult neurogenic niche in the hippocampus of mice,” *Front. Neuroanat.*, vol. 9, no. MAY, May 2015, doi: 10.3389/fnana.2015.00053.
- [165] G. A. Pilz *et al.*, “Live imaging of neurogenesis in the adult mouse hippocampus,” *Science*, vol. 359, no. 6376, pp. 658–662, Feb. 2018, doi: 10.1126/SCIENCE.AAO5056.
- [166] M. Biebl, C. M. Cooper, J. Winkler, and H. G. Kuhn, “Analysis of neurogenesis and programmed cell death reveals a self-renewing capacity in the adult rat brain,” *Neurosci. Lett.*, vol. 291, no. 1, pp. 17–20, Sep. 2000, doi: 10.1016/S0304-3940(00)01368-9.
- [167] H. G. Kuhn, M. Biebl, D. Wilhelm, M. Li, R. M. Friedlander, and J. Winkler, “Increased generation of granule cells in adult Bcl-2-overexpressing mice: A role for cell death during continued hippocampal neurogenesis,” *Eur. J. Neurosci.*, vol. 22, no. 8, pp. 1907–1915, Oct. 2005, doi: 10.1111/j.1460-9568.2005.04377.x.
- [168] H. A. Cameron and R. D. G. McKay, “Adult neurogenesis produces a large pool of new granule cells in the dentate gyrus,” *J. Comp. Neurol.*, vol. 435, no. 4, pp. 406–417, Jul. 2001, doi: 10.1002/CNE.1040.
- [169] A. G. Dayer, A. A. Ford, K. M. Cleaver, M. Yassaee, and H. A. Cameron, “Short-term and long-term survival of new neurons in the rat dentate gyrus,” *J. Comp. Neurol.*, vol. 460, no. 4, pp. 563–572, Jun. 2003, doi: 10.1002/CNE.10675.
- [170] W. Sun, A. Winseck, S. Vinsant, O. H. Park, H. Kim, and R. W. Oppenheim, “Programmed cell death of adult-generated hippocampal neurons is mediated by the proapoptotic gene Bax,” *J. Neurosci.*, vol. 24, no. 49, pp. 11205–11213, Dec. 2004, doi: 10.1523/JNEUROSCI.1436-04.2004.
- [171] A. Sierra *et al.*, “Microglia shape adult hippocampal neurogenesis through apoptosis-coupled phagocytosis,” *Cell Stem Cell*, vol. 7, no. 4, p. 483, Oct. 2010, doi: 10.1016/J.STEM.2010.08.014.
- [172] A. Tashiro, V. M. Sandler, N. Toni, C. Zhao, and F. H. Gage, “NMDA-receptor-

- mediated, cell-specific integration of new neurons in adult dentate gyrus,” *Nature*, vol. 442, no. 7105, pp. 929–933, Aug. 2006, doi: 10.1038/NATURE05028.
- [173] C. Zhao, E. M. Teng, R. G. Summers, G. L. Ming, and F. H. Gage, “Distinct morphological stages of dentate granule neuron maturation in the adult mouse hippocampus,” *J. Neurosci.*, vol. 26, no. 1, pp. 3–11, Jan. 2006, doi: 10.1523/JNEUROSCI.3648-05.2006.
- [174] K. A. Huckleberry and R. M. Shansky, “The unique plasticity of hippocampal adult-born neurons: Contributing to a heterogeneous dentate,” *Hippocampus*, vol. 31, no. 6, pp. 543–556, Jun. 2021, doi: 10.1002/HIPO.23318.
- [175] J. Liu, K. Solway, R. O. Messing, and F. R. Sharp, “Increased neurogenesis in the dentate gyrus after transient global ischemia in gerbils,” *J. Neurosci.*, vol. 18, no. 19, pp. 7768–7778, Oct. 1998, doi: 10.1523/JNEUROSCI.18-19-07768.1998.
- [176] J. M. Parent, T. W. Yu, R. T. Leibowitz, D. H. Geschwind, R. S. Sloviter, and D. H. Lowenstein, “Dentate granule cell neurogenesis is increased by seizures and contributes to aberrant network reorganization in the adult rat hippocampus,” *J. Neurosci.*, vol. 17, no. 10, pp. 3727–3738, 1997, doi: 10.1523/JNEUROSCI.17-10-03727.1997.
- [177] A. Dranovsky *et al.*, “Experience dictates stem cell fate in the adult hippocampus,” *Neuron*, vol. 70, no. 5, pp. 908–923, Jun. 2011, doi: 10.1016/J.NEURON.2011.05.022.
- [178] H. Van Praag, G. Kempermann, and F. H. Gage, “Running increases cell proliferation and neurogenesis in the adult mouse dentate gyrus,” *Nat. Neurosci.*, vol. 2, no. 3, pp. 266–270, Mar. 1999, doi: 10.1038/6368.
- [179] C. Mirescu, J. D. Peters, and E. Gould, “Early life experience alters response of adult neurogenesis to stress,” *Nat. Neurosci.*, vol. 7, no. 8, pp. 841–846, Aug. 2004, doi: 10.1038/NN1290.
- [180] C. L. Coe *et al.*, “Prenatal stress diminishes neurogenesis in the dentate gyrus of juvenile Rhesus monkeys,” *Biol. Psychiatry*, vol. 54, no. 10, pp. 1025–1034, Nov. 2003, doi: 10.1016/S0006-3223(03)00698-X.
- [181] V. Lemaire, M. Koehl, M. Le Moal, and D. N. Abrous, “Prenatal stress produces learning deficits associated with an inhibition of neurogenesis in the hippocampus,” *Proc. Natl. Acad. Sci. U. S. A.*, vol. 97, no. 20, pp. 11032–11037, Sep. 2000, doi: 10.1073/PNAS.97.20.11032.

- [182] M. L. Monje, H. Toda, and T. D. Palmer, "Inflammatory blockade restores adult hippocampal neurogenesis," *Science*, vol. 302, no. 5651, pp. 1760–1765, Dec. 2003, doi: 10.1126/SCIENCE.1088417.
- [183] C. T. Ekdahl, J. H. Claasen, S. Bonde, Z. Kokaia, and O. Lindvall, "Inflammation is detrimental for neurogenesis in adult brain," *Proc. Natl. Acad. Sci. U. S. A.*, vol. 100, no. 23, pp. 13632–13637, Nov. 2003, doi: 10.1073/PNAS.2234031100.
- [184] S. A. Villeda *et al.*, "The ageing systemic milieu negatively regulates neurogenesis and cognitive function," *Nature*, vol. 477, no. 7362, pp. 90–96, Sep. 2011, doi: 10.1038/NATURE10357.
- [185] N. Urbán and F. Guillemot, "Neurogenesis in the embryonic and adult brain: same regulators, different roles," *Front. Cell. Neurosci.*, vol. 8, no. NOV, Nov. 2014, doi: 10.3389/FNCEL.2014.00396.
- [186] B. Yao, K. M. Christian, C. He, P. Jin, G. L. Ming, and H. Song, "Epigenetic mechanisms in neurogenesis," *Nat. Rev. Neurosci.* 2016 179, vol. 17, no. 9, pp. 537–549, Jun. 2016, doi: 10.1038/nrn.2016.70.
- [187] M. V. Niklison-Chirou, M. Agostini, I. Amelio, and G. Melino, "Regulation of Adult Neurogenesis in Mammalian Brain," *Int. J. Mol. Sci.* 2020, Vol. 21, Page 4869, vol. 21, no. 14, p. 4869, Jul. 2020, doi: 10.3390/IJMS21144869.
- [188] D. K. Ma, M. C. Marchetto, J. U. Guo, G. L. Ming, F. H. Gage, and H. Song, "Epigenetic choreographers of neurogenesis in the adult mammalian brain," *Nature Neuroscience*, vol. 13, no. 11. NIH Public Access, pp. 1338–1344, Nov. 2010, doi: 10.1038/nn.2672.
- [189] S. Zocher *et al.*, "De novo DNA methylation controls neuronal maturation during adult hippocampal neurogenesis," *EMBO J.*, vol. 40, no. 18, p. e107100, Sep. 2021, doi: 10.15252/EMBJ.2020107100.
- [190] J. B. Aimone, Y. Li, S. W. Lee, G. D. Clemenson, W. Deng, and F. H. Gage, "Regulation and function of adult neurogenesis: from genes to cognition," *Physiological reviews*, vol. 94, no. 4. American Physiological Society, pp. 991–1026, Oct. 01, 2014, doi: 10.1152/physrev.00004.2014.
- [191] J. Hsieh and X. Zhao, "Genetics and epigenetics in adult neurogenesis," *Cold Spring Harb. Perspect. Biol.*, vol. 8, no. 6, Jun. 2016, doi: 10.1101/cshperspect.a018911.
- [192] V. Chesnokova, R. N. Pechnick, and K. Wawrowsky, "Chronic Peripheral Inflammation, Hippocampal Neurogenesis, and Behavior," *Brain. Behav. Immun.*,

- vol. 58, p. 1, Nov. 2016, doi: 10.1016/J.BBI.2016.01.017.
- [193] S. Martín-Suárez, J. Valero, T. Muro-García, and J. M. Encinas, “Phenotypical and functional heterogeneity of neural stem cells in the aged hippocampus,” *Aging Cell*, vol. 18, no. 4, p. e12958, Aug. 2019, doi: 10.1111/ACEL.12958.
- [194] C. V Borlongan *et al.*, “Stem Cells of the Aging Brain,” 2020, doi: 10.3389/fnagi.2020.00247.
- [195] B. Becher, S. Spath, and J. Goverman, “Cytokine networks in neuroinflammation,” *Nat. Rev. Immunol.* 2016 171, vol. 17, no. 1, pp. 49–59, Dec. 2016, doi: 10.1038/nri.2016.123.
- [196] Q. Yang, J. Zhou, C. Qiaoqiao Yang, and J. Zhou, “Neuroinflammation in the central nervous system: Symphony of glial cells,” *Glia*, vol. 67, no. 6, pp. 1017–1035, Jun. 2019, doi: 10.1002/GLIA.23571.
- [197] D. M. Teleanu *et al.*, “An Overview of Oxidative Stress, Neuroinflammation, and Neurodegenerative Diseases,” *Int. J. Mol. Sci.* 2022, Vol. 23, Page 5938, vol. 23, no. 11, p. 5938, May 2022, doi: 10.3390/IJMS23115938.
- [198] L. Guzman-Martinez, R. B. Maccioni, V. Andrade, L. P. Navarrete, M. G. Pastor, and N. Ramos-Escobar, “Neuroinflammation as a common feature of neurodegenerative disorders,” *Front. Pharmacol.*, vol. 10, no. SEP, p. 452270, Sep. 2019, doi: 10.3389/FPHAR.2019.01008/BIBTEX.
- [199] V. Haage and P. L. De Jager, “Neuroimmune contributions to Alzheimer’s disease: a focus on human data,” *Mol. Psychiatry* 2022 278, vol. 27, no. 8, pp. 3164–3181, Jun. 2022, doi: 10.1038/s41380-022-01637-0.
- [200] M. G. Tansey, R. L. Wallings, M. C. Houser, M. K. Herrick, C. E. Keating, and V. Joers, “Inflammation and immune dysfunction in Parkinson disease,” *Nat. Rev. Immunol.* 2022 2211, vol. 22, no. 11, pp. 657–673, Mar. 2022, doi: 10.1038/s41577-022-00684-6.
- [201] A. Musella *et al.*, “Interplay between age and neuroinflammation in multiple sclerosis: Effects on motor and cognitive functions,” *Front. Aging Neurosci.*, vol. 10, no. AUG, p. 380748, Aug. 2018, doi: 10.3389/FNAGI.2018.00238/BIBTEX.
- [202] S. M. Matta, E. L. Hill-Yardin, and P. J. Crack, “The influence of neuroinflammation in Autism Spectrum Disorder,” *Brain. Behav. Immun.*, vol. 79, pp. 75–90, Jul. 2019, doi: 10.1016/J.BBI.2019.04.037.
- [203] V. X. Han, S. Patel, H. F. Jones, and R. C. Dale, “Maternal immune activation and

- neuroinflammation in human neurodevelopmental disorders,” *Nat. Rev. Neurol.* 2021 179, vol. 17, no. 9, pp. 564–579, Aug. 2021, doi: 10.1038/s41582-021-00530-8.
- [204] F. Benedetti, V. Aggio, M. L. Pratesi, G. Greco, and R. Furlan, “Neuroinflammation in Bipolar Depression,” *Front. Psychiatry*, vol. 11, p. 449957, Feb. 2020, doi: 10.3389/FPSYT.2020.00071/BIBTEX.
- [205] F. Bright *et al.*, “Neuroinflammation in frontotemporal dementia,” *Nat. Rev. Neurol.* 2019 159, vol. 15, no. 9, pp. 540–555, Jul. 2019, doi: 10.1038/s41582-019-0231-z.
- [206] R. L. Jayaraj, S. Azimullah, R. Beiram, F. Y. Jalal, and G. A. Rosenberg, “Neuroinflammation: friend and foe for ischemic stroke,” *J. Neuroinflammation* 2019 161, vol. 16, no. 1, pp. 1–24, Jul. 2019, doi: 10.1186/S12974-019-1516-2.
- [207] F. Leng and P. Edison, “Neuroinflammation and microglial activation in Alzheimer disease: where do we go from here?,” *Nat. Rev. Neurol.* 2020 173, vol. 17, no. 3, pp. 157–172, Dec. 2020, doi: 10.1038/s41582-020-00435-y.
- [208] H. S. Kwon and S. H. Koh, “Neuroinflammation in neurodegenerative disorders: the roles of microglia and astrocytes,” *Transl. Neurodegener.* 2020 91, vol. 9, no. 1, pp. 1–12, Nov. 2020, doi: 10.1186/S40035-020-00221-2.
- [209] M. Colonna and O. Butovsky, “Microglia function in the central nervous system during health and neurodegeneration,” *Annual Review of Immunology*, vol. 35. Annual Reviews Inc., pp. 441–468, Apr. 26, 2017, doi: 10.1146/annurev-immunol-051116-052358.
- [210] P. del Rio-Hortega, “del Rio-Hortega, P. (1932) Microglia. In Penfield, W., Ed., *Cytology & Cellular Pathology of the Nervous System*, P.B. Hoeber, New York, 483-534. - References - Scientific Research Publishing,” 1932. [https://www.scirp.org/\(S\(vtj3fa45qm1ean45vvffcz55\)\)/reference/referencespapers.aspx?referenceid=3065815](https://www.scirp.org/(S(vtj3fa45qm1ean45vvffcz55))/reference/referencespapers.aspx?referenceid=3065815) (accessed Dec. 03, 2023).
- [211] Q. Li and B. A. Barres, “Microglia and macrophages in brain homeostasis and disease,” *Nat. Rev. Immunol.* 2017 184, vol. 18, no. 4, pp. 225–242, Nov. 2017, doi: 10.1038/nri.2017.125.
- [212] T. L. Tay, J. C. Savage, C. W. Hui, K. Bisht, and M. È. Tremblay, “Microglia across the lifespan: from origin to function in brain development, plasticity and cognition,” *J. Physiol.*, vol. 595, no. 6, pp. 1929–1945, Mar. 2017, doi: 10.1113/JP272134.
- [213] K. Kierdorf *et al.*, “Microglia emerge from erythromyeloid precursors via Pu.1- and

- Irf8-dependent pathways," *Nat. Neurosci.*, vol. 16, no. 3, pp. 273–280, Mar. 2013, doi: 10.1038/NN.3318.
- [214] C. Schulz *et al.*, "A lineage of myeloid cells independent of Myb and hematopoietic stem cells," *Science*, vol. 336, no. 6077, pp. 86–90, Apr. 2012, doi: 10.1126/SCIENCE.1219179.
- [215] F. Ginhoux *et al.*, "Fate mapping analysis reveals that adult microglia derive from primitive macrophages," *Science*, vol. 330, no. 6005, pp. 841–845, Nov. 2010, doi: 10.1126/SCIENCE.1194637.
- [216] C. Stremmel *et al.*, "Yolk sac macrophage progenitors traffic to the embryo during defined stages of development," *Nat. Commun.*, vol. 9, no. 1, Dec. 2018, doi: 10.1038/S41467-017-02492-2.
- [217] B. Ajami, J. L. Bennett, C. Krieger, W. Tetzlaff, and F. M. V. Rossi, "Local self-renewal can sustain CNS microglia maintenance and function throughout adult life," *Nat. Neurosci.*, vol. 10, no. 12, pp. 1538–1543, Dec. 2007, doi: 10.1038/NN2014.
- [218] K. Askew *et al.*, "Coupled Proliferation and Apoptosis Maintain the Rapid Turnover of Microglia in the Adult Brain," *Cell Rep.*, vol. 18, no. 2, pp. 391–405, Jan. 2017, doi: 10.1016/J.CELREP.2016.12.041.
- [219] F. Alliot, I. Godin, and B. Pessac, "Microglia derive from progenitors, originating from the yolk sac, and which proliferate in the brain," *Dev. Brain Res.*, vol. 117, no. 2, pp. 145–152, Nov. 1999, doi: 10.1016/S0165-3806(99)00113-3.
- [220] C. Rigato, R. Buckinx, H. Le-Corronc, J. M. Rigo, and P. Legendre, "Pattern of invasion of the embryonic mouse spinal cord by microglial cells at the time of the onset of functional neuronal networks," *Glia*, vol. 59, no. 4, pp. 675–695, Apr. 2011, doi: 10.1002/GLIA.21140.
- [221] V. H. Perry, D. A. Hume, and S. Gordon, "Immunohistochemical localization of macrophages and microglia in the adult and developing mouse brain," *Neuroscience*, vol. 15, no. 2, pp. 313–326, 1985, doi: 10.1016/0306-4522(85)90215-5.
- [222] L. Muzio, A. Viotti, and G. Martino, "Microglia in Neuroinflammation and Neurodegeneration: From Understanding to Therapy," *Front. Neurosci.*, vol. 15, Sep. 2021, doi: 10.3389/FNINS.2021.742065.
- [223] T. Goldmann *et al.*, "Origin, fate and dynamics of macrophages at central nervous system interfaces," *Nat. Immunol.*, vol. 17, no. 7, pp. 797–805, Jun. 2016, doi:

- 10.1038/NI.3423.
- [224] M. Prinz, T. Masuda, M. A. Wheeler, and F. J. Quintana, "Microglia and Central Nervous System–Associated Macrophages—From Origin to Disease Modulation," *Annu. Rev. Immunol.*, vol. 39, p. 251, Apr. 2021, doi: 10.1146/ANNUREV-IMMUNOL-093019-110159.
- [225] I. Dermitzakis *et al.*, "CNS Border-Associated Macrophages: Ontogeny and Potential Implication in Disease," *Curr. Issues Mol. Biol. 2023, Vol. 45, Pages 4285-4300*, vol. 45, no. 5, pp. 4285–4300, May 2023, doi: 10.3390/CIMB45050272.
- [226] G. T. Norris and J. Kipnis, "Immune cells and CNS physiology: Microglia and beyond," *Journal of Experimental Medicine*, vol. 216, no. 1. Rockefeller University Press, pp. 60–70, Jan. 01, 2019, doi: 10.1084/jem.20180199.
- [227] A. Nimmerjahn, F. Kirchhoff, and F. Helmchen, "Resting microglial cells are highly dynamic surveillants of brain parenchyma in vivo," *Science*, vol. 308, no. 5726, pp. 1314–1318, May 2005, doi: 10.1126/SCIENCE.1110647.
- [228] D. Davalos *et al.*, "ATP mediates rapid microglial response to local brain injury in vivo," *Nat. Neurosci. 2005 86*, vol. 8, no. 6, pp. 752–758, May 2005, doi: 10.1038/nn1472.
- [229] H. Wake, A. J. Moorhouse, S. Jinno, S. Kohsaka, and J. Nabekura, "Resting microglia directly monitor the functional state of synapses in vivo and determine the fate of ischemic terminals," *J. Neurosci.*, vol. 29, no. 13, pp. 3974–3980, Apr. 2009, doi: 10.1523/JNEUROSCI.4363-08.2009.
- [230] D. Gosselin *et al.*, "An environment-dependent transcriptional network specifies human microglia identity," *Science (80-.)*, vol. 356, no. 6344, pp. 1248–1259, Jun. 2017, doi: 10.1126/SCIENCE.AAL3222/SUPPL_FILE/AAL3222_GOSSELIN_TABLES6.XLSX.
- [231] T. L. Tay *et al.*, "A new fate mapping system reveals context-dependent random or clonal expansion of microglia," *Nat. Neurosci. 2017 206*, vol. 20, no. 6, pp. 793–803, Apr. 2017, doi: 10.1038/nn.4547.
- [232] B. Ajami *et al.*, "Single-cell mass cytometry reveals distinct populations of brain myeloid cells in mouse neuroinflammation and neurodegeneration models," *Nat. Neurosci. 2018 214*, vol. 21, no. 4, pp. 541–551, Mar. 2018, doi: 10.1038/s41593-018-0100-x.
- [233] T. R. Hammond *et al.*, "Single-Cell RNA Sequencing of Microglia throughout the

- Mouse Lifespan and in the Injured Brain Reveals Complex Cell-State Changes,” *Immunity*, vol. 50, no. 1, pp. 253-271.e6, Jan. 2019, doi: 10.1016/j.immuni.2018.11.004.
- [234] C. Sousa *et al.*, “Single-cell transcriptomics reveals distinct inflammation-induced microglia signatures,” *EMBO Rep.*, vol. 19, no. 11, p. e46171, Nov. 2018, doi: 10.15252/EMBR.201846171.
- [235] S. A. Wolf, H. W. G. M. Boddeke, and H. Kettenmann, “Microglia in Physiology and Disease,” *Annu. Rev. Physiol.*, vol. 79, pp. 619–643, Feb. 2017, doi: 10.1146/ANNUREV-PHYSIOL-022516-034406.
- [236] O. Butovsky and H. L. Weiner, “Microglial signatures and their role in health and disease,” *Nat. Rev. Neurosci. 2018 1910*, vol. 19, no. 10, pp. 622–635, Sep. 2018, doi: 10.1038/s41583-018-0057-5.
- [237] R. C. Paolicelli *et al.*, “Microglia states and nomenclature: A field at its crossroads,” *Neuron*, vol. 110, no. 21, pp. 3458–3483, Nov. 2022, doi: 10.1016/J.NEURON.2022.10.020.
- [238] C. L. Cunningham, V. Martínez-Cerdeño, and S. C. Noctor, “Microglia regulate the number of neural precursor cells in the developing cerebral cortex,” *J. Neurosci.*, vol. 33, no. 10, pp. 4216–4233, Mar. 2013, doi: 10.1523/JNEUROSCI.3441-12.2013.
- [239] K. Takahashi, C. D. P. Rochford, and H. Neumann, “Clearance of apoptotic neurons without inflammation by microglial triggering receptor expressed on myeloid cells-2,” *J. Exp. Med.*, vol. 201, no. 4, pp. 647–657, Feb. 2005, doi: 10.1084/JEM.20041611.
- [240] H. Lui *et al.*, “Progranulin Deficiency Promotes Circuit-Specific Synaptic Pruning by Microglia via Complement Activation,” *Cell*, vol. 165, no. 4, pp. 921–935, May 2016, doi: 10.1016/J.CELL.2016.04.001.
- [241] R. C. Paolicelli and M. T. Ferretti, “Function and dysfunction of microglia during brain development: Consequences for synapses and neural circuits,” *Front. Synaptic Neurosci.*, vol. 9, no. MAY, p. 257452, May 2017, doi: 10.3389/FNSYN.2017.00009/BIBTEX.
- [242] R. C. Paolicelli *et al.*, “Synaptic pruning by microglia is necessary for normal brain development,” *Science*, vol. 333, no. 6048, pp. 1456–1458, Sep. 2011, doi: 10.1126/SCIENCE.1202529.
- [243] D. P. Schafer *et al.*, “Microglia sculpt postnatal neural circuits in an activity and

- complement-dependent manner," *Neuron*, vol. 74, no. 4, pp. 691–705, May 2012, doi: 10.1016/J.NEURON.2012.03.026.
- [244] M. Ě. Tremblay, R. L. Lowery, and A. K. Majewska, "Microglial interactions with synapses are modulated by visual experience," *PLoS Biol.*, vol. 8, no. 11, Nov. 2010, doi: 10.1371/JOURNAL.PBIO.1000527.
- [245] N. B. McNamara *et al.*, "Microglia regulate central nervous system myelin growth and integrity," *Nat. 2022 6137942*, vol. 613, no. 7942, pp. 120–129, Dec. 2022, doi: 10.1038/s41586-022-05534-y.
- [246] N. Hagemeyer *et al.*, "Microglia contribute to normal myelinogenesis and to oligodendrocyte progenitor maintenance during adulthood," *Acta Neuropathol.*, vol. 134, no. 3, pp. 441–458, Sep. 2017, doi: 10.1007/S00401-017-1747-1.
- [247] S. Safaiyan *et al.*, "Age-related myelin degradation burdens the clearance function of microglia during aging," *Nat. Neurosci.*, vol. 19, no. 8, pp. 995–998, Aug. 2016, doi: 10.1038/NN.4325.
- [248] A. D. Umpierre and L. J. Wu, "How microglia sense and regulate neuronal activity," *Glia*, vol. 69, no. 7, pp. 1637–1653, Jul. 2021, doi: 10.1002/GLIA.23961.
- [249] A. Badimon *et al.*, "Negative feedback control of neuronal activity by microglia," *Nature*, vol. 586, no. 7829, p. 417, Oct. 2020, doi: 10.1038/S41586-020-2777-8.
- [250] M. M. A. de Almeida, K. Goodkey, and A. Voronova, "Regulation of microglia function by neural stem cells," *Front. Cell. Neurosci.*, vol. 17, p. 1130205, Mar. 2023, doi: 10.3389/FNCEL.2023.1130205/BIBTEX.
- [251] I. Diaz-Aparicio *et al.*, "Microglia Actively Remodel Adult Hippocampal Neurogenesis through the Phagocytosis Secretome," *J. Neurosci.*, vol. 40, no. 7, pp. 1453–1482, Feb. 2020, doi: 10.1523/JNEUROSCI.0993-19.2019.
- [252] K. Sato, "Effects of Microglia on Neurogenesis," *Glia*, vol. 63, no. 8, p. 1394, Aug. 2015, doi: 10.1002/GLIA.22858.
- [253] K. I. Mosher *et al.*, "Neural progenitor cells regulate microglia functions and activity," *Nat. Neurosci.*, vol. 15, no. 11, pp. 1485–1487, Nov. 2012, doi: 10.1038/NN.3233.
- [254] O. Butovsky *et al.*, "Microglia activated by IL-4 or IFN-gamma differentially induce neurogenesis and oligodendrogenesis from adult stem/progenitor cells," *Mol. Cell. Neurosci.*, vol. 31, no. 1, pp. 149–160, Jan. 2006, doi: 10.1016/J.MCN.2005.10.006.
- [255] J. Aarum, K. Sandberg, S. L. B. Haeberlein, and M. A. A. Persson, "Migration and

- differentiation of neural precursor cells can be directed by microglia," *Proc. Natl. Acad. Sci. U. S. A.*, vol. 100, no. 26, pp. 15983–15988, Dec. 2003, doi: 10.1073/PNAS.2237050100.
- [256] M. E. Woodbury *et al.*, "miR-155 Is Essential for Inflammation-Induced Hippocampal Neurogenic Dysfunction," *J. Neurosci.*, vol. 35, no. 26, pp. 9764–9781, Jul. 2015, doi: 10.1523/JNEUROSCI.4790-14.2015.
- [257] J. Guadagno, X. Xu, M. Karajgikar, A. Brown, and S. P. Cregan, "Microglia-derived TNF α induces apoptosis in neural precursor cells via transcriptional activation of the Bcl-2 family member Puma," *Cell Death Dis.* 2013 43, vol. 4, no. 3, pp. e538–e538, Mar. 2013, doi: 10.1038/cddis.2013.59.
- [258] Z. Kokaia, G. Martino, M. Schwartz, and O. Lindvall, "Cross-talk between neural stem cells and immune cells: the key to better brain repair?," *Nat. Neurosci.*, vol. 15, no. 8, pp. 1078–1087, Aug. 2012, doi: 10.1038/NN.3163.
- [259] S. U. Vay *et al.*, "The plasticity of primary microglia and their multifaceted effects on endogenous neural stem cells in vitro and in vivo," *J. Neuroinflammation*, vol. 15, no. 1, Aug. 2018, doi: 10.1186/S12974-018-1261-Y.
- [260] S. Pluchino *et al.*, "Neurosphere-derived multipotent precursors promote neuroprotection by an immunomodulatory mechanism," *Nature*, vol. 436, no. 7048, pp. 266–271, Jul. 2005, doi: 10.1038/NATURE03889.
- [261] S. Pluchino *et al.*, "Injection of adult neurospheres induces recovery in a chronic model of multiple sclerosis," *Nature*, vol. 422, no. 6933, pp. 688–694, Apr. 2003, doi: 10.1038/NATURE01552.
- [262] S. Pluchino *et al.*, "Human neural stem cells ameliorate autoimmune encephalomyelitis in non-human primates," *Ann. Neurol.*, vol. 66, no. 3, pp. 343–354, 2009, doi: 10.1002/ANA.21745.
- [263] K. Haruwaka *et al.*, "Dual microglia effects on blood brain barrier permeability induced by systemic inflammation," *Nat. Commun.* 2019 101, vol. 10, no. 1, pp. 1–17, Dec. 2019, doi: 10.1038/s41467-019-13812-z.
- [264] G. S. Gullotta, G. Costantino, M. A. Sortino, and S. F. Spampinato, "Microglia and the Blood-Brain Barrier: An External Player in Acute and Chronic Neuroinflammatory Conditions," *Int. J. Mol. Sci.*, vol. 24, no. 11, Jun. 2023, doi: 10.3390/IJMS24119144.
- [265] X. Zhao, U. B. Eyo, M. Murugan, and L. J. Wu, "Microglial interactions with the neurovascular system in physiology and pathology," *Dev. Neurobiol.*, vol. 78, no. 6,

- pp. 604–617, Jun. 2018, doi: 10.1002/DNEU.22576.
- [266] S. F. Rymo, H. Gerhardt, F. W. Sand, R. Lang, A. Uv, and C. Betsholtz, “A Two-Way Communication between Microglial Cells and Angiogenic Sprouts Regulates Angiogenesis in Aortic Ring Cultures,” *PLoS One*, vol. 6, no. 1, p. e15846, 2011, doi: 10.1371/JOURNAL.PONE.0015846.
- [267] J. Moss *et al.*, “Fine processes of Nestin-GFP-positive radial glia-like stem cells in the adult dentate gyrus ensheath the local synapses and vasculature,” *Proc. Natl. Acad. Sci. U. S. A.*, vol. 113, no. 18, pp. E2536–E2545, May 2016, doi: 10.1073/PNAS.1514652113.
- [268] S. E. Hickman *et al.*, “The microglial sensome revealed by direct RNA sequencing,” *Nat. Neurosci.*, vol. 16, no. 12, pp. 1896–1905, 2013, doi: 10.1038/NN.3554.
- [269] K. Borst, A. A. Dumas, and M. Prinz, “Microglia: Immune and non-immune functions,” *Immunity*, vol. 54, no. 10, pp. 2194–2208, Oct. 2021, doi: 10.1016/J.IMMUNI.2021.09.014.
- [270] H. Liu, R. K. Leak, and X. Hu, “Neurotransmitter receptors on microglia,” *Stroke Vasc. Neurol.*, vol. 1, no. 2, pp. 52–58, Jun. 2016, doi: 10.1136/SVN-2016-000012.
- [271] U. B. Eyo *et al.*, “Regulation of Physical Microglia–Neuron Interactions by Fractalkine Signaling after Status Epilepticus,” *eNeuro*, vol. 3, no. 6, Dec. 2016, doi: 10.1523/ENEURO.0209-16.2016.
- [272] A. E. Cardona *et al.*, “Control of microglial neurotoxicity by the fractalkine receptor,” *Nat. Neurosci.*, vol. 9, no. 7, pp. 917–924, Jul. 2006, doi: 10.1038/NN1715.
- [273] L. Maggi, M. Scianni, I. Branchi, I. D’Andrea, C. Lauro, and C. Limatola, “CX 3CR1 deficiency alters hippocampal-dependent plasticity phenomena blunting the effects of enriched environment,” *Front. Cell. Neurosci.*, vol. 5, no. OCTOBER, pp. 1–10, Oct. 2011, doi: 10.3389/FNCEL.2011.00022/BIBTEX.
- [274] Z. Tang *et al.*, “CX3CR1 deficiency suppresses activation and neurotoxicity of microglia/macrophage in experimental ischemic stroke,” *J. Neuroinflammation*, vol. 11, no. 1, pp. 1–13, Feb. 2014, doi: 10.1186/1742-2094-11-26/FIGURES/6.
- [275] F. Xiao, J. M. Xu, and X. H. Jiang, “CX3 chemokine receptor 1 deficiency leads to reduced dendritic complexity and delayed maturation of newborn neurons in the adult mouse hippocampus,” *Neural Regen. Res.*, vol. 10, no. 5, pp. 772–777, May 2015, doi: 10.4103/1673-5374.156979.
- [276] M. Bolós *et al.*, “Absence of microglial CX3CR1 impairs the synaptic integration of

- adult-born hippocampal granule neurons,” *Brain. Behav. Immun.*, vol. 68, pp. 76–89, Feb. 2018, doi: 10.1016/J.BBI.2017.10.002.
- [277] Y. Wolf, S. Yona, K. W. Kim, and S. Jung, “Microglia, seen from the CX3CR1 angle,” *Front. Cell. Neurosci.*, vol. 7, no. MAR, Mar. 2013, doi: 10.3389/FNCEL.2013.00026.
- [278] D. Bérangère Ré and S. Przedborski, “Fractalkine: moving from chemotaxis to neuroprotection,” *Nat. Neurosci.* 2006 97, vol. 9, no. 7, pp. 859–861, Jul. 2006, doi: 10.1038/nn0706-859.
- [279] S. Thoma-Uszynski *et al.*, “Induction of direct antimicrobial activity through mammalian toll-like receptors,” *Science*, vol. 291, no. 5508, pp. 1544–1547, Feb. 2001, doi: 10.1126/SCIENCE.291.5508.1544.
- [280] H. Hemmi *et al.*, “A Toll-like receptor recognizes bacterial DNA,” *Nat.* 2000 4086813, vol. 408, no. 6813, pp. 740–745, Dec. 2000, doi: 10.1038/35047123.
- [281] J. Lunney and G. Ashwell, “A hepatic receptor of avian origin capable of binding specifically modified glycoproteins,” *Proc. Natl. Acad. Sci. U. S. A.*, vol. 73, no. 2, pp. 341–343, 1976, doi: 10.1073/PNAS.73.2.341.
- [282] F. Heil *et al.*, “Species-specific recognition of single-stranded RNA via toll-like receptor 7 and 8,” *Science*, vol. 303, no. 5663, pp. 1526–1529, Mar. 2004, doi: 10.1126/SCIENCE.1093620.
- [283] S. S. Diebold, T. Kaisho, H. Hemmi, S. Akira, and C. Reis E Sousa, “Innate antiviral responses by means of TLR7-mediated recognition of single-stranded RNA,” *Science*, vol. 303, no. 5663, pp. 1529–1531, Mar. 2004, doi: 10.1126/SCIENCE.1093616.
- [284] G. M. Barton, J. C. Kagan, and R. Medzhitov, “Intracellular localization of Toll-like receptor 9 prevents recognition of self DNA but facilitates access to viral DNA,” *Nat. Immunol.*, vol. 7, no. 1, pp. 49–56, Jan. 2006, doi: 10.1038/NI1280.
- [285] L. Alexopoulou, A. C. Holt, R. Medzhitov, and R. A. Flavell, “Recognition of double-stranded RNA and activation of NF- κ B by Toll-like receptor 3,” *Nat.* 2001 4136857, vol. 413, no. 6857, pp. 732–738, Oct. 2001, doi: 10.1038/35099560.
- [286] Y. G. Kim, J. H. Park, M. H. Shaw, L. Franchi, N. Inohara, and G. Núñez, “The cytosolic sensors Nod1 and Nod2 are critical for bacterial recognition and host defense after exposure to Toll-like receptor ligands,” *Immunity*, vol. 28, no. 2, pp. 246–257, Feb. 2008, doi: 10.1016/J.IMMUNI.2007.12.012.
- [287] J. Rehwinkel and M. U. Gack, “RIG-I-like receptors: their regulation and roles in RNA

- sensing," *Nat. Rev. Immunol.* 2020 209, vol. 20, no. 9, pp. 537–551, Mar. 2020, doi: 10.1038/s41577-020-0288-3.
- [288] M. Yoneyama *et al.*, "The RNA helicase RIG-I has an essential function in double-stranded RNA-induced innate antiviral responses," *Nat. Immunol.*, vol. 5, no. 7, pp. 730–737, Jul. 2004, doi: 10.1038/NI1087.
- [289] J. J. Siew and Y. Chern, "Microglial lectins in health and neurological diseases," *Front. Mol. Neurosci.*, vol. 11, p. 356252, May 2018, doi: 10.3389/FNMOL.2018.00158/BIBTEX.
- [290] K. S. Midwood and A. M. Piccinini, "DAMPening inflammation by modulating TLR signalling," *Mediators Inflamm.*, vol. 2010, 2010, doi: 10.1155/2010/672395.
- [291] J. K. Olson and S. D. Miller, "Microglia initiate central nervous system innate and adaptive immune responses through multiple TLRs," *J. Immunol.*, vol. 173, no. 6, pp. 3916–3924, Sep. 2004, doi: 10.4049/JIMMUNOL.173.6.3916.
- [292] M. Bsibsi, R. Ravid, D. Gveric, and J. M. Van Noort, "Broad Expression of Toll-Like Receptors in the Human Central Nervous System," *J. Neuropathol. Exp. Neurol.*, vol. 61, no. 11, pp. 1013–1021, Nov. 2002, doi: 10.1093/JNEN/61.11.1013.
- [293] V. Kumar, "Toll-like receptors in the pathogenesis of neuroinflammation," *J. Neuroimmunol.*, vol. 332, pp. 16–30, Jul. 2019, doi: 10.1016/J.JNEUROIM.2019.03.012.
- [294] J. A. Rodríguez-Gómez *et al.*, "Microglia: Agents of the CNS Pro-Inflammatory Response," *Cells* 2020, Vol. 9, Page 1717, vol. 9, no. 7, p. 1717, Jul. 2020, doi: 10.3390/CELLS9071717.
- [295] C. S. Subhramanyam, C. Wang, Q. Hu, and S. T. Dheen, "Microglia-mediated neuroinflammation in neurodegenerative diseases," *Semin. Cell Dev. Biol.*, vol. 94, pp. 112–120, Oct. 2019, doi: 10.1016/J.SEMCDB.2019.05.004.
- [296] S. T. T. Schetters, D. Gomez-Nicola, J. J. Garcia-Vallejo, and Y. Van Kooyk, "Neuroinflammation: Microglia and T cells get ready to tango," *Front. Immunol.*, vol. 8, no. JAN, p. 294587, Jan. 2018, doi: 10.3389/FIMMU.2017.01905/BIBTEX.
- [297] S. A. Amici, J. Dong, and M. Guerau-de-Arellano, "Molecular Mechanisms Modulating the Phenotype of Macrophages and Microglia," *Front. Immunol.*, vol. 8, no. NOV, Nov. 2017, doi: 10.3389/FIMMU.2017.01520.
- [298] A. Shemer *et al.*, "Interleukin-10 Prevents Pathological Microglia Hyperactivation following Peripheral Endotoxin Challenge," *Immunity*, vol. 53, no. 5, pp. 1033-

- 1049.e7, Nov. 2020, doi: 10.1016/J.IMMUNI.2020.09.018.
- [299] C. Cunningham, D. C. Wilcockson, S. Campion, K. Lunnon, and V. H. Perry, "Central and systemic endotoxin challenges exacerbate the local inflammatory response and increase neuronal death during chronic neurodegeneration," *J. Neurosci.*, vol. 25, no. 40, pp. 9275–9284, Oct. 2005, doi: 10.1523/JNEUROSCI.2614-05.2005.
- [300] I. C. M. Hoogland, C. Houbolt, D. J. van Westerloo, W. A. van Gool, and D. van de Beek, "Systemic inflammation and microglial activation: systematic review of animal experiments," *J. Neuroinflammation*, vol. 12, no. 1, Jun. 2015, doi: 10.1186/S12974-015-0332-6.
- [301] C. R. A. Batista, G. F. Gomes, E. Candelario-Jalil, B. L. Fiebich, and A. C. P. de Oliveira, "Lipopolysaccharide-Induced Neuroinflammation as a Bridge to Understand Neurodegeneration," *Int. J. Mol. Sci.*, vol. 20, no. 9, May 2019, doi: 10.3390/IJMS20092293.
- [302] E. Hetier *et al.*, "Brain macrophages synthesize interleukin-1 and interleukin-1 mRNAs in vitro," *J. Neurosci. Res.*, vol. 21, no. 2–4, pp. 391–397, 1988, doi: 10.1002/JNR.490210230.
- [303] M. Sawada, N. Kondo, A. Suzumura, and T. Marunouchi, "Production of tumor necrosis factor-alpha by microglia and astrocytes in culture," *Brain Res.*, vol. 491, no. 2, pp. 394–397, Jul. 1989, doi: 10.1016/0006-8993(89)90078-4.
- [304] A. Poltorak *et al.*, "Defective LPS signaling in C3H/HeJ and C57BL/10ScCr mice: mutations in Tlr4 gene," *Science*, vol. 282, no. 5396, pp. 2085–2088, Dec. 1998, doi: 10.1126/SCIENCE.282.5396.2085.
- [305] R. Medzhitov, P. Preston-Hurlburt, and C. A. Janeway, "A human homologue of the Drosophila Toll protein signals activation of adaptive immunity," *Nat.* 1997 3886640, vol. 388, no. 6640, pp. 394–397, 1997, doi: 10.1038/41131.
- [306] K. A. Fitzgerald *et al.*, "Mal (MyD88-adaptor-like) is required for Toll-like receptor-4 signal transduction," *Nat.* 2001 4136851, vol. 413, no. 6851, pp. 78–83, Sep. 2001, doi: 10.1038/35092578.
- [307] T. Kawai and S. Akira, "The role of pattern-recognition receptors in innate immunity: update on Toll-like receptors," *Nat. Immunol.* 2010 115, vol. 11, no. 5, pp. 373–384, Apr. 2010, doi: 10.1038/ni.1863.
- [308] S. Lehnardt *et al.*, "Activation of innate immunity in the CNS triggers neurodegeneration through a Toll-like receptor 4-dependent pathway," *Proc. Natl.*

- Acad. Sci. U. S. A.*, vol. 100, no. 14, pp. 8514–8519, Jul. 2003, doi: 10.1073/PNAS.1432609100.
- [309] S. Bachiller *et al.*, “Microglia in neurological diseases: A road map to brain-disease dependent-inflammatory response,” *Front. Cell. Neurosci.*, vol. 12, p. 403344, Dec. 2018, doi: 10.3389/FNCEL.2018.00488/BIBTEX.
- [310] M. Song *et al.*, “TLR4 mutation reduces microglial activation, increases A β deposits and exacerbates cognitive deficits in a mouse model of Alzheimer’s disease,” *J. Neuroinflammation*, vol. 8, p. 92, Aug. 2011, doi: 10.1186/1742-2094-8-92.
- [311] J. M. Pocock and H. Kettenmann, “Neurotransmitter receptors on microglia,” *Trends Neurosci.*, vol. 30, no. 10, pp. 527–535, Oct. 2007, doi: 10.1016/j.tins.2007.07.007.
- [312] S. V. V. JL, T. MÈ, and J. B, “Microglial subtypes: diversity within the microglial community,” *EMBO J.*, vol. 38, no. 17, Sep. 2019, doi: 10.15252/EMBJ.2019101997.
- [313] V. A *et al.*, “Sex-Specific Features of Microglia from Adult Mice,” *Cell Rep.*, vol. 23, no. 12, pp. 3501–3511, Jun. 2018, doi: 10.1016/J.CELREP.2018.05.048.
- [314] S. Ghosh, E. Castillo, E. S. Frias, and R. A. Swanson, “Bioenergetic regulation of microglia,” *Glia*, vol. 66, no. 6, pp. 1200–1212, Jun. 2018, doi: 10.1002/GLIA.23271.
- [315] C. Lauro and C. Limatola, “Metabolic Reprograming of Microglia in the Regulation of the Innate Inflammatory Response,” *Front. Immunol.*, vol. 11, p. 523362, Mar. 2020, doi: 10.3389/FIMMU.2020.00493/BIBTEX.
- [316] I. R. Holtman, D. Skola, and C. K. Glass, “Transcriptional control of microglia phenotypes in health and disease,” *J. Clin. Invest.*, vol. 127, no. 9, p. 3220, Sep. 2017, doi: 10.1172/JCI90604.
- [317] E. Sun, A. Motolani, L. Campos, and T. Lu, “The Pivotal Role of NF- κ B in the Pathogenesis and Therapeutics of Alzheimer’s Disease,” 2022, doi: 10.3390/ijms23168972.
- [318] T. Liu, L. Zhang, D. Joo, and S. C. Sun, “NF- κ B signaling in inflammation,” *Signal Transduct. Target. Ther.* 2017 21, vol. 2, no. 1, pp. 1–9, Jul. 2017, doi: 10.1038/sigtrans.2017.23.
- [319] T. Kawai and S. Akira, “Signaling to NF- κ B by Toll-like receptors,” *Trends Mol. Med.*, vol. 13, no. 11, pp. 460–469, Nov. 2007, doi: 10.1016/j.molmed.2007.09.002.
- [320] I. Amit, D. R. Winter, and S. Jung, “The role of the local environment and epigenetics in shaping macrophage identity and their effect on tissue homeostasis,” *Nat. Immunol.*, vol. 17, no. 1, pp. 18–25, Jan. 2016, doi: 10.1038/NI.3325.

- [321] H. Yeh and T. Ikezu, "Transcriptional and Epigenetic Regulation of Microglia in Health and Disease," *Trends Mol. Med.*, vol. 25, no. 2, pp. 96–111, Feb. 2019, doi: 10.1016/j.molmed.2018.11.004.
- [322] M. Cheray and B. Joseph, "Epigenetics control microglia plasticity," *Front. Cell. Neurosci.*, vol. 12, p. 389563, Aug. 2018, doi: 10.3389/FNCEL.2018.00243/BIBTEX.
- [323] X. Li *et al.*, "Transcriptional and epigenetic decoding of the microglial aging process," *Nat. Aging* 2023 310, vol. 3, no. 10, pp. 1288–1311, Sep. 2023, doi: 10.1038/s43587-023-00479-x.
- [324] R. Martins-Ferreira, B. Leal, P. P. Costa, and E. Ballestar, "Microglial innate memory and epigenetic reprogramming in neurological disorders," *Prog. Neurobiol.*, vol. 200, p. 101971, May 2021, doi: 10.1016/J.PNEUROBIO.2020.101971.
- [325] M. Huang *et al.*, "Microglial immune regulation by epigenetic reprogramming through histone H3K27 acetylation in neuroinflammation," *Front. Immunol.*, vol. 14, p. 1052925, Mar. 2023, doi: 10.3389/FIMMU.2023.1052925/BIBTEX.
- [326] X. Zhang *et al.*, "Epigenetic regulation of innate immune memory in microglia," *J. Neuroinflammation*, vol. 19, no. 1, pp. 1–19, Dec. 2022, doi: 10.1186/S12974-022-02463-5/FIGURES/2.
- [327] E. K. Greenwood and D. R. Brown, "Senescent microglia: The key to the ageing brain?," *International Journal of Molecular Sciences*, vol. 22, no. 9. MDPI AG, p. 4402, May 01, 2021, doi: 10.3390/ijms22094402.
- [328] H. Keren-Shaul *et al.*, "A Unique Microglia Type Associated with Restricting Development of Alzheimer's Disease," *Cell*, vol. 169, no. 7, pp. 1276–1290.e17, Jun. 2017, doi: 10.1016/J.CELL.2017.05.018.
- [329] H. Mathys *et al.*, "Temporal Tracking of Microglia Activation in Neurodegeneration at Single-Cell Resolution," *Cell Rep.*, vol. 21, no. 2, pp. 366–380, Oct. 2017, doi: 10.1016/J.CELREP.2017.09.039.
- [330] B. A. Friedman *et al.*, "Diverse Brain Myeloid Expression Profiles Reveal Distinct Microglial Activation States and Aspects of Alzheimer's Disease Not Evident in Mouse Models," *Cell Rep.*, vol. 22, no. 3, pp. 832–847, Jan. 2018, doi: 10.1016/J.CELREP.2017.12.066.
- [331] S. Wang *et al.*, " α -Synuclein, a chemoattractant, directs microglial migration via H2O2-dependent Lyn phosphorylation," *Proc. Natl. Acad. Sci. U. S. A.*, vol. 112, no. 15, pp. E1926–E1935, Apr. 2015, doi: 10.1073/PNAS.1417883112.

- [332] I. M. Chiu *et al.*, “A neurodegeneration-specific gene expression signature and immune profile of acutely isolated microglia from an ALS mouse model,” *Cell Rep.*, vol. 4, no. 2, p. 385, Jul. 2013, doi: 10.1016/J.CELREP.2013.06.018.
- [333] Q. Li *et al.*, “Developmental Heterogeneity of Microglia and Brain Myeloid Cells Revealed by Deep Single-Cell RNA Sequencing,” *Neuron*, vol. 101, no. 2, pp. 207-223.e10, Jan. 2019, doi: 10.1016/J.NEURON.2018.12.006.
- [334] S. Smajic *et al.*, “Single-cell sequencing of human midbrain reveals glial activation and a Parkinson-specific neuronal state,” *Brain*, vol. 145, no. 3, pp. 964–978, Mar. 2022, doi: 10.1093/BRAIN/AWAB446.
- [335] H. A. Vecchiarelli and M.-È. Tremblay, “Microglial Transcriptional Signatures in the Central Nervous System: Toward A Future of Unraveling Their Function in Health and Disease,” *Annu. Rev. Genet.*, vol. 57, no. 1, Nov. 2023, doi: 10.1146/ANNUREV-GENET-022223-093643.
- [336] S. Hickman, S. Izzy, P. Sen, L. Morsett, and J. El Khoury, “Microglia in neurodegeneration,” *Nat. Neurosci.*, vol. 21, no. 10, pp. 1359–1369, Oct. 2018, doi: 10.1038/S41593-018-0242-X.
- [337] G. Y *et al.*, “MicroRNAs in Microglia: How do MicroRNAs Affect Activation, Inflammation, Polarization of Microglia and Mediate the Interaction Between Microglia and Glioma?,” *Front. Mol. Neurosci.*, vol. 12, Feb. 2019, doi: 10.3389/FNMOL.2019.00125.
- [338] D. Brites, “Regulatory function of microRNAs in microglia,” *Glia*, vol. 68, no. 8, pp. 1631–1642, Aug. 2020, doi: 10.1002/GLIA.23846.
- [339] R. W. Freilich, M. E. Woodbury, and T. Ikezu, “Integrated Expression Profiles of mRNA and miRNA in Polarized Primary Murine Microglia,” *PLoS One*, vol. 8, no. 11, p. e79416, Nov. 2013, doi: 10.1371/JOURNAL.PONE.0079416.
- [340] A. L. Cardoso, J. R. Guedes, L. Pereira de Almeida, and M. C. Pedroso de Lima, “miR-155 modulates microglia-mediated immune response by down-regulating SOCS-1 and promoting cytokine and nitric oxide production,” *Immunology*, vol. 135, no. 1, pp. 73–88, Jan. 2012, doi: 10.1111/J.1365-2567.2011.03514.X.
- [341] D. Marangon, J. H. Castro e Silva, and D. Lecca, “Neuronal and Glial Communication via Non-Coding RNAs: Messages in Extracellular Vesicles,” *Int. J. Mol. Sci.*, vol. 24, no. 1, Jan. 2022, doi: 10.3390/IJMS24010470.
- [342] L. Zuo, Z. Wang, Y. Tan, X. Chen, and X. Luo, “piRNAs and Their Functions in the

- Brain," *Int. J. Hum. Genet.*, vol. 16, no. 1–2, p. 53, Mar. 2016, doi: 10.1080/09723757.2016.11886278.
- [343] M. DiGiacomo *et al.*, "Multiple Epigenetic Mechanisms and the piRNA Pathway Enforce LINE1 Silencing during Adult Spermatogenesis," *Mol. Cell*, vol. 50, no. 4, pp. 601–608, May 2013, doi: 10.1016/j.molcel.2013.04.026.
- [344] M. Pons-Espinal *et al.*, "MiR-135a-5p Is Critical for Exercise-Induced Adult Neurogenesis," *Stem Cell Reports*, vol. 12, no. 6, pp. 1298–1312, Jun. 2019, doi: 10.1016/j.stemcr.2019.04.020.
- [345] H. Babu, J. H. Claasen, S. Kannan, A. E. Rünker, T. Palmer, and G. Kempermann, "A protocol for isolation and enriched monolayer cultivation of neural precursor cells from mouse dentate gyrus," *Front. Neurosci.*, vol. 5, no. JUL, 2011, doi: 10.3389/fnins.2011.00089.
- [346] T. L. Walker and G. Kempermann, "One mouse, two cultures: Isolation and culture of adult neural stem cells from the two neurogenic zones of individual mice," *J. Vis. Exp.*, no. 84, Feb. 2014, doi: 10.3791/51225.
- [347] M. Pons-Espinal *et al.*, "Synergic Functions of miRNAs Determine Neuronal Fate of Adult Neural Stem Cells," *Stem Cell Reports*, vol. 8, no. 4, pp. 1046–1061, Apr. 2017, doi: 10.1016/j.stemcr.2017.02.012.
- [348] S. Jung *et al.*, "Analysis of fractalkine receptor CX(3)CR1 function by targeted deletion and green fluorescent protein reporter gene insertion," *Mol. Cell. Biol.*, vol. 20, no. 11, pp. 4106–4114, Jun. 2000, doi: 10.1128/MCB.20.11.4106-4114.2000.
- [349] P. B. Andersson, V. H. Perry, and S. Gordon, "The acute inflammatory response to lipopolysaccharide in cns parenchyma differs from that in other body tissues," *Neuroscience*, vol. 48, no. 1, pp. 169–186, May 1992, doi: 10.1016/0306-4522(92)90347-5.
- [350] J. Rodhe, "Cell Culturing of Human and Murine Microglia Cell Lines," *Methods Mol. Biol.*, vol. 1041, pp. 11–16, 2013, doi: 10.1007/978-1-62703-520-0_2.
- [351] C. Dello Russo *et al.*, "The human microglial HMC3 cell line: where do we stand? A systematic literature review," *J. Neuroinflammation* 2018 151, vol. 15, no. 1, pp. 1–24, Sep. 2018, doi: 10.1186/S12974-018-1288-0.
- [352] S. Srakočić, P. Josić, S. Trifunović, S. Gajović, D. Grčević, and A. Glasnović, "Proposed practical protocol for flow cytometry analysis of microglia from the healthy adult mouse brain: Systematic review and isolation methods' evaluation," *Front. Cell.*

- Neurosci.*, vol. 16, p. 1017976, Oct. 2022, doi: 10.3389/FNCEL.2022.1017976/BIBTEX.
- [353] B. Czech *et al.*, “piRNA-Guided Genome Defense: From Biogenesis to Silencing,” *Annu. Rev. Genet.*, vol. 52, pp. 131–157, Nov. 2018, doi: 10.1146/ANNUREV-GENET-120417-031441.
- [354] M. Simon, M. Van Meter, J. Ablaeva, J. M. Sedivy, A. Seluanov, and V. Gorbunova, “LINE1 Derepression in Aged Wild-Type and SIRT6-Deficient Mice Drives Inflammation,” *Cell Metab.*, vol. 30, pp. 871–885, 2019, doi: 10.1016/j.cmet.2019.02.014.
- [355] N. Teerawattanapong, W. Udomsinprasert, S. Ngarmukos, A. Tanavalee, and S. Honsawek, “Blood leukocyte LINE-1 hypomethylation and oxidative stress in knee osteoarthritis,” 2017, doi: 10.1016/j.heliyon.2019.e01774.
- [356] K. E. Copley and J. Shorter, “Repetitive elements in aging and neurodegeneration,” 2023, doi: 10.1016/j.tig.2023.02.008.
- [357] M. A. Bonaguidi *et al.*, “In vivo clonal analysis reveals self-renewing and multipotent adult neural stem cell characteristics,” *Cell*, vol. 145, no. 7, p. 1142, Jun. 2011, doi: 10.1016/J.CELL.2011.05.024.
- [358] L. E. Clarke, S. A. Liddelow, C. Chakraborty, A. E. Münch, M. Heiman, and B. A. Barres, “Normal aging induces A1-like astrocyte reactivity,” *Proc. Natl. Acad. Sci. U. S. A.*, vol. 115, no. 8, pp. E1896–E1905, Feb. 2018, doi: 10.1073/pnas.1800165115.
- [359] M. Schouten *et al.*, “Circadian glucocorticoid oscillations preserve a population of adult hippocampal neural stem cells in the aging brain,” *Mol. Psychiatry*, vol. 25, no. 7, pp. 1382–1405, Jul. 2020, doi: 10.1038/s41380-019-0440-2.
- [360] A. Sierra *et al.*, “Neuronal hyperactivity accelerates depletion of neural stem cells and impairs hippocampal neurogenesis,” *Cell Stem Cell*, vol. 16, no. 5, pp. 488–503, May 2015, doi: 10.1016/j.stem.2015.04.003.
- [361] S. Camandola and M. P. Mattson, “Brain metabolism in health, aging, and neurodegeneration,” *EMBO J.*, vol. 36, no. 11, pp. 1474–1492, Jun. 2017, doi: 10.15252/EMBJ.201695810.
- [362] I. Antignano, Y. Liu, N. Offermann, and M. Capasso, “Aging microglia,” *Cell. Mol. Life Sci.*, vol. 80, no. 5, p. 126, May 2023, doi: 10.1007/S00018-023-04775-Y.
- [363] R. S. Balaban, S. Nemoto, and T. Finkel, “Mitochondria, oxidants, and aging,” *Cell*, vol. 120, no. 4, pp. 483–495, Feb. 2005, doi: 10.1016/J.CELL.2005.02.001.

- [364] I. Liguori *et al.*, "Oxidative stress, aging, and diseases," *Clin. Interv. Aging*, vol. 13, pp. 757–772, Jan. 2018, doi: 10.2147/CIA.S158513.
- [365] X. Z. Li *et al.*, "An ancient transcription factor initiates the burst of piRNA production during early meiosis in mouse testes," *Mol. Cell*, vol. 50, no. 1, pp. 67–81, Apr. 2013, doi: 10.1016/J.MOLCEL.2013.02.016.
- [366] N. A. Wallace, V. P. Belancio, and P. L. Deininger, "L1 mobile element expression causes multiple types of toxicity," *Gene*, vol. 419, no. 1–2, pp. 75–81, Aug. 2008, doi: 10.1016/J.GENE.2008.04.013.
- [367] Y. A. Savva *et al.*, "RNA editing regulates transposon-mediated heterochromatic gene silencing," *Nat. Commun.*, vol. 4, Nov. 2013, doi: 10.1038/NCOMMS3745.
- [368] J. G. Wood *et al.*, "Chromatin-modifying genetic interventions suppress age-associated transposable element activation and extend life span in *Drosophila*," *Proc. Natl. Acad. Sci. U. S. A.*, vol. 113, no. 40, pp. 11277–11282, Oct. 2016, doi: 10.1073/PNAS.1604621113/-/DCSUPPLEMENTAL.
- [369] N. F. Page *et al.*, "Alterations in Retrotransposition, Synaptic Connectivity, and Myelination Implicated by Transcriptomic Changes Following Maternal Immune Activation in Nonhuman Primates," *Biol. Psychiatry*, vol. 89, no. 9, pp. 896–910, May 2021, doi: 10.1016/j.biopsych.2020.10.016.
- [370] S. Ikhlas, A. Usman, D. Kim, and D. Cai, "Exosomes/microvesicles target SARS-CoV-2 via innate and RNA-induced immunity with PIWI-piRNA system," *Life Sci. alliance*, vol. 5, no. 3, p. e202101240, Mar. 2021, doi: 10.26508/LSA.202101240.
- [371] B. Yu, S. Ikhlas, C. Ruan, X. Zhong, and D. Cai, "Innate and Adaptive Immunity of Murine Neural Stem Cell-Derived piRNA Exosomes/Microvesicles against Pseudotyped SARS-CoV-2 and HIV-Based Lentivirus," *iScience*, vol. 23, no. 12, Dec. 2020, doi: 10.1016/J.ISCI.2020.101806.
- [372] Y. Ophinni, U. Palatini, Y. Hayashi, and N. F. Parrish, "piRNA-Guided CRISPR-like Immunity in Eukaryotes," *Trends Immunol.*, vol. 40, no. 11, pp. 998–1010, Nov. 2019, doi: 10.1016/J.IT.2019.09.003.
- [373] T. Deierborg, "Preparation of Primary Microglia Cultures from Postnatal Mouse and Rat Brains," *Methods Mol. Biol.*, vol. 1041, pp. 25–31, 2013, doi: 10.1007/978-1-62703-520-0_4.
- [374] Y. Lu, A. S. Baras, and M. K. Halushka, "miRge 2.0 for comprehensive analysis of microRNA sequencing data," *BMC Bioinformatics*, vol. 19, no. 1, Jul. 2018, doi:










10.1186/S12859-018-2287-Y.

- [375] "Index of /pub/release-67/fasta/mus_musculus/ncrna."
https://ftp.ensembl.org/pub/release-67/fasta/mus_musculus/ncrna/ (accessed Dec. 04, 2023).
- [376] R. H. Waterston *et al.*, "Initial sequencing and comparative analysis of the mouse genome," *Nat. 2003 4206915*, vol. 420, no. 6915, pp. 520–562, Dec. 2002, doi: 10.1038/nature01262.
- [377] "piRBase." <http://bigdata.ibp.ac.cn/piRBase/download.php> (accessed Dec. 04, 2023).

6 Appendix

SOURCE
DATATRANSPARENT
PROCESSOPEN
ACCESS

Piwi2 (Mili) sustains neurogenesis and prevents cellular senescence in the postnatal hippocampus

Caterina Gasperini¹ , Kiril Tuntevski^{1,2}, Silvia Beatini¹ , Roberta Pelizzoli¹, Amanda Lo Van¹, Damiano Mangoni³ , Rosa M Cossu³, Giovanni Pascarella⁴, Paolo Bianchini⁵, Pascal Bielefeld⁶, Margherita Scarpato³, Meritxell Pons-Espinal¹, Remo Sanges^{3,7} , Alberto Diaspro⁵ , Carlos P Fitzsimons⁶ , Piero Carninci^{4,8} , Stefano Gustincich³  & Davide De Pietri Tonelli^{1,*} 

Abstract

Adult neural progenitor cells (aNPCs) ensure lifelong neurogenesis in the mammalian hippocampus. Proper regulation of aNPC fate has thus important implications for brain plasticity and healthy aging. Piwi proteins and the small noncoding RNAs interacting with them (piRNAs) have been proposed to control memory and anxiety, but the mechanism remains elusive. Here, we show that Piwil2 (Mili) is essential for proper neurogenesis in the postnatal mouse hippocampus. RNA sequencing of aNPCs and their differentiated progeny reveal that Mili and piRNAs are dynamically expressed in neurogenesis. Depletion of Mili and piRNAs in the adult hippocampus impairs aNPC differentiation toward a neural fate, induces senescence, and generates reactive glia. Transcripts modulated upon Mili depletion bear sequences complementary or homologous to piRNAs and include repetitive elements and mRNAs encoding essential proteins for proper neurogenesis. Our results provide evidence of a critical role for Mili in maintaining fitness and proper fate of aNPCs, underpinning a possible involvement of the piRNA pathway in brain plasticity and successful aging.

Keywords hippocampal neurogenesis; Mili; Piwi-interacting RNAs; Piwil2; senescence

Subject Categories Neuroscience; RNA Biology

DOI 10.15252/embr.202153801 | Received 12 August 2021 | Revised 25 October 2022 | Accepted 10 November 2022 | Published online 6 December 2022

EMBO Reports (2023) 24: e53801

Introduction

A regulated balance of aNPC quiescence, proliferation, and differentiation guarantees lifelong neurogenesis in the adult hippocampus

(Altman, 1962; Doetsch *et al*, 1999), prevents the generation of reactive glia (Encinas *et al*, 2011; Sierra *et al*, 2015; Clarke *et al*, 2018), and curbs neurodegeneration (Toda *et al*, 2019). Understanding the molecular control of aNPCs fate is pivotal to develop novel therapies aimed at preventing or delay age-dependent loss of neurogenesis and related pathological conditions.

The *Piwi* genes encode for an evolutionary conserved subfamily of Argonaute proteins that bind to Piwi-interacting RNAs (piRNAs), a class of single-stranded noncoding RNAs of 21–35 nucleotides. Piwi proteins and piRNAs (henceforth referred to as the piRNA pathway) are highly abundant in gonads, where they mainly target transposable elements (TEs) for degradation to maintain germline stem cell pools and male fertility (Czech *et al*, 2018; Ozata *et al*, 2019). Since its initial discovery, the piRNA pathway has been also implicated in regulating gene expression outside gonads, particularly in somatic stem cells (Rojas-Riós & Simonelig, 2018). In fact, Piwi proteins are present in human hematopoietic stem cells, but their functions are dispensable for normal hematopoiesis in the mouse (Nolde *et al*, 2013), suggesting a possible role of the piRNA pathway in the control of self-renewal, rather than differentiation of these cells (Sharma *et al*, 2001).

Besides gonads, the highest piRNA expression in the adult mouse has been observed in the hippocampus (Perera *et al*, 2019), and proposed to control synaptic plasticity, memory, and anxiety (Lee *et al*, 2011; Zhao *et al*, 2015; Nandi *et al*, 2016; Leighton *et al*, 2019). piRNA abundance in neurons, however, is low compared to that of germline cells (Lee *et al*, 2011; Ghosheh *et al*, 2016; Nandi *et al*, 2016). Moreover, TE expression increases following the differentiation of NPC (Muotri *et al*, 2005), in parallel with the number of somatic TE insertions found in hippocampal neurons (Upton *et al*, 2015), arguing against functions of the piRNA pathway in postmitotic nerve cells. Given that the hippocampus is one of the niches in which neurogenesis persists beyond embryonic age, we

¹ Neurobiology of miRNA Laboratory, Istituto Italiano di Tecnologia, Genoa, Italy

² The Open University Affiliated Research Centre at Istituto Italiano di Tecnologia (ARC@IIT), Genoa, Italy

³ Central RNA Laboratory, Istituto Italiano di Tecnologia, Genoa, Italy

⁴ Division of Genomic Technologies, RIKEN Center for Life Science Technologies, Yokohama, Japan

⁵ Nanoscopy, CHT Erzelli, Istituto Italiano di Tecnologia, Genoa, Italy

⁶ Swammerdam Institute for Life Sciences, Faculty of Science, University of Amsterdam, Amsterdam, The Netherlands

⁷ Area of Neuroscience, SISSA, Trieste, Italy

⁸ Human Technopole, Milan, Italy

*Corresponding author. Tel: +39 010 2896 725; E-mail: davide.depietri@iit.it

hypothesize that the piRNA pathway may be present in aNPCs, possibly contributing to maintain the neurogenesis capacity lifelong (Penning *et al*, 2022).

Here, we studied the piRNA pathway in aNPCs of the postnatal mouse hippocampus *in vivo* and *in vitro*. By knockdown (KD) of Mili (i.e., one of the essential endoribonucleases for piRNA biogenesis and function) and Mili-dependent piRNAs, we investigated the consequences of their depletion for proliferation, survival, differentiation, and fate of aNPCs. With this approach, we aim to address functions of the piRNA pathway in adult neurogenesis, hence providing a system-level biological understanding of scientific and therapeutic value for brain plasticity and successful aging.

Results

Mili is preferentially expressed in aNPCs and depleted in neurogenesis

As an entry point to investigate the piRNA pathway in aNPCs we quantified the expression of *Piwi1* (Miwi) *Piwi2* (Mili) and *Piwi4* (Miwi2) transcripts, encoding the three main Piwi proteins present in the adult mouse (Czech *et al*, 2018; Ozata *et al*, 2019). Analysis of deep RNA sequencing (RNA seq) of total RNA from cultured aNPCs derived from neural stem cells (NSC) of the adult mouse Dentate Gyrus (DG) (Walker & Kempermann, 2014; Pons-Espinal *et al*, 2017) indicated that *Mili* is the most abundantly expressed of the three *Piwi* genes in neurogenesis (Fig 1A). In addition, other genes encoding for piRNA biogenesis cofactors were expressed in neurogenesis, including the transcription factors *Zic2*, *Mybl1*, and *Meis1*, the Tudor and KH domain-containing protein *Tdrkh*, and the helicase *Mov10* (Dataset EV1). Interestingly, *Mili* expression showed a dynamic trend in neurogenesis. Indeed, its expression increased transiently from proliferating aNPCs (here referred to as days of differentiation (DIF0)) showing a peak at DIF4 upon onset of their spontaneous differentiation, whereas it decreased in differentiated progeny (DIF7-14) (Fig 1A). Similarly, the Mili protein abundance was higher in undifferentiated aNPCs (DIF0), or early upon onset of vector-induced neurogenesis (DIF4), compared with neuroblasts and neurons (DIF7 and 14, respectively) (Fig 1B). Next, we quantified the abundance of Miwi and Mili proteins in the mouse testis, whole hippocampus, and undifferentiated aNPCs (Fig 1C and D). As expected, the Miwi protein was very abundant in the testis but almost undetectable in the whole hippocampus or aNPCs (Fig 1C), whereas the Mili protein abundance in aNPCs was about 40% of the one in the testes (Fig 1D), and about four-fold higher than in primary hippocampal neurons (Fig 1E).

To validate this finding *in vivo*, we used the split-Cre viral approach to selectively label NSCs and their progeny in the postnatal hippocampus of Td-Tomato Cre-reporter mice (Pons-Espinal *et al*, 2017). Five days postviral injection (dpi), we found Mili protein in Td-Tomato positive (Td⁺) NSCs of the subgranular zone (SGZ) of the DG (Fig 1F). To corroborate the immunofluorescence result, and to follow *Mili* expression during neurogenesis *in vivo*, we sorted Td⁺ NSCs and their differentiated progeny at 10 and 30 dpi in the postnatal mouse hippocampus, respectively, and quantified *Mili* by real-time quantitative PCR (qPCR). The *Mili* transcript was significantly more abundant in Td⁺ NSCs (10 dpi) than in

adult-born Td⁺ neurons (30 dpi) or Td⁻ cells (Fig 1G). These results indicate that Mili expression is dynamic in neurogenesis, being enriched in neural stem/progenitor cells and depleted in their differentiated progeny.

Identification and validation of piRNAs in aNPCs

Next, we used RNA seq. to investigate the presence of endogenous piRNAs in undifferentiated aNPCs (DIF0), or upon onset of vector-induced neurogenesis (DIF4-7). To eliminate the possibility of ribosomal RNA (rRNA) or full-length transfer RNA (tRNA) contaminations, we performed small RNA size selection during library preparation. Following a previously published analysis pipeline (Ghosheh *et al*, 2016), we identified a total of 725,472 putative piRNAs, and using stringent criteria, we focused the subsequent analyses on the 571,439 small noncoding RNAs that perfectly aligned (i.e., no mismatch) with mouse piRNA previously annotated in the piRNA database (piRBase, Zhang *et al*, 2014). Putative piRNAs in aNPCs had a peak length of 30 nt (Fig 2A) and bore a 5' uridine (U) bias (Fig 2B), in agreement with previous reports in the brain of adult mice (Ghosheh *et al*, 2016). Moreover, the nucleotide-pair distance probability between the 5' termini of putative primary and secondary piRNAs was distributed similarly to that of other animals (Gainetdinov *et al*, 2018), with asymptotic convergence around the "0" mark on the abscissa (Fig 2C). Mature piRNAs typically bear 2'-O-methylation at their 3' termini, which confers them stability and enables stronger binding to Piwi proteins (Czech *et al*, 2018; Ozata *et al*, 2019). Thereby, we asked whether the endogenous piRNAs isolated from aNPCs were also methylated by evaluating their resistance to periodate oxidation and alkaline β -elimination, as previously reported (Kirino & Mourelatos, 2007). As controls, we used a synthetic piRNA bearing or lacking, a 2'-O-methylation in its 3' end. As expected, the unmethylated synthetic piRNA was degraded after sodium periodate treatment, whereas the methylated one was preserved, as indicated by (qPCR)-based small RNA assay (TaqMan) (Fig 2D). Small RNAs isolated from aNPCs were subject to periodate treatment in the same experiment. As expected, endogenous unmethylated small noncoding RNAs, such as snoRNA-202 and -135, were degraded; whereas four of the most abundant endogenous piRNA-cluster consensus sequences (piCS, i.e., extended by qPCR primers bearing specificity for shared sequences among different clusters) identified in aNPCs exhibited resistance to periodate treatment, thus indicating their methylation (Fig 2D). We then addressed the Mili-dependence of the endogenous piRNAs. To this aim, we used three independent strategies to achieve *Mili* KD in aNPCs (Figs 2E and EV1A and B). Specifically, we transduced short-hairpin RNAs targeting *Mili* transcripts through a lentiviral vector, and transfected two different synthetic antisense oligonucleotides (GapmeRs) targeting distinct *Mili* regions (Fig 4A). Indeed, KD of *Mili* in aNPCs was sufficient to deplete four of the most abundant endogenous piCS (Figs 2F and EV1C), in agreement with the observation that Mili is the main Piwi protein in these cells (Fig 1). Of note, this manipulation did not affect *Miwi* expression, excluding possible compensatory effects on piRNA biogenesis in aNPCs (Fig EV1D). PiRNAs interact with Piwi proteins to form functional complexes. To examine whether endogenous Mili and piRNAs associate in aNPCs, we immunoprecipitated (IP) the Mili protein from differentiating aNPCs (DIF4, i.e., at the peak of Mili expression; the

specificity of the anti-Mili antibody used for the IP was validated by western blotting of lysates from the testis of Mili null and control adult mice, Fig EV1E). IP with IgG was also included as a control for nonspecific binding (Fig 2G). To determine the size distribution of RNAs co-precipitated with Mili, we used capillary electrophoresis on

microfluidic chips. This analysis indicated that the peak size distribution of Mili-bound RNAs in aNPCs was 25 nt (Fig 2H), in agreement with the known size of Mili-bound piRNAs in the mouse testis (Ding et al, 2017). Real-time qPCR confirmed that five of the most abundant endogenous piCS identified in aNPCs were enriched in the

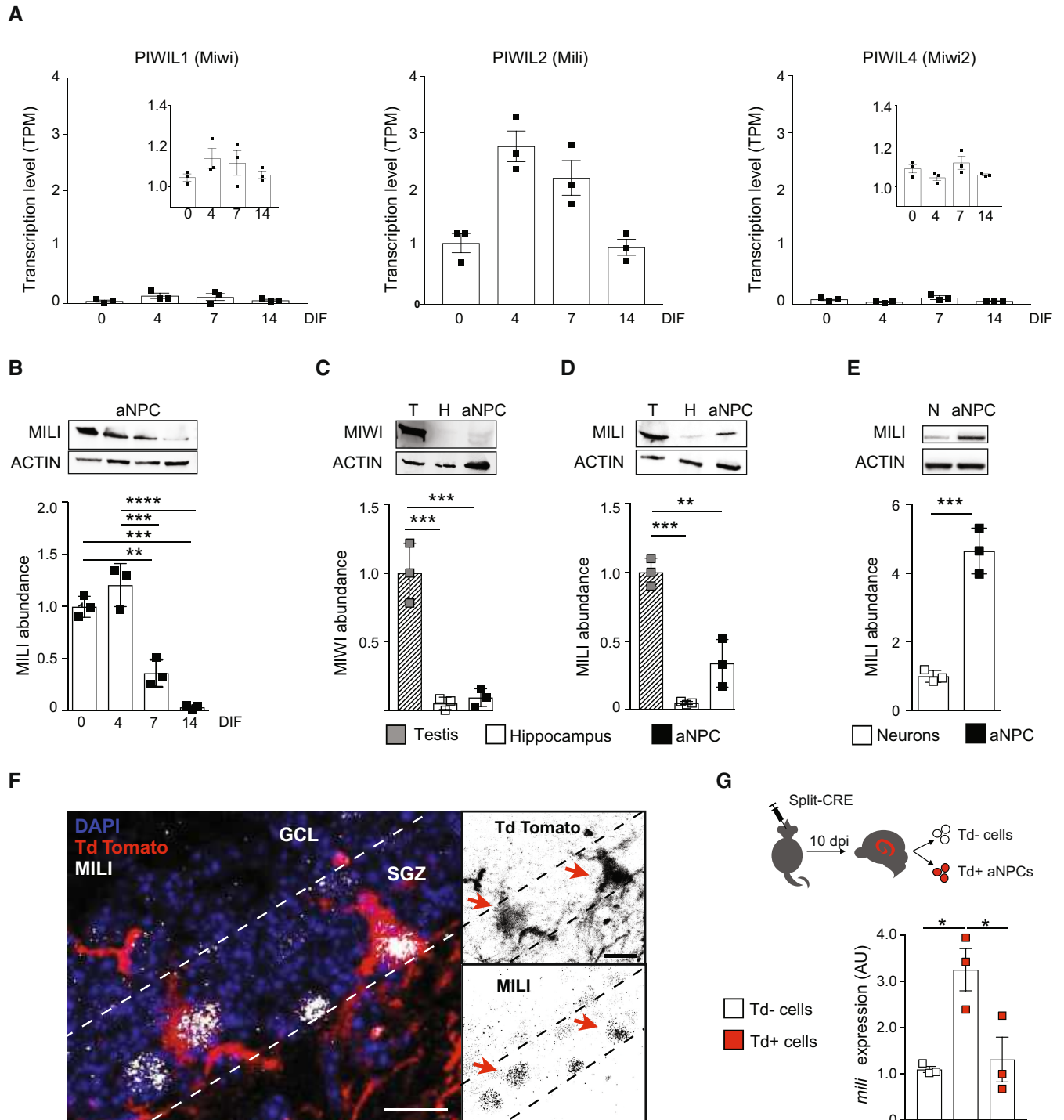


Figure 1.

Figure 1. Mili is preferentially expressed in aNPCs and depleted in neurogenesis.

- A Levels of *Piwi1* (*Miwi*), *Piwi2* (*Mili*), and *Piwi4* (*Miwi2*) transcripts in RNA seq. data from undifferentiated aNPCs (Days of differentiation—DIF—0) and differentiating neuroblasts (DIF4–14); insets in left and right panels show the same data with smaller scales in the ordinate axes.
- B Western blot (inset) and quantification (bar graph) of *Mili* protein abundance in DIF0 aNPCs and differentiating neuroblasts upon viral-induced neurogenesis (DIF4–14).
- C, D Western blot (insets) and quantification (bar graphs) of *Miwi* and *Mili* protein abundance in lysates from postnatal mouse testis, hippocampus, and undifferentiated aNPCs cultures.
- E Western blot (inset) and quantification (bar graph) of *Mili* protein abundance in lysates from cultured mouse hippocampal neurons and undifferentiated aNPCs.
- F Representative immunofluorescence micrograph of *Mili* (white) and Td⁺ NSCs (red) in hippocampal subgranular zone (SGZ); arrows indicate Td⁺ *Mili*⁺ double-positive cells.
- G Scheme of the experiment (top) and *Mili* mRNA expression in sorted Td⁺ and Td⁻ cells after *in vivo* transduction with split-Cre viruses in the hippocampus (bottom).

Data information: data are expressed as mean \pm SEM, $n = 3$ biological replicates. * $P < 0.05$, ** $P < 0.01$, *** $P < 0.001$, **** $P < 0.0001$ as assessed by one-way ANOVA with the Bonferroni test (in B–D, G) and the two-tailed Student's t -test (in E). In (F): GCL, granular cell layer; H, Hilus. The scale bars represent 10 μ m. Source data are available online for this figure.

Mili-IP compared with the control IP (Fig 2I). Together these results indicate that *Mili* and piRNAs are co-expressed and interact in aNPCs.

Expression of piRNAs parallels *Mili* abundance in neurogenesis

Analysis of small RNAs seq in undifferentiated aNPCs (DIF0), or upon onset of vector-induced neurogenesis (DIF4–7) showed that piRNAs were dynamically expressed, peaking at the onset of differentiation (DIF4) (Figs 3A and EV2A), in agreement with the *Mili* expression pattern (Fig 1). To validate this observation, we sorted Td⁺ NSCs from the adult hippocampus and quantified levels of four of the most abundant piCS, confirming their expression *in vivo* (Fig 3B). Genomic mapping of the piRNA reads from aNPCs and their progeny identified 298 clusters perfectly aligning to the mouse genome (Fig 3C and Dataset EV2). These clusters had an average length of 168 bases, with some exceeding 2,000 bases, as previously seen in mouse testis (Aravin *et al.*, 2006; Girard *et al.*, 2006). The piRNA raw reads/cluster averaged around 4,700 reads, with two clusters, one located in chromosome 13 and one in the 17, giving rise to more than 80,000 piRNA reads (Fig 3C). Analysis of small RNA seq data for directionality suggested a strand bias, where the majority of the piRNAs arise unidirectionally, although some piRNAs were found to be homologous to both strands and at different loci. Of note, one of the clusters in our dataset (hereafter referred to piR-cluster 1, Dataset EV2) is homologous to the human piR-61648 that was recently shown to be selectively expressed in somatic tissues but depleted in gonads (Torres *et al.*, 2019; Fig EV2B). In agreement, analysis of small RNA datasets from the RIKEN FANTOM5 project (De Rie *et al.*, 2017) showed an enriched expression of the piRNAs bearing sequence homology to piR-cluster 1, as well as of many additional piRNA clusters in human NSCs compared with differentiated brain cells (Fig EV2C and Dataset EV3). Together, these results indicate that *Mili*-dependent piRNAs are more abundant in neural stem/progenitor cells than in their differentiated progeny, thus matching the expression of *Mili*.

Depletion of *Mili* and piRNAs impairs neurogenesis and increases astrogliosis

To infer functions of the piRNA pathway in neurogenesis, we KD *Mili* in aNPCs and investigated the consequences of *Mili* and

piRNA depletion for their proliferation, survival, differentiation, and fate. *Mili* KD did not alter aNPC stemness or proliferation (Fig EV3A), but it led to a dramatic increase in the expression of the astrocyte marker glial fibrillary acidic protein (GFAP) *in vitro* (Fig EV3B). Next, we KD *Mili* *in vivo* by injecting two different GapmeRs antisense to the *Mili* transcript (GapmeR1 shown in Fig 4; GapmeR3 shown in Fig EV3C), or a scrambled GapmeR (Control) in the DG of postnatal mouse hippocampus (Figs 4A–G and EV3D and E). Inspection of brain sections 30 days after bilateral injections indicated a marked increase in GFAP⁺ cells that showed enlarged somas in the ipsilateral hippocampus injected with GapmeR antisense to *Mili*, compared with the contralateral side injected with control GapmeR (Figs 4D and EV3D). Quantification of GFAP protein (fluorescence intensity) and transcript in *Mili* KD hippocampus (Figs 4E and EV3D) confirmed this observation. To ascertain whether GFAP⁺ cells were actively generated upon *Mili* KD, we labeled dividing cells by administration of bromodeoxyuridine (BrdU) in a third cohort of mice, immediately after GapmeRs injection (Figs 4F and EV3E). Thirty days after, we found that *Mili* KD led to a significant increase in adult-born GFAP⁺BrdU⁺ glial cells at the expense of NeuN⁺BrdU⁺ neurons (Figs 4F and EV3E). This result was corroborated by RNA seq dataset analysis from differentiating aNPCs *in vitro*, showing an enrichment in the expression of astrocyte-related genes and a concomitant deregulation of neuronal fate genes upon *Mili* KD (Fig EV3F). These results indicate that *Mili* sustains neurogenesis in the postnatal hippocampus, at the expense of gliogenesis. Increased GFAP expression is generally regarded as a hallmark of astrocytic reactivity (Escartin *et al.*, 2021). In agreement, we observed a significant increase in the levels of known reactive glial markers (Liddelov *et al.*, 2017; Clarke *et al.*, 2018) upon *Mili* KD in the postnatal hippocampus (Fig 4G). To corroborate this result, we took advantage of Kainic Acid (KA) injection in the postnatal hippocampus of mice expressing GFP under the control of the NSCs/NPCs specific promoter *Nestin* (Fig 4H), a treatment previously shown to induce aNSC conversion into reactive glia (Sierra *et al.*, 2015; Bielefeld *et al.*, 2017). Indeed, this treatment reduced the levels of *Mili* and one of the most abundant piCS-bearing sequence homology to piR-cluster 1 in sorted *Nestin*-GFP⁺ NSCs (Fig 4H). Altogether, these results demonstrate that *Mili* functions are essential for proper neurogenesis and prevent reactive gliogenesis in the postnatal mouse hippocampus.

Depletion of Mili and piRNAs in aNPCs results in senescence-associated phenotypes

Conversion of hippocampal NSC into reactive glia at the expense of neurogenesis has been related to increased neuroinflammation and cellular senescence (Martín-Suárez *et al*, 2019; Babcock *et al*, 2021), and it has been observed in normal aging (Clarke *et al*, 2018). The involvement of the piRNA pathway in these mechanisms is unknown. We investigated whether the depletion of Mili and piRNA induces senescence-associated secretory phenotype (SASP), β -galactosidase activity (β -gal) and cell cycle exit, known hallmarks of

an aged hippocampal niche (Ahlenius *et al*, 2009; Encinas *et al*, 2011; Jin *et al*, 2021). In agreement with the *in vivo* phenotypes, Mili KD in aNPCs cultures induced a significant increase in the expression of several genes encoding immune-modulatory and SASP proteins in neuroblasts (DIF4), compared with control cells (Fig 5A). Moreover, Mili KD resulted in a higher proportion of cells positive for β -gal as early as 48 h upon induction of their spontaneous differentiation (Fig 5B). At the same time point, we immunostained aNPCs with anti-Ki67 (a protein that is expressed in all phases of the cell cycle except G0 and early G1; Yu, 1992) and anti-BrdU antibodies. Quantification of the BrdU⁺ and Ki67⁻ cells over

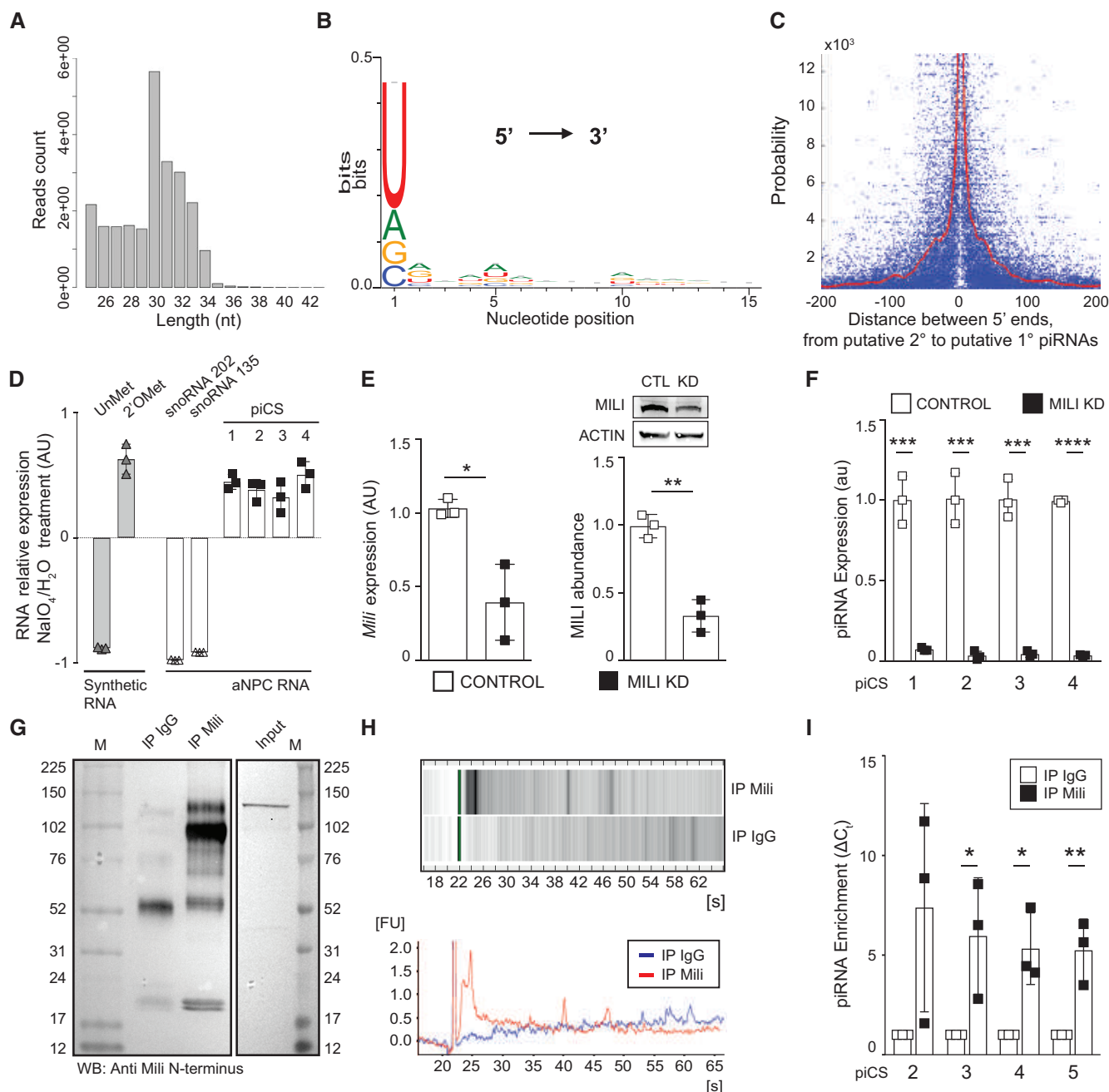
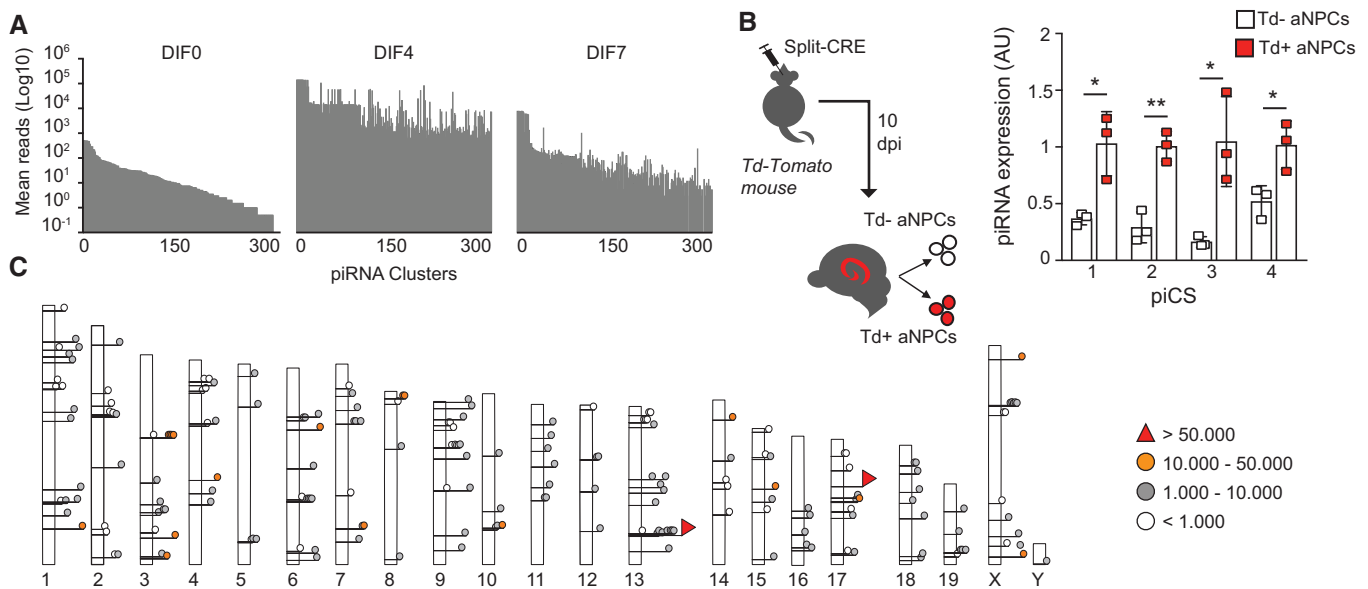


Figure 2.

Figure 2. Identification and validation of piRNAs in aNPCs.

- A–C (A) Size distribution of the piRNA reads showing (B) uridine bias at piRNA 5' ends and (C) probability of distances from the 5' ends of putative secondary piRNAs to the 5' ends of putative primary piRNAs. Note in panel C that 5' termini of putative primary and secondary piRNAs derived from the same cluster tend to concatenate around the "0" mark, as reported in other animals. Distance probability was assayed for unique piRNAs (length between 15–35 nucleotides), without taking into account abundance, by locally weighted smoothing linear regression (LOWESS).
- D Relative expression of transcripts bearing piRNA-cluster consensus sequences (piCS) of the top abundant piRNAs, and two control snoRNAs (202 and 135) in aNPC, upon treatment with sodium periodate (NaIO₄) or water and alkaline β-elimination. Synthetic RNA oligos were used as negative (Unmethylated, UnMet) and positive (2'-O-methylated, 2'OMet) controls, respectively. Note that the presence of 3'-end 2'-O-methylation in positive control and piRNAs confers them resistance to periodate oxidation and alkaline β-elimination, in contrast to the depletion in UnMet negative control and snoRNAs.
- E *Mili* mRNA expression (left bar graph); western blot (inset) and quantification (right bar graph) of *Mili* protein abundance in aNPCs upon viral transduction of scrambled shRNA (Control) or shRNA targeting *Mili* (*Mili* KD).
- F Expression of four of the most abundant piCS in control and *Mili* KD aNPCs.
- G–I Western blot (G), analysis by capillary electrophoresis (H), or quantification by qPCR (I) of the endogenous piCS after co-immunoprecipitation (IP) with endogenous *Mili* (IP *Mili*), or control IgG (IP IgG) in lysates of DIF4 aNPCs. In the qPCR abundance of the indicated piCS in the IP *Mili* was normalized to its respective level in the control co-immunoprecipitation (IgG); error bars in (I) represent standard deviation.

Data information: data are expressed as mean ± SEM unless differently indicated, $n = 2$ biological replicates (A–C) and $n = 3$ biological replicates (D–F, I). * $P < 0.05$, ** $P < 0.01$, *** $P < 0.001$, **** $P < 0.0001$, as assessed by the two-tailed Student's *t*-test. Source data are available online for this figure.

**Figure 3. Expression of piRNAs parallels *Mili* abundance in neurogenesis.**

- A Mean reads of the piRNA clusters in undifferentiated aNPCs (DIF0) and neuroblasts (DIF4–7) upon viral-induced neurogenesis, where the total number of filtered reads in each library ranges between 1.4 – 4.4×10^6 .
- B (left) Schematic representation of the experiment; (right) expression of four of the most abundant piCS in sorted Td⁺ and Td⁻ cells 10 dpi of split-Cre viruses in hippocampus.
- C Genomic location of the 298 piRNA clusters found in the *Mus musculus* genome (assembly MGScv37; mm9).

Data information: data are expressed as mean ± SEM, $n = 2$ biological replicates (A, C) and $n = 3$ biological replicates (B). * $P < 0.05$, ** $P < 0.01$, as assessed by the two-tailed Student's *t*-test carried out for each piCS between Td⁺ and Td⁻ cells.

total BrdU⁺ indicated a premature cycle exit upon *Mili* KD (Fig 5C). Similarly, by propidium iodide incorporation and flow cytometry analysis we found a significant increase in the proportion of cells in G0/G1 phase and a concomitant decrease in S phase cells upon *Mili* KD (Fig 5D; *Mili* KD G0/G1 = 89.8%, S = 6.03%, G2/M = 4.03%; Control G0/G1 = 84.7%, S = 8.97% G2/M = 6.27%). *Mili* KD did not lead to apoptosis (Fig EV4A and B), whereas it led to altered expression of genes encoding proteins associated with oxidative stress, circadian mechanism (Fig EV4C and D, and Dataset EV4), and

senescence-induced cell cycle exit (Fig 5E and F) in agreement with previous reports (Schouten *et al*, 2020; Adusumilli *et al*, 2021; Babcock *et al*, 2021). Strengthening this evidence, we found increased β-gal activity in the ipsilateral hippocampus injected with different GapmeRs antisense to *Mili*, compared with the contralateral side injected with control GapmeR (Figs 5G and EV4E and F). Next, we sorted *Nestin*-GFP⁺ NSCs from the DG of young (6 weeks) and ~12 months old mice (i.e., when the majority of hippocampal NSCs turn into an aged phenotype; Martín-Suárez *et al*, 2019) and found

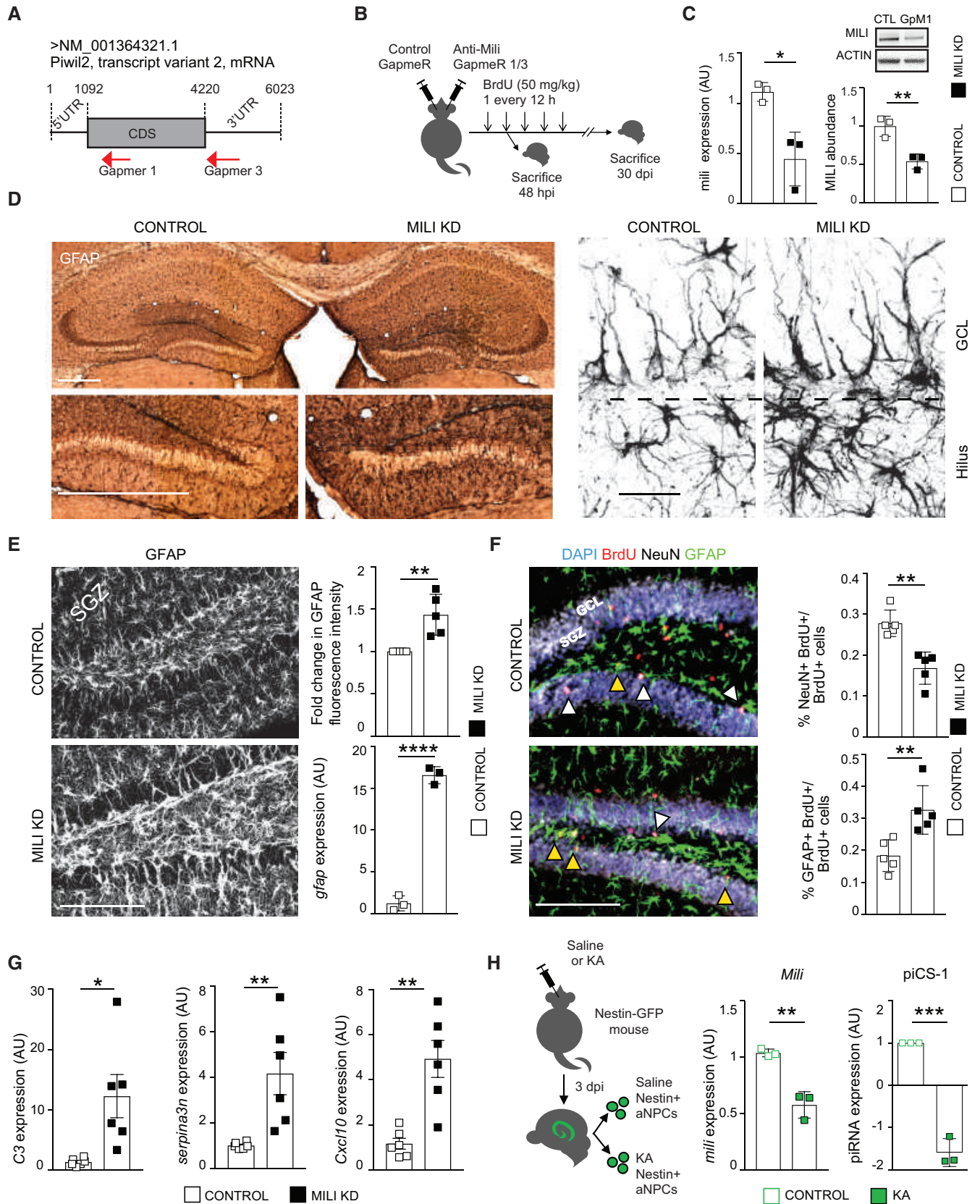


Figure 4.

Figure 4. Depletion of *Mili* and piRNAs impairs neurogenesis and increases astroglia.

- A Representation of the targeting regions of GapmeR1 and 3 on the *Mili* transcript.
- B Scheme of the *in vivo* experiment.
- C *Mili* mRNA expression (left bar graph); western blot (inset) and quantification (right bar graph) of *Mili* protein abundance in lysates from the DG of mouse hippocampi 48 h after the injection of scrambled (Control) or GapmeR1 against *Mili* (Mili KD).
- D Representative light microscopy (left) and confocal (right) micrographs of postnatal hippocampal sections, immunostained for GFAP at 30 dpi of scrambled (Control, left hemisphere) and GapmeR1 against *Mili* (Mili KD, right hemisphere).
- E Representative immunofluorescence micrograph of postnatal hippocampal sections immunostained for GFAP at 30 dpi of scrambled (Control) and GapmeR1 against *Mili* (Mili KD); Right panels: Fold change in GFAP fluorescence intensity level (upper graph) in a hippocampal region of interest (ROI) of 500 μm^2 in brain slices upon *Mili* KD compared with Control; *Gfap* mRNA levels (lower graph) in the DG from mouse hippocampi 48 h after the injection of scrambled (Control) or GapmeR1 (Mili KD).
- F (left) Representative immunofluorescence micrograph of postnatal hippocampal sections immunostained for GFAP (green), BrdU (red), NeuN (white), and nuclear DNA (blue) at 30 dpi of scrambled (Control) or GapmeR1 against *Mili* (Mili KD); (right graphs) percentages of NeuN⁺BrdU⁺ (white arrowheads in the images), or GFAP⁺BrdU⁺ (yellow arrowheads in the images) double-positive cells over total BrdU⁺ cells.
- G Relative mRNAs expression of reactive astrocyte markers in the hippocampus 48 h upon injection of scrambled (control, $n = 6$ mice) or GapmeRs against *Mili* (Mili KD, $n = 3$ mice GapmeR1 and $n = 3$ GapmeR3).
- H (left) Schematic representation of the experiment; *Mili* mRNA (left graph) and piCS1 (right graph) expression in sorted GFP⁺ NSCs from *Nestin*-GFP mice treated with Saline (Control) or Kainic Acid (KA).

Data information: data are expressed as mean \pm SEM, $n = 3$ (C, D, E mRNA, H) and 5 (E, F) biological replicates. * $P < 0.05$, ** $P < 0.01$, *** $P < 0.001$, **** $P < 0.0001$, as assessed by the two-tailed Student's *t*-test. UTR, untranslated region; CDS, coding sequence; GCL, granular cell layer; SGZ, subgranular zone. The scale bars represent 1 mm (D, left), 10 μm (D, right), and 100 μm (E, F).

Source data are available online for this figure.

that *Mili* transcript was significantly reduced in aged NSCs compared with the young (Fig 5H). These results indicate that *Mili* functions likely prevent the senescence of aNPCs and their progeny.

Identification of piRNA targets in neurogenesis

Next, we sought to identify targets of piRNAs in aNPCs lineages. In contrast to germline piRNAs, which primarily target TEs, somatic piRNAs have also homology with, or pair by sequence complementarity, to a variety of noncoding RNAs including tRNAs and others from repetitive elements (Keam *et al*, 2014; Rojas-Riós & Simonelig, 2018). Thereby, we first performed *in silico* prediction of non-coding RNAs targeted by the piRNAs identified in our model. Accordingly, TEs were just a minor percentage of the predicted non-coding RNA targets in both undifferentiated aNPCs and progeny (Fig 6A and B), despite their proportion being increased upon induction of neurogenesis (Fig 6B). The latter finding is in agreement with

the activation of TEs (e.g., LINE1) observed during neuronal differentiation (Muotri *et al*, 2005; Coufal *et al*, 2009; Upton *et al*, 2015). Interestingly, transcripts from repeats such as 5S rRNA and tRNAs were the main predicted targets in both undifferentiated (47% and 40%, respectively) and progeny (35% and 16%, respectively, Fig 6A and B). To ascertain whether these noncoding RNAs are modulated upon *Mili* and piRNA depletion, we quantified their levels in *Mili* KD aNPCs and progeny (Fig 6C). Indeed, *Mili* depletion significantly elevated levels of 5S rRNA and SINEB1 family of TEs in both undifferentiated aNPCs and progeny, compared with scrambled control (Fig 6C), whereas LINE1, here quantified with a qPCR assay detecting the full-length transcript, was initially refractory to *Mili* depletion and its level only increased late in differentiation (Fig 6C).

To identify which protein-coding transcripts are modulated upon *Mili* depletion in aNPCs lineages, we analyzed RNA seq data from *Mili* KD or scrambled control cells during their spontaneous

Figure 5. Depletion of *Mili* and piRNAs in aNPCs results in senescence-associated phenotypes.

- A Heatmap illustrating the expression of genes encoding proteins involved in immune-modulatory and senescence-associated phenotype in differentiating neuroblasts (DIF4) upon *Mili* KD, compared with control cells. Expression heatmap correlation plots were computed by the k-means clustering method. Scale bar indicates Z-scores.
- B Representative bright-field microscopy images (left) and quantification (right) of β -galactosidase⁺ aNPCs as percent of total cells upon *Mili* KD, or control 48 h after induction of spontaneous differentiation.
- C Representative fluorescence microscopy images (left) and quantification (right) of control or *Mili* KD neuroblasts 48 h after spontaneous differentiation, immunostained with anti-BrdU (white) and Ki67 (purple) antibodies. (Right) Percentage of BrdU⁺ and Ki67⁻ cells over BrdU⁺ cells.
- D Representative cell cycle analysis of propidium iodide staining by flow cytometry in neuroblasts 48 h after spontaneous differentiation; Percentage of cells in G0/G1 and S is reported in the text.
- E Relative mRNA expression of genes encoding proteins involved in the regulation of cell cycle in control and *Mili* KD neuroblasts 48 h after spontaneous differentiation.
- F Transcript abundance expressed in transcripts per million (TPM) of genes encoding proteins involved in the regulation of cell cycle and differentiation (left) or cell cycle (right) in DIF4 neuroblasts upon *Mili* KD, compared with control cells.
- G Representative light-microscopy images of the β -galactosidase staining of postnatal hippocampal sections, 30 dpi of scrambled (Control, left hemisphere) and GapmeR1 against *Mili* (Mili KD, right hemisphere). See Fig EV4E for a larger image of this section.
- H (left) Scheme of the *in vivo* experiment; (right) *Mili* mRNA expression in *Nestin*-GFP⁺ sorted cells from young (6 weeks) and old (56 weeks) mice.

Data information: data are expressed as mean \pm SEM, $n = 3$ (A, D–F, H) and 5 (B, C) biological replicates (in A each biological replicate was sequenced with two separate flow cells). * $P < 0.05$, ** $P < 0.01$, *** $P < 0.001$, **** $P < 0.0001$, as assessed by the two-tailed Student's *t*-test. The scale bars represent 50 μm (B, C) and 500 μm (G).

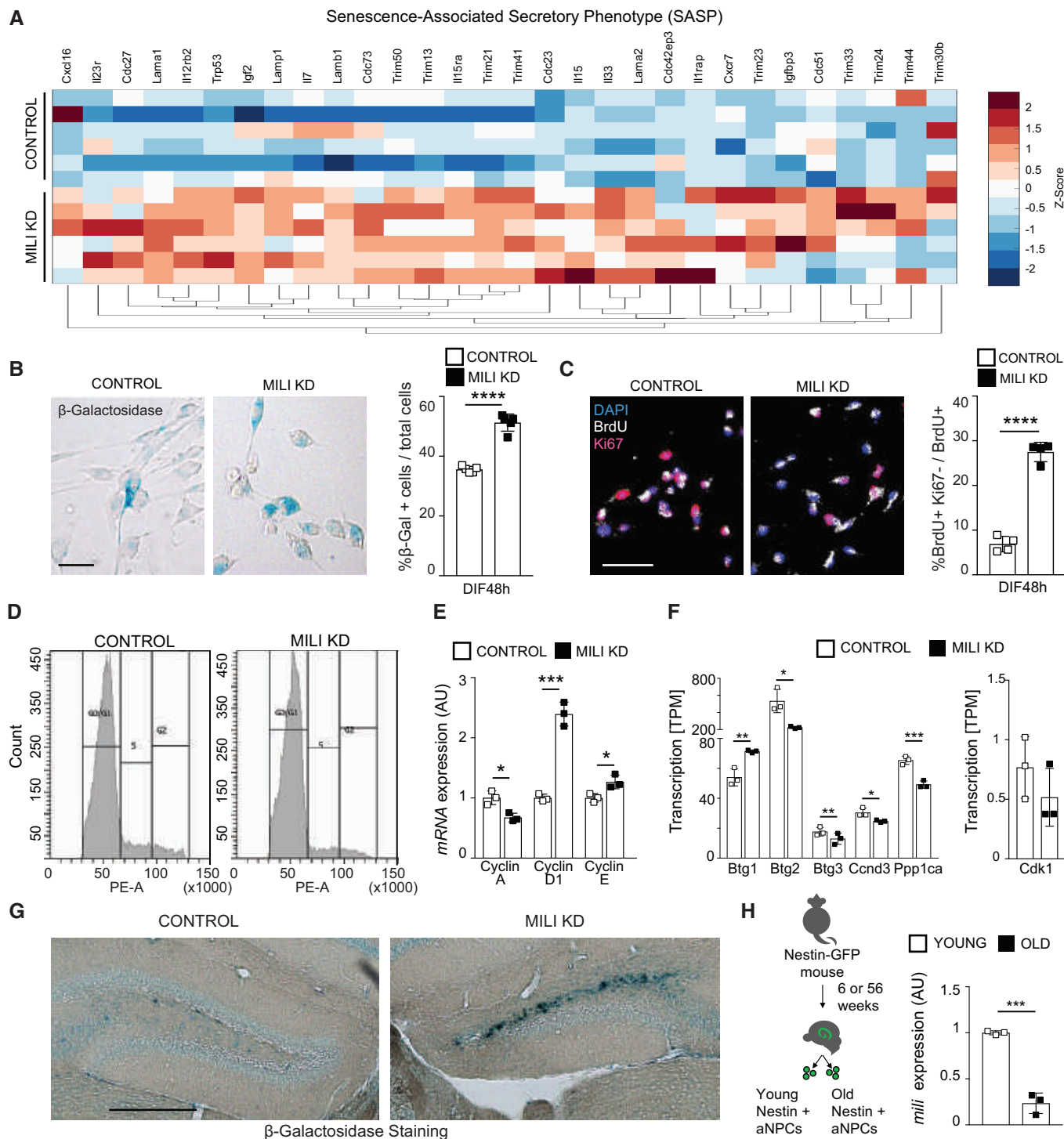


Figure 5.

differentiation, at the peak of Mili and piRNA expression (i.e., DIF4). Most of the transcripts modulated upon Mili depletion were upregulated (Fig 6D), and most of them bore sequences antisense to piRNAs and/or harbored homologous sequences to piRNAs (Fig 6D and E). More specifically, we observed that transcripts from individual genes are targeted by multiple unique piRNAs, with a maximum of 11,904 piRNAs targeting a single modulated gene (Fig 6F), and a

maximum of 9,870 piRNA transcripts per million (TPM) targeting a single mRNA (Fig 6C).

To address possible functions of the piRNA targets in aNPCs we searched the Gene ontology (GO) and Kyoto Encyclopedia of Genes and Genomes (KEGG) databases. GO analysis of the upregulated protein-coding targets upon Mili depletion indicated a prevalence of genes involved in the regulation of chromatin, transcription, mRNA

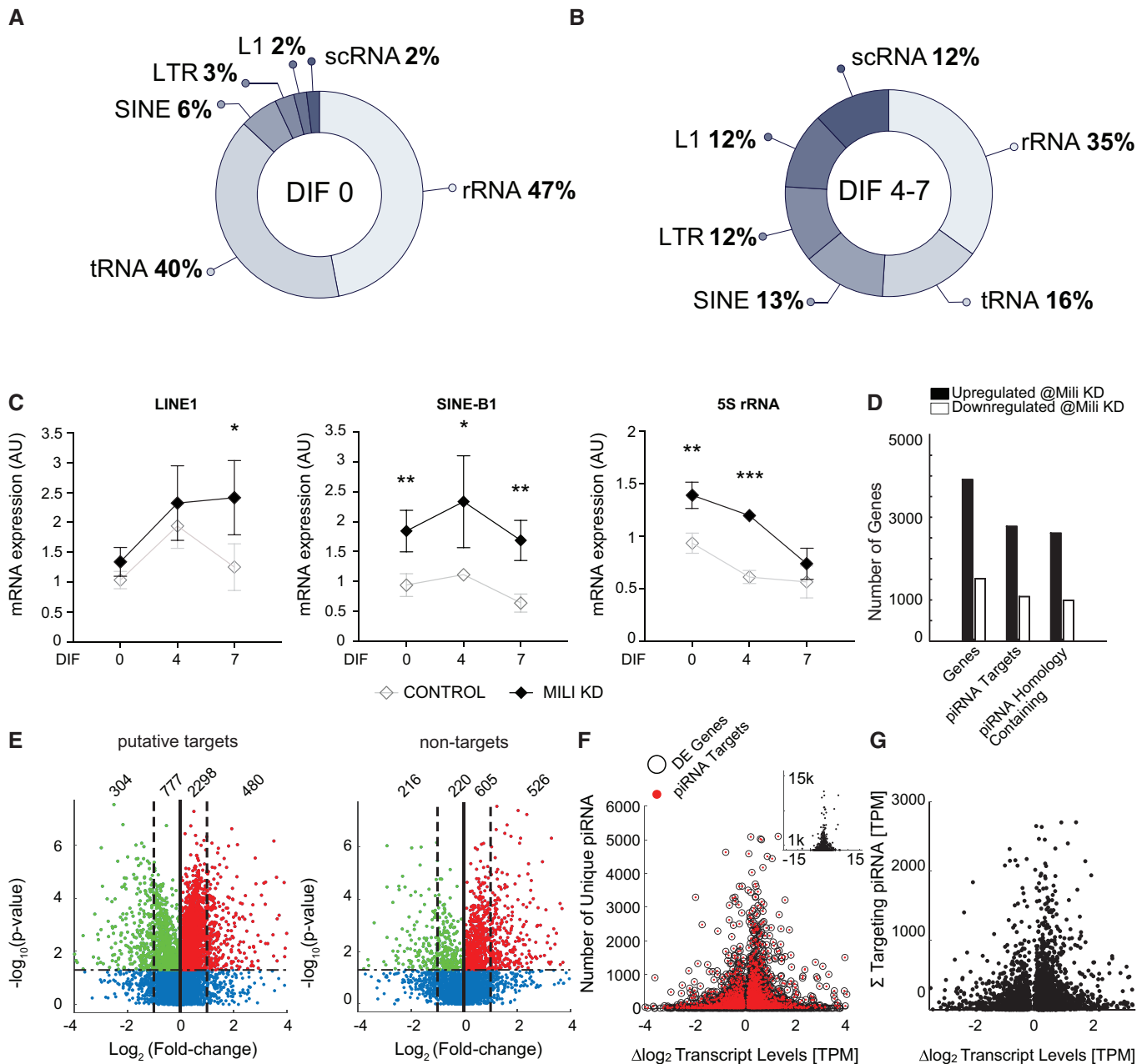


Figure 6. piRNAs target repetitive elements and mRNAs in neurogenesis.

A, B Pie plots showing proportions of noncoding RNAs predicted targets of piRNAs in undifferentiated aNPCs (DIF0) and differentiating neuroblasts (DIF4-7).

C Transcript levels of *LINE1* 5'UTR, *SINEB1*, and *5S rRNA* in the Mili KD or control aNPCs (DIF0) and differentiating neuroblasts (DIF4-7).

D Total counts of upregulated (black bars) and downregulated protein-coding genes (white bars) in Mili KD versus scrambled control neuroblasts at DIF4.

E Volcano plots showing the \log_2 fold change of significantly altered mRNA transcripts (numbers of each category indicated) that are target or nontarget of the piRNAs.

F The \log_2 fold change of significantly altered mRNA transcripts (abscissa) plotted with the raw number of unique piRNA sequences qualified as targeting molecules (ordinate) for all modulated genes (black circles), and piRNA-targeted genes (red dots), identified by RNA seq. The modulated genes without piRNA target sequences concatenate at the bottom at the "y = 0" value; total range, inset.

G The \log_2 fold change of significantly altered piRNA-targeted mRNA transcripts (abscissa) plotted with the summed levels of all mRNA-targeted (complementary) piRNA molecules (ordinate), identified by RNA seq.

Data information: data are expressed as mean \pm SEM, $n = 3$ (C) biological replicates. Data are expressed in transcripts per million (TPM) as the mean levels of six sequencing runs (three biological replicates sequenced with two separate flow cells) profiles at DIF4 (D-G). Outliers (mean calculation) were detected by more than three mean absolute deviations, for a final "n" value between 4 and 6 samples. * $P < 0.05$, ** $P < 0.01$, *** $P < 0.001$, as assessed by the two-tailed Student's *t*-test. (G) The two-sample Kolmogorov-Smirnov test on the change in expression between piRNA target and nontarget genes, P -value = 3.21e-260.



Figure 7. Analysis of genes and pathways modulated upon Mili and piRNA depletion.

A, B Bar graph showing the top biological pathways of significantly upregulated (A) and downregulated (B) protein-coding genes in Mili KD neuroblasts at DIF4; Numbers in each category indicate gene counts and percentages are normalized on the total number of genes for each category.
C Most significant terms generated from KEGG pathway analysis of the modulated targets.

processing, translation, and DNA repair (Fig 7A), which are well-known functions regulated by the piRNA pathway in both germline and somatic tissues (Czech *et al*, 2018; Rojas-Riós & Simonelig, 2018; Ozata *et al*, 2019). Among the downregulated protein-coding targets, we found genes involved in the regulation of apoptosis, cell proliferation, oxidative pathway, and differentiation (Fig 7B), in agreement with the main phenotypes that we observed upon Mili depletion in neurogenesis. “Ribosome” and “Spliceosome” were the top terms among upregulated genes in the KEGG pathway analysis; whereas, cancer-related terms were common among the downregulated pathways (Fig 7C), in agreement with the known oncogenic role of Piwil2 in various human tumors (Lee *et al*, 2006). As 5S rRNA and SINEB1, both involved in the control of ribosome biogenesis and translation, are among the piRNA targets in aNPCs and because the dysregulation of ribosome biogenesis has been associated with cellular senescence (Liu & Sabatini, 2020), we investigated ribosome density and translation in Mili KD aNPCs and progeny. Accordingly, Mili depletion increased the density of polyribosomes in both undifferentiated and differentiating aNPCs compared with control cells (Fig EV5A and B), as revealed by immunostaining for the ribosomal

protein RPL26 imaged with stimulated emission depletion (STED) nanoscopy (Viero *et al*, 2015). Furthermore, the protein synthesis rate, measured by OPP (O-propargyl-puromycin) labeling of nascent proteins, was significantly increased upon Mili depletion in differentiating neuroblasts (DIF7), but not in undifferentiated aNPCs (DIF0) (Fig EV5C), in agreement with the notion that the density of ribosomes over a transcript does not necessarily correlate with its translation (Mills & Green, 2017).

In sum, these results indicate that the piRNA pathway is present and preferentially expressed in adult hippocampal NSC/NPCs compared with their progeny, where it exerts a wide range of gene-modulatory functions essential for their fitness and neurogenesis.

Discussion

This study provides the first evidence of the role of the piRNA pathway in neurogenesis. By investigating the presence of Mili and Mili-dependent piRNAs in aNPCs and by inferring functions of this

pathway in the regulation of adult hippocampal neurogenesis, we provide evidence of an essential role for Mili in maintaining NSC fitness and proper fate. This finding adds a new layer of complexity to the understanding of adult brain plasticity and entails implications for aging and neuronal disorders, where dysregulated expression of the piRNA pathway has been reported, such as neurodegeneration (Jain *et al*, 2019; Wakisaka, 2019) and various psychiatric conditions (Page *et al*, 2021).

At the functional level, the Piwi proteins in gonads and bone marrow maintain stem cell pools by preserving their fitness (De Luca *et al*, 2016; Rojas-Riós & Simonelig, 2018). Similarly, our data indicate that Mili is required to maintain the fitness of NSC/NPCs in the adult hippocampus. We find that piRNAs are enriched in aNPCs and their expression is dynamic along neurogenesis, mirroring Mili. Moreover, Mili depletion in aNPCs leads to premature cell cycle exit, increases generation of reactive glia, and alters the expression of several inflammatory, reactive oxygen, and circadian-related genes, which are known hallmarks of an aged hippocampal niche (Bonaguidi *et al*, 2011; Encinas *et al*, 2011; Clarke *et al*, 2018; Martín-Suárez *et al*, 2019; Schouten *et al*, 2020); accordingly, we find a reduced expression of Mili in hippocampal NSCs of aged mice. In contrast to the dispensable role of Piwi proteins for hematopoiesis (Nolde *et al*, 2013), however, Mili is required for the proper neurogenesis fate. Thereby, our data support the idea that Mili regulates the fate choice in the hippocampal niche, implicating functions of the piRNA pathway in the maintenance of lifelong neurogenesis, possibly to prevent or delay its drift toward reactive gliogenesis. While some of these conclusions require further longitudinal investigations in Mili knockout mice (ideally, bearing Lox-P sites to selectively restrict the deletion of Mili to distinct NSC subpopulations), this study underpins a possible involvement of the piRNA pathway in brain plasticity and aging.

At the mechanistic level, several unresolved questions arise from this study. Perhaps the most crucial one is whether Mili functions in neurogenesis are mediated through piRNAs. Indeed, Piwi proteins regulate targets at both the transcriptional and post-transcriptional levels. However, these mechanisms are very complex and differ according to the cell type, the Piwi proteins involved, effectors, and their subcellular localization and do not necessarily require cleavage-competent Piwi or piRNAs (Czech *et al*, 2018; Ozata *et al*, 2019). Our data indicate the presence of key players of the piRNA pathway, such as Mili, several cofactors, as well as piRNAs (fulfilling most of the criteria characterizing them, such as length, U-Bias, 2'-O-Methylation at their 3' ends, inter-distance, Mili-dependence and -interaction) in aNPCs. We also uncover that this pathway targets, either directly or indirectly, more than 6,000 genes in neurogenesis including repetitive elements, and several genes are known to be regulated by piRNAs in other tissues and cell types; however, given this level of complexity, the mechanisms mediating gene-regulatory functions of the Mili-piRNA complexes in our model certainly warrant further investigation. Future exploitation of the “simplified” aNPC model (where Mili is the main Piwi protein, while other cofactors such as the testis-specific methyl transferase Hen1 are missing), would disentangle the mechanism of piRNA biogenesis and function in neurogenesis, providing the biological understanding of scientific and therapeutic value for brain plasticity and successful aging.

Materials and Methods

Reagents and Tools table

| Reagent/resource | Reference or source | Identifier or catalog number |
|---|--|--------------------------------|
| Experimental models | | |
| C57BL/6j (<i>M. musculus</i>) | Jackson Lab | B6.129P2Gpr37tm1Dgen/J |
| Td-Tomato ^{fllox/wt} (<i>M. musculus</i>) | Jackson Lab | Madisen <i>et al</i> (2010) |
| Mili null mice (<i>M. musculus</i>) | European mouse mutant archive (EMMA) | Di Giacomo <i>et al</i> (2013) |
| Nestin-GFP (<i>M. musculus</i>) | C. Fitzsimons' Lab | Mignone <i>et al</i> (2004) |
| Antibodies | | |
| Mouse-anti-MILI | Santa Cruz 1:100 WB | Cat # sc-377347 |
| Mouse-anti-MILI | Santa Cruz 1:100 WB, 1:25 IP | Cat # sc-377258 |
| Rabbit-anti-MILI | G. Hannon's Lab 1:150 WB, 1:100 IF/IHC | |
| Rabbit-anti-MIWI | G. Hannon's Lab 1:200 WB | |
| Rabbit-anti-ACTIN | Abcam 1:1,000 WB | Cat # ab13970 |
| Rabbit-anti-GADPH | Santa Cruz 1:1,000 WB | Cat # sc-25778 |
| Rabbit-anti-GFAP | Dako 1:1,000 WB, IF/IHC | Cat # Z-0334 |
| Rat-anti-BrdU | Abcam 1:200 IF/IHC | Cat # ab6326 |
| Rabbit-anti-KI67 | Abcam 1:250 IF/IHC | Cat # ab15580 |
| Mouse-anti-NeuN | Millipore 1:250 IF/IHC | Cat # MAB377 |
| Rabbit-anti-RPL26 | Abcam 1:500 IF/IHC | Cat # ab59567 |
| Mouse-anti-Nestin | Millipore 1:250 IF/IHC | Cat # MAB353 |
| Rabbit-anti-cleaved caspase-3 | Cell Signaling Technology 1:400 IF/IHC | Cat # 9664 |
| IgG | Millipore-Sigma 1:100 IP | |

Methods and Protocols

Experimental mice

C57BL/6 and Td-Tomato^{fllox/wt} knock-in reporter mice (Jackson Laboratory stock number 007908) (Madisen *et al*, 2010) and Mili null mice (Di Giacomo *et al*, 2013) were housed at Istituto Italiano di Tecnologia (IIT); Nestin-GFP mice (Mignone *et al*, 2004) were housed at the Swammerdam Institute for Life Sciences, University of Amsterdam, The Netherlands. All animal procedures were approved by the IIT animal use committee and the Italian Ministry of health, or by the Commission for Animal Welfare at the University of Amsterdam (DEC protocol 4925, AVD1110020184925), respectively, and

conducted in accordance with the Guide for the Care and Use of Laboratory Animals of the European Community Council Directives. All mice were group-housed under a 12-h light–dark cycle in a temperature and humidity-controlled environment with *ad libitum* access to food and water.

Virus and GapmeR injection

Split-cre viruses or GapmeRs injection was done as previously published (Pons-Espinal *et al*, 2019); briefly, 8 weeks-old mice Td-Tomato^{flox/wt} or WT C57BL6/J were anesthetized with isoflurane and 1.5 μ l of virus mix (Split-Cre N-Cre:C-Cre), or 1.5 μ l of 50 μ M antisense GapmeR targeting *Mili* or negative control (custom design probes, MILI 339512, Control 339516, Qiagen), were stereotaxically injected in the dentate gyrus. Bilateral injection of Control GapmeR in the left hemisphere and *Mili* KD GapmeR in the right hemisphere allowed the analysis of the phenotypes within the same brain. To assess the GapmeRs uptake and the efficacy of *Mili* KD, the first group of mice ($n = 3$ for each GapmeR) was sacrificed 48 h after the injection and the DG and tissue processed for RNA or protein extraction. Another set of animals received 2 BrdU intraperitoneal injections per day for 5 days (50 mg/kg) (one every 12 h) starting 24 h after GapmeRs injection. Animals were sacrificed 30 days after GapmeRs injection ($n = 5$ for each oligo) and tissue processed for histological analysis (Pons-Espinal *et al*, 2019). GapmeR sequences are listed in the Table EV1.

Kainic acid (KA) administration and aNPC collection by fluorescence-activated cell sorting (FACS)

Kainic acid to elicit tonic, nonconvulsive epileptic seizures, was administered as described before (Bielefeld *et al*, 2019). Briefly, 50 nl of 2.22 mM Kainic Acid dissolved in PBS (pH 7.4) was injected bilaterally into the hippocampus at the following coordinates (AP -2.0 , ML ± 1.5 , DV -2.0 mm) (between 9 AM and 1 PM). Control animals were administered saline (pH 7.4). Bilateral dentate gyri from three animals per condition were pooled to allow sufficient recovery of NSC/NPCs. A single-cell suspension was created using a Neural Tissue Dissociation kit (Miltenyi Biotec), according to the manufacturer's protocol. In order to enrich aNPCs from the DG, we used the endogenous GFP expression driven by the Nestin promoter in combination with FACS. Propidium Iodide (5 μ g/ml) was added to the single-cell suspension to assess cell viability. Cells were sorted using a FACS Aria III system (BD) with a 488 nm excitation laser. Cell duplets were removed based on forward and side scatters, and viable cells were selected based on PI negativity. GFP-positive (corrected for autofluorescence) cells were sorted ($\cong 50,000$ cells/pool) and collected in PBS containing 1% FBS. Trizol LS (Thermo Scientific) was added and after resuspension samples were snap-frozen and stored at -20°C .

For RNA extraction and cDNA preparation, Td-Tomato^{flox/wt} or Nestin-GFP mice were used. Six to ten Td-Tomato^{flox/wt} mice were euthanized 10 or 30 days after the split-Cre virus injection. DG cells were dissociated with the Neural Tissue Dissociation Kit P (Miltenyi Biotec) and FACS-sorted as previously published (Pons-Espinal *et al*, 2019). FACS-sorted cells were immediately processed for RNA extraction. Cell cycle length was measured by propidium iodide (PI), which binds to DNA by intercalating between the bases, as previously described (Krishan, 1975). Briefly, cells were trypsinized, resuspended in PBS, and fixed with 70% of ethanol for 40 min on

ice. Cells were then centrifuged, resuspended in PBS for 15 min, and then incubated for 1 h at 37°C with 60 μ g/ml of PI (Sigma). Cells were collected by centrifuge and resuspended in ice-cold PBS for FACS analysis.

Primary aNPC isolation and culture

Hippocampal NPCs were prepared and expanded as described previously and induction of spontaneous differentiation by growth factor removal was done as previously described (Pons-Espinal *et al*, 2017, 2019); viral-induced neuronal differentiation of aNPCs was done by transduction of a viral construct expressing Ascl1-ERT2 as previously described (Braun *et al*, 2013).

Histology, immunofluorescence, and imaging

Immunofluorescence staining on brain slices was performed on sections covering the entire dorsal hippocampus as previously described (Pons-Espinal *et al*, 2019). Forty micrometer-thick brain sections were generated using a sliding microtome and were stored in a -20°C freezer as floating sections in 48 well plates filled with cryoprotectant solution (glycerol, ethylene glycol, and 0.2 M phosphate buffer, pH 7.4, 1:1:2 by volume).

To detect Ki67 staining, citrate buffer 10 mM pH = 6 treatment for 10 min at 95°C was used. Secondary fluorescent antibodies were diluted 1:1,000 (Goat Alexa 488, 568, and 647 nm, Invitrogen). Confocal stack images of brain slices (40 μ m) were obtained with the Confocal A1 Nikon Inverted SFC with 20 \times objective (Nikon Instruments, Yokohama, Japan). Cell quantification and analysis were performed using NIS-Elements software (Nikon Instruments) and the Cell-counter plugin in Fiji. GFAP intensity fluorescence analysis was done on fluorescence microscopy images acquired by the Confocal A1 Nikon Inverted SFC with 20 \times objective (Nikon Instruments), with the same parameters for all the sections. Quantification of fluorescence intensity was performed using ImageJ measuring the integrated density of a region of interest (ROI) of 500 μm^2 for each hippocampal slice. Fold change in fluorescence intensity of *Mili* KD hippocampi compared with control ones has been plotted in the graph. For all the quantification analysis, six sections were analyzed from each animal, and the mean of the measures from consecutive sections was used for that individual. DAB staining was performed as previously reported (Bielefeld *et al*, 2019). Briefly, sections were incubated with peroxidase block (Vectashield) and permeabilized with 0.3% PBS-Triton X (PBS-T) and 0.1% PBS-T. Sections were blocked with 0.1% PBS-T and 5% Normal Goat Serum (NGS), incubated with primary antibodies, and subsequently with the corresponding biotinylated secondary antibodies (1:1,000 Goat anti-rabbit, Invitrogen). Signal amplification was performed using the ABC complex (Vectashield), according to the manufacturer's instructions. Sections were incubated with the solution for DAB reaction (Sigma) and counterstained with Hoechst (1:300), mounted, and coverslipped with Vectashield reagent (VECTOR Labs). β -galactosidase detection was obtained with the Senescence Cells Histochemical Staining Kit (Sigma-Aldrich), according to the manufacturer's instructions. Briefly, cells were plated on coverslip in proliferating medium. Forty-eight hours after the induction of spontaneous differentiation, cells were washed twice with PBS 1 \times and incubated with Fixation Buffer 1 \times for 7 min at RT. Next, cells were rinsed with PBS 1 \times and incubated with fresh senescence-associated β -Gal (SA- β -Gal) stain solution at 37°C (no

CO₂) for 4 h. Reaction was blocked with PBS 1×, and coverslips were mounted on slides using Vectashield reagent (Vector Labs). Images were obtained using the microscope Nikon Eclipse 80i (Nikon Instruments, Yokohama, Japan) and the percentage of cells expressing β-galactosidase was quantified over the number of total cells using a Cell-counter plugin in Fiji software. To detect β-galactosidase *in vivo*, brain slices of 40 μm were collected from perfused animals, and the reaction was carried out in free-floating sections as previously described for cells. Images (DAB and β-galactosidase) were obtained using the microscope Olympus BX51 equipped with Neurolucida software (MBF Bioscience), and a full brain slice was reconstructed from acquired fields. Immunofluorescence staining on cell cultures was performed as reported (Pons-Espinal *et al*, 2019). To detect BrdU incorporation, cells were pre-treated with 2 N HCl for 30 min at 37°C. Cells were mounted in a mounting medium and counterstained with fluorescent nuclear dye DAPI (Invitrogen). Images were obtained using the microscope Nikon Eclipse 80i at 20× or 40× magnification and quantification was performed using a Cell-counter plugin in Fiji. For the quantification analysis, six fields were analyzed from each coverslip, and the mean of the measures was used for that experimental replica.

Mili knockdown (KD) *in vitro*

Adult neural progenitor cells were infected at MOI = 5 with a lentivirus encoding for a *Mili*-targeted short hairpin (shMILI, pKO.1, Sigma) or for a short hairpin scramble lentivirus (Control, SHC202, Sigma) both decorated with an eGFP reporter. GFP-positive cells were first selected by FACS after three passages and then plated in proliferating or differentiating media, as previously described. We also performed the knockdown using two different synthetic antisense LNA GapmeRs for *Mili* KD or negative control (as for the *in vivo*: *Mili* 339512, Control 339516, Qiagen). Cells were transfected with 150 pmol of GapmeRs 50 μM using Lipofectamin stem transfection reagent (STEM00015, Thermo Fisher) according to the manufacturer's protocol and collected 72 h after treatment. GapmeRs uptake and *Mili* knockdown were assessed by real-time qPCR and Western Blot.

Protein extraction and Western blot

For total protein extraction, adult testes or hippocampus or cell pellets were homogenized in RIPA buffer and the protein concentration was determined using a Bradford Assay kit (Bio-Rad). For blot analysis, equal amounts of protein (30 μg) were run on homemade 10% polyacrylamide gels and transferred on nitrocellulose membranes (GE Healthcare). Membranes were probed with the primary antibodies, followed by HRP-conjugated secondary antibody anti-rabbit or mouse (Invitrogen, A16104, A16072; 1:2,000). LAS 4000 Mini Imaging System (GE Healthcare) was used to digitally acquire chemiluminescence signals, and the band intensities were quantified using Fiji software (Macbiophotonics) (Schindelin *et al*, 2012).

Co-immunoprecipitation of *Mili* and piRNA

Adult NPCs were suspended in ice-cold lysis buffer supplemented with protease inhibitor (Roche) and RNase inhibitor (Promega) and lysed with a 30G syringe needle. Equal concentrations of cell lysate were incubated overnight at 4°C in rotation with either IgG (Millipore-Sigma), or the anti-*Mili* primary antibody (Santa Cruz, sc-37258) and UV cross-linked. Dnase I (Sigma) was added, and the

suspensions were incubated with Dynabeads Protein G (Thermo Fisher) to immunoprecipitate the antigen–antibody complex for 2 h at room temperature in rotation. The magnetic beads were captured on a magnetic rack and washed five times each with buffers at increasing salt concentrations. Ten percent of the final wash solution was removed for RNA extraction and subject to real-time qPCR or analysis with the Bioanalyzer RNA chips (Agilent). The remainder of the beads was captured on a magnetic rack, and the protein content was eluted in RIPA buffer supplemented with 150 mM TCEP, incubated on ice for 10 min, and resolved on a 4–12% polyacrylamide gel. Proteins were transferred and processed for Western blotting as above.

RNA extraction and real-time qPCR

Total RNA was extracted from aNPCs (proliferating and differentiating conditions), or DG dissected from adult C57BL/6, Nestin-GFP, or Td-Tomato^{flox/wt} mice with QIAzol protocol (Qiagen) according to the manufacturer's instructions. One microgram of total RNA was treated with DNase I (Sigma) and cDNA was synthesized using iScript cDNA Synthesis kit (Bio-Rad) or with ImProm-II reverse transcriptase (Promega). Real-time qPCR was performed in a duplex with Actin as a reference gene, with QuantiFast SYBR Green PCR Kit (Qiagen) or TaqMan Assay (Thermo Fisher) on ABI-7500 Real-Time PCR System (Applied Biosystems). Expression levels were determined relative to Actin, using the delta-delta Ct method. Primers were designed using NCBI/UCSC Genome Browser and Primer3 software tools and then checked in PrimerBLAST for their specificity to amplify the desired genes. For piRNA real-time qPCR, total RNA enriched in the fraction of small RNAs was extracted using miRNeasy Mini kit (Qiagen) following the manufacturer's instructions from aNPCs, microdissected DG from hippocampi of C57BL/6/J or Td-Tomato^{flox/wt} mice. cDNA was obtained using the TaqMan MicroRNA Reverse Transcription Kit (Thermo Fisher) according to the manufacturer's instructions and quantified using the Custom TaqMan Small RNA Assay (Thermo Fisher) on a ABI-7500 Real-Time PCR System (Applied Biosystems). Each sample was normalized to U6 snRNA level (Thermo Fisher). Oligonucleotide sequences are listed in the Table EV1.

RNA library preparation

For small RNA libraries, the quantity and quality of the total RNA isolated from aNPCs/neuroblasts cultures were measured by Nanodrop spectrophotometer (Thermo Fisher) and Experion RNA chips (Bio-Rad). RNA with RNA integrity number (RIN) values ≥ 9.5 were selected for the study. One microgram of high-quality RNA for each sample was used for library preparation according to the Illumina TruSeq small RNA library protocol (Illumina Inc., CA). Briefly, 3' adapters were ligated to 3' end of small RNAs using a truncated RNA ligase enzyme followed by 5' adaptor ligation using an RNA ligase enzyme. Reverse transcription followed by PCR was used to prepare cDNA using primers specific for the 3' and 5' adapters. The amplification of those fragments having adapter molecules on both ends was carried out with 13 PCR cycles. The amplified libraries were pooled together and run on a 6% polyacrylamide gel. The 145–160 bp bands (which correspond to inserts of 24–32 nt cDNAs) were extracted and purified using the Wizard® SV Gel and PCR Clean-Up System (Promega). The quality of the library was assessed by the Experion DNA 1 K chips (Bio-Rad). Small RNA sequencing

using HiSeq2000 (Illumina Inc., CA) was performed by the IIT genomics facility at the Center for Genomic Science (IIT@SEMM, Milan, Italy). For Long RNA Libraries, quantity and quality of the total RNA extracted from WT/Mili KD aNPCs were measured by Qubit 4 Fluorometer (Thermo Fisher) and Bioanalyzer RNA chips (Agilent). RNA with RIN values ≥ 8 were selected for the study. Thirty nanogram of high-quality RNA for each sample was used for library preparation according to the Illumina Stranded Total RNA Prep, Ligation with Ribo-Zero Plus Kit (20040529, Illumina Inc., CA) using the IDT for Illumina Indexes Set A (20040553). Briefly, after ribosomal RNA depletion, RNA was fragmented, denatured and cDNA synthesized. The 3' ends were adenylated and anchors ligated. After amplification and clean-up, the quality of the libraries was assessed by the Bioanalyzer DNA chips (Agilent). Paired-End stranded total RNA sequencing on NovaSeq 6000 Sequencing System instrument (Illumina Inc., CA), was performed by the IIT Genomic facility at the Center for Human Technologies, Genoa, Italy. Sequencing was performed bidirectionally, and in duplicate by two flow cell pairs of 100 and 150 base pairs, for a total of six measurements produced from three independent samples for each differentiation time point and genotype.

Small RNA sequencing data processing

Was done essentially as previously published (Ghosheh *et al*, 2016). Briefly, Illumina reads were trimmed to remove the 3' adapter using Cutadapt, with parameters `-m 25 -q 20`. Since piRNA size ranges from 26 to 31 bases, all sequences with length ≤ 24 bases were discarded. Reads mapped to known noncoding RNAs (RNAcentral v6.0 snoRNA, UCSC tRNA, miRBase Release 21 miRNA hairpin and mature miRNA annotation, NCBI complete ribosomal DNA unit) were removed from the datasets. The comparison was performed using NCBI BLASTN v2.6.0 with parameters `-max_hsps = 1, -max_target_seqs = 1, -perc_identity = 80, mismatches ≤ 1 , qcovhsp ≥ 90` . Reads were aligned on the nonrepeat-masked UCSC release 9 of the mouse genome (MM9) using *bowtie* (Langmead & Salzberg, 2012) v2.2.6 with the sensitive preset option and allowed a maximum of 100 alignments. All the reads that aligned to the genome were retained and used for subsequent analysis. piRNA clusters were identified collapsing overlapped piRNA sequences (piRBase Release 1; Zhang *et al*, 2014) into one cluster (mergeBed with preset options; Quinlan & Hall, 2010). piRNA clusters and all the reads that aligned to the genome were intersected (intersectBed with option `-f 1`). Intersection files were then parsed using a custom perl script in order to evaluate alignment counts. Differential expression was assessed using DESeq2 (Love *et al*, 2014). piRNA clusters were considered differentially expressed when the adjusted *P*-value was ≤ 0.05 , and down- and up-regulation was established in the range of ≤ -1 to ≥ 1 log₂ fold change, respectively. piRNA sequences were then categorized for the putative mRNA transcript targets (for each gene). In order to obtain a count of piRNA target levels, which target individual gene transcripts, for each differentiation time point (DIF0-7), piRNA transcripts were expressed in transcripts per million (TPM) and summed for each target category. Spearman correlation was performed between the levels of the piRNA in the Sh-Scramble (control) genotype and compared with the fold-change level of the putative target genes, which were found to be significantly altered (up and down) in the Sh-Mili-KD genotype. In order to assess the clustering behavior of putative piRNAs,

the 5' termini positions of each cluster-associated putative primary and putative secondary piRNA sequences were analyzed for distance, represented as probability, within a range of 200 nucleotides in the 5' direction and 200 nucleotides in the 3' direction of the putative primary piRNAs, as reported previously (Gainetdinov *et al*, 2018). The positional distance between piRNAs for each cluster was sampled iteratively for each assigned piRNA and normalized by the total number of diverse piRNAs associated with each cluster. The distance probability distribution was assayed by the locally weighted smoothing linear regression method (LOWESS), by using the built-in MATLAB "fit" function (MathWorks, Natick, MA), with a span value of 0.1.

mRNA sequencing data processing

Adapter sequences were trimmed using *Cutadapt*, after which a quality control trim was implemented on a sliding window of 25 nucleotides, for 2 base pairs with a minimum quality score of 26, with the *Bowtie* build for the MATLAB bioinformatics suite (MathWorks, Natick, MA). Transcript quantification was performed with the Salmon suite (Patro *et al*, 2017), on the NCBI mouse genome, release 67, obtained from the ENSEMBL FASTA directory. The identified ENSEMBL gene accessions were grouped for the different transcript reads, and the read counts, expressed in TPM, were summed for the annotated transcripts. Outlier reads for each gene transcript level in TPM were detected by the mean absolute deviations method (MAD), where reads with more than 3 scaled MAD distances from the mean were eliminated from statistical analysis. Then, the mean and SD for each gene were used for statistical analysis among the different genotypes by one-way ANOVA with multiple comparisons. *P*-values lower than, or equal to, 0.05 were selected as the threshold of significance, for a minimum count of 4 of 6 samples per gene. Database for Annotation, Visualization and Integrated Discovery (DAVID, <https://david.ncifcrf.gov/>) (Huang *et al*, 2009), was used to perform Gene ontology (GO) and Kyoto Encyclopedia of Genes and Genomes (KEGG) signaling pathway analysis using whole *Mus musculus* genome as background. Expression heatmap correlation plots were computed by the k-means clustering method, with imputation performed by the nearest-neighbor method by the MATLAB "clustergram" function (MathWorks, Natick, MA, USA), as described previously (Eisen *et al*, 1999).

Periodate oxidation/alkaline β -elimination

Periodate oxidation and alkaline β -elimination were performed as previously described (Balaratnam *et al*, 2018). Briefly, total small RNA fractions were collected from 8×10^6 aNPCs (per replica). Two portions, each containing 25 μ g of small RNA were dissolved in 87.5 μ l 0.06 M borate buffer (pH 8.6). Then, 12.5 μ l of nuclease-free water (to control group) or 200 mM sodium periodate (to treatment group) were added to the reaction and samples were incubated for 1 h at room temperature. After the incubation, the reaction was stopped by adding 10 μ l of glycerol for another 30 min. For the control group (treated with water), 12.5 μ l sodium periodate was incubated with glycerol for 60 min prior to adding to the samples to maintain the same ion strength between the control and treatment. RNA was then precipitated by ethanol precipitation method 1 h at -80°C . Precipitated RNA was dissolved in 100 μ l of 0.055 M borate buffer (pH 9.5) and incubated for 60 min at 45°C . RNA was precipitated again as before, washed, and used for TaqMan small RNA

assay. As an internal control for the assay, a synthetic piRNA sequence (corresponding to one of the most abundant piRNA found in aNPCs bearing homology to piR-cluster-1) either modified with the 3'-end 2'-O-methylation (positive control) or bearing a terminal 2',3'-hydroxyl group (negative control) were subject to the periodate treatment as above.

Protein synthesis assay

To quantify the protein synthesis rate of cells, we used the Global Protein Synthesis Assay Kit (FACS/Microscopy) and Red Fluorescence kit (Abcam), following the manufacturer's instructions. Briefly, cells in proliferating or differentiating media (DIF7) were treated with Cycloheximide as an inhibitor of protein synthesis, for 30 min at 37°C. Media were replaced with fresh aliquots containing Protein Label (400×) diluted to 1× final concentration and the cells were incubated for additional 30 min at 37°C. Negative control cells were not incubated with the protein label. Samples were analyzed by FACS for red fluorescence generated by *de novo* synthesized protein during click reaction. Translation rate is directly proportional to emitted fluorescence. Cells emitting fluorescence lower than 10^3 were considered negative (P3) and higher than 10^4 were considered positive (P2).

Immunofluorescence, STED nanoscopy, and particle analysis

Confocal and Stimulated Emission Depletion (STED) nanoscopy were performed as previously reported (Vicidomini *et al*, 2018; Diaspro & Bianchini, 2020). aNPCs were plated on glass coverslips 24 h before fixation. Cells were fixed with PFA 4%, permeabilized with PBS-T 0.1%, blocked for 1 h at room temperature with PBS-T 0.1% NGS 5%, and incubated according to the dilution suggested by the manufacturer's instructions with 0.01 µg/ml rabbit polyclonal antibody against the N terminus of RPL26 (Abcam) for 1 h at room temperature. Cells were washed extensively and incubated with the secondary antibody goat anti-rabbit ATTO-647N (0.8 µg/ml; Sigma) for 45 min. Nuclei were stained while mounting the coverslip with DAPI-ProLong antifade (Invitrogen). Confocal and STED images were acquired at 23°C with a modified TCS SP5 STED-CW gated and operated with its own imaging software, LAS X (Leica Microsystems, Mannheim, Germany). The microscope has been customized with a second pulsed STED laser line at 775 nm. The beam originates from a Onefive Katana HP 8 (NKT, Birkerød, Denmark)

and passes through a vortex phase plate (RPC photonics, Rochester, NY, USA) before entering the microscope through the IR port. The depletion laser pulses are electronically synchronized with the Leica's supercontinuum pulsed and visible excitation laser. The ATTO-647N fluorescence was excited at 633 nm, and the fluorescence depletion was performed at 775 nm. The maximal focal power of the STED beam was 200 mW at 80 MHz. Both beams were focused into the 1.4 NA objective lens (HCX PL APO 100× 1.40 NA Oil STED Orange; Leica). Fluorescence was collected by the same lens, filtered with a 775 nm notch filter, and imaged in the spectral range 660–710 nm by the hybrid detector with a time gating of 1 ns. All the images have a 14 nm pixel size and 37-µs pixel dwell time. The analysis of polysome clusters in aNPC lineages was performed on more than 20 images likewise different cells. Image analysis was performed using the Fiji software.

In silico piRNA targets prediction

For piRNA targets analysis, we divided the sequencing data into one set of 100 piRNA clusters enriched in proliferating aNPCs (DIF0) and a second set of 198 clusters specifically expressed at DIF4/7 stage. The Differential Expression analysis for piRNAs mapping on repeat elements (REs) in DIF4 and DIF7 compared with DIF0 was done using EdgeR software package (Robinson & Oshlack, 2010). Identification of piRNA targets was divided into: piRNAs mapping on REs only/piRNAs mapping on GENCODE elements/piRNAs mapping on REs within GENCODE elements/unannotated piRNAs/piRNAs clusters. Gene Ontology analysis for piRNAs mapping on GENCODE protein-coding genes (but NOT mapping on REs) has been done with the R package GOFuncR (<https://bioconductor.org/packages/release/bioc/html/GOFuncR.html>).

Quantification and statistical analysis

Data are presented as mean ± SEM and were analyzed using Prism 6 (GraphPad). Statistical significance was assessed with a two-tailed unpaired *t*-test for two experimental groups. For experiments with three or more groups, one-way ANOVA with the Bonferroni's multiple comparison test was used. Results were considered significant when $P < 0.05$. The number of samples (*n*) in each group is reported in the figure legend. Exact *P*-values of the experiments are shown in Table 1.

Table 1. Exact *P*-values of the experiments presented in the paper.

| Figure | Comparison | <i>P</i> -value | Statistical test |
|--------|---|------------------------|---|
| 1B | DIF0/DIF7 | ** <i>P</i> = 0.0022 | One-way ANOVA, <i>post-hoc</i> Bonferroni |
| | DIF0/DIF14 | *** <i>P</i> = 0.0001 | |
| | DIF4/DIF7 | *** <i>P</i> = 0.0003 | |
| | DIF4/DIF14 | **** <i>P</i> < 0.0001 | |
| 1C | Testis/Hippocampus | *** <i>P</i> = 0.0004 | One-way ANOVA, <i>post-hoc</i> Bonferroni |
| | Testis/aNPCs | *** <i>P</i> = 0.0005 | |
| 1D | Testis/Hippocampus | *** <i>P</i> = 0.0002 | One-way ANOVA, <i>post-hoc</i> Bonferroni |
| | Testis/aNPCs | ** <i>P</i> = 0.0013 | |
| 1E | Neurons/aNPCs | *** <i>P</i> = 0.0008 | Two-tailed Student's <i>t</i> -test |
| 1G | Td ⁻ /Td ⁺ 10 dpi | * <i>P</i> = 0.0224 | One-way ANOVA, <i>post-hoc</i> Bonferroni |
| | Td ⁺ 30/10 dpi | * <i>P</i> = 0.0355 | |

Table 1 (continued)

| Figure | Comparison | P-value | Statistical test |
|--------|---|----------------------------|---|
| 2E | mRNA Ctl/Mili KD | * $P = 0.014$ | Two-tailed Student's <i>t</i> -test |
| | WB Ctl/Mili KD | ** $P = 0.0015$ | |
| 2F | piCS1 Ctl/Mili KD | *** $P = 0.0004$ | Two-tailed Student's <i>t</i> -test |
| | piCS2 Ctl/Mili KD | *** $P = 0.0005$ | |
| | piCS3 Ctl/Mili KD | *** $P = 0.0002$ | |
| | piCS4 Ctl/Mili KD | **** $P < 0.0001$ | |
| 2I | piCS2 anti-Piwil2/IgG | ⁿ⁵ $P = 0.1018$ | Two-tailed Student's <i>t</i> -test |
| | piCS3 anti-Piwil2/IgG | * $P = 0.0423$ | |
| | piCS4 anti-Piwil2/IgG | * $P = 0.0142$ | |
| | piCS5 anti-Piwil2/IgG | ** $P = 0.0097$ | |
| 3B | piCS1 Td ⁻ /Td ⁺ | * $P = 0.0164$ | Two-tailed Student's <i>t</i> -test |
| | piCS2 Td ⁻ /Td ⁺ | ** $P = 0.0028$ | |
| | piCS3 Td ⁻ /Td ⁺ | * $P = 0.0184$ | |
| | piCS4 Td ⁻ /Td ⁺ | * $P = 0.0278$ | |
| 4C | mRNA Ctl/Mili KD | * $P = 0.0152$ | Two-tailed Student's <i>t</i> -test |
| | WB Ctl/Mili KD | ** $P = 0.0083$ | |
| 4E | GFAP Ctl/Mili KD | ** $P = 0.0061$ | Two-tailed Student's <i>t</i> -test |
| | mRNA Ctl/Mili KD | **** $P < 0.0001$ | |
| 4F | NeuN Ctl/Mili KD | ** $P = 0.0013$ | Two-tailed Student's <i>t</i> -test |
| | GFAP Ctl/Mili KD | ** $P = 0.0077$ | |
| 4G | C3 Ctl/Mili KD | * $P = 0.0124$ | Two-tailed Student's <i>t</i> -test |
| | Serpin Ctl/Mili KD | ** $P = 0.0068$ | |
| | Cxcl10 Ctl/Mili KD | ** $P = 0.0013$ | |
| 4H | Mili Ctl/KA | ** $P = 0.0028$ | Two-tailed Student's <i>t</i> -test |
| | piCS1 Ctl/KA | *** $P = 0.0002$ | |
| 5B | β-Gal Ctl/Mili KD | **** $P < 0.0001$ | Two-tailed Student's <i>t</i> -test |
| 5C | BrdU Ki67 Ctl/Mili KD | **** $P < 0.0001$ | Two-tailed Student's <i>t</i> -test |
| 5D | G0-G1 Ctl/Mili KD | * $P = 0.0186$ | Two-tailed Student's <i>t</i> -test |
| | S Ctl/Mili KD | ** $P = 0.0056$ | |
| 5E | Cyclin A Ctl/Mili KD | * $P = 0.0132$ | Two-tailed Student's <i>t</i> -test |
| | Cyclin D1 Ctl/Mili KD | *** $P = 0.0003$ | |
| | Cyclin E Ctl/Mili KD | * $P = 0.0266$ | |
| 5F | Btg1 Ctl/Mili KD | ** $P = 0.0068$ | Two-tailed Student's <i>t</i> -test |
| | Btg2 Ctl/Mili KD | * $P = 0.0174$ | |
| | Btg3 Ctl/Mili KD | ** $P = 0.0068$ | |
| | Ccnd3 Ctl/Mili KD | * $P = 0.0279$ | |
| | Ppp1ca Ctl/Mili KD | *** $P = 0.0005$ | |
| 5H | Mili young/old | *** $P = 0.0003$ | Two-tailed Student's <i>t</i> -test |
| 6C | SINE DIF0 Ctl/Mili KD | ** $P = 0.0079$ | One-way ANOVA, <i>post-hoc</i> Bonferroni |
| | SINE DIF4 Ctl/Mili KD | * $P = 0.0405$ | |
| | SINE DIF7 Ctl/Mili KD | ** $P = 0.0059$ | |
| | rRNA DIF0 Ctl/Mili KD | ** $P = 0.0074$ | |
| | rRNA DIF4 Ctl/Mili KD | *** $P = 0.0002$ | |
| 6D | LINE1 DIF7 Ctl/Mili KD | * $P = 0.00472$ | Two-tailed Student's <i>t</i> -test |
| 6G | mRNA Target Mili KD/CtlmRNA Nontarget Mili KD/Ctl | $P = 3.21E-260$ | Two-sample Kolmogorov-Smirnov test |

Table 1 (continued)

| Figure | Comparison | P-value | Statistical test |
|--------|--------------------|-------------------|---|
| EV1A | mRNA Ctl/GpM1 | * $P = 0.0133$ | Two-tailed Student's <i>t</i> -test |
| | mRNA Ctl/GpM3 | * $P = 0.038$ | |
| EV1B | WB Ctl/GpM1 | *** $P = 0.001$ | |
| | WB Ctl/GpM3 | * $P = 0.014$ | |
| EV1C | piCS Ctl/GpM1/GpM3 | **** $P < 0.0001$ | One-way ANOVA, <i>post-hoc</i> Bonferroni |
| EV3B | mRNA Ctl/Mili KD | ** $P = 0.098$ | Two-tailed Student's <i>t</i> -test |
| | WB Ctl/Mili KD | **** $P < 0.0001$ | |
| EV3C | mRNA Ctl/Mili KD | * $P = 0.0477$ | Two-tailed Student's <i>t</i> -test |
| | WB Ctl/Mili KD | * $P = 0.017$ | |
| EV3D | GFAP Ctl/Mili KD | ** $P = 0.0039$ | Two-tailed Student's <i>t</i> -test |
| EV3E | NeuN Ctl/Mili KD | ** $P = 0.012$ | Two-tailed Student's <i>t</i> -test |
| | GFAP Ctl/Mili KD | **** $P < 0.0001$ | |
| EV4B | Bcl2 Ctl/Mili KD | ** $P = 0.098$ | Two-tailed Student's <i>t</i> -test |
| EV5C | DIF7 Ctl/Mili KD | * $P = 0.0338$ | One-way ANOVA, <i>post-hoc</i> Bonferroni |

Data availability

Mouse Small RNA sequencing data have been deposited in the European Nucleotide Archive (ENA) under the accession: PRJEB40241 (<https://www.ebi.ac.uk/ena/browser/view/PRJEB40241?show=reads>) and the long RNA sequencing data in the Gene Expression Omnibus (GEO) database under the accession GSE182848 (<https://www.ncbi.nlm.nih.gov/geo/query/acc.cgi?acc=GSE182848>); human datasets (De Rie *et al*, 2017) are available through RIKEN FANTOM5.

Expanded View for this article is available [online](#).

Acknowledgements

We are grateful to G. Hannon (Cambridge, UK), H. Siomi (Keyo University Japan), and Z. Mourelatos (University of Pennsylvania, USA) for providing Mili and/or Miwi antibodies; G. Enikolopov (Stony Brook University NY, USA) for the *Nestin*-GFP mouse and to D. O'Carroll (University of Edinburgh, UK) for the *Mili* null mice. We thank IIT technical staff (S. Bianchi; M. Pesce; E. Albanesi, M. Morini, D. Vozzi) for excellent assistance; L. Pandolfini (IIT-CHT) for advice in the protocol for piRNA resistance to periodate and M. Veronesi and F. Saccoliti (IIT-CCT) for advice on protein chemistry. We are grateful to N. Tirelli Director of the Open University Affiliated Research Centre at IIT (ARC@IIT), part of the Open University, Milton Keynes MK7 6AA, United Kingdom, for advice and support to KT during his training as a PhD student. This study was funded by Fondazione Istituto Italiano di Tecnologia; and partly by Fondazione Cariplo Grant #2015-0590; AIRC-IG 2017 # 20106; PNR—CENTRO NAZIONALE 3—“Sviluppo di terapia genica e farmaci con tecnologia a RNA”. CPF was funded by an ERA-NET-NEURON EJTC 2016 grant and by The Netherlands organization for scientific research (NWO). We apologize to those colleagues whose work could not be cited due to space limitations.

Author contributions

Caterina Gasperini: Conceptualization; data curation; formal analysis; investigation; visualization; methodology; writing – original draft; writing – review and editing. **Kiril Tuntevski:** Data curation; formal analysis; investigation; visualization; methodology; writing – review and editing. **Silvia**

Beatini: Data curation; formal analysis; investigation; visualization; methodology; writing – review and editing. **Roberta Pelizzoli:** Data curation; formal analysis; investigation; methodology. **Amanda Lo Van:** Data curation; formal analysis; visualization. **Damiano Mangoni:** Data curation; formal analysis; investigation; visualization; methodology; writing – review and editing. **Rosa M Cossu:** Data curation; formal analysis; investigation; visualization; methodology; writing – review and editing. **Giovanni Pascarella:** Data curation; software; formal analysis; investigation; visualization; methodology; writing – review and editing. **Paolo Bianchini:** Formal analysis; investigation; visualization; methodology; writing – review and editing. **Pascal Bielefeld:** Formal analysis; investigation; methodology; writing – review and editing. **Margherita Scarpato:** Formal analysis; methodology. **Meritxell Pons-Espinal:** Supervision; methodology; writing – review and editing. **Remo Sanges:** Software; formal analysis; supervision; methodology; writing – review and editing. **Alberto Diaspro:** Supervision; funding acquisition; methodology; writing – review and editing. **Carlos P Fitzsimons:** Formal analysis; supervision; funding acquisition; methodology; writing – review and editing. **Piero Carninci:** Supervision; funding acquisition; methodology; writing – review and editing. **Stefano Gustincich:** Supervision; funding acquisition; methodology; writing – review and editing. **Davide De Pietri Tonelli:** Conceptualization; data curation; formal analysis; supervision; funding acquisition; investigation; visualization; methodology; writing – original draft; project administration; writing – review and editing.

Disclosure and competing interests statement

The authors declare that they have no conflict of interest.

References

- Adusumilli VS, Walker TL, Overall RW, Klatt GM, Zeidan SA, Zocher S, Kirova DG, Ntitsias K, Fischer TJ, Sykes AM *et al* (2021) ROS dynamics delineate functional states of hippocampal neural stem cells and link to their activity-dependent exit from quiescence. *Cell Stem Cell* 28: 300–314
- Ahlenius H, Visan V, Kokaia M, Lindvall O, Kokaia Z (2009) Neural stem and progenitor cells retain their potential for proliferation and differentiation

- into functional neurons despite lower number in aged brain. *J Neurosci* 29: 4408–4419
- Altman J (1962) Are new neurons formed in the brains of adult mammals? *Science* 135: 1127–1128
- Aravin A, Gaidatzis D, Pfeffer S, Lagos-Quintana M, Landgraf P, Iovino N, Morris P, Brownstein MJ, Kuramochi-Miyagawa S, Nakano T et al (2006) A novel class of small RNAs bind to MILI protein in mouse testes. *Nature* 442: 203–207
- Babcock KR, Page JS, Fallon JR, Webb AE (2021) Adult hippocampal neurogenesis in aging and Alzheimer's disease. *Stem Cell Reports* 16: 1–13
- Balaratnam S, West N, Basu S (2018) A piRNA utilizes HILI and HIWI2 mediated pathway to down-regulate ferritin heavy chain 1 mRNA in human somatic cells. *Nucleic Acids Res* 46: 10635–10648
- Bielefeld P, Sierra A, Encinas JM, Maletic-Savatic M, Anderson A, Fitzsimons CP (2017) A standardized protocol for stereotaxic intrahippocampal administration of kainic acid combined with electroencephalographic seizure monitoring in mice. *Front Neurosci* 11: 1–9
- Bielefeld P, Schouten M, Meijer GM, Breuk MJ, Geijtenbeek K, Karayel S, Tiaglik A, Vuuregge AH, Willems RAL, Witkamp D et al (2019) Co-administration of anti microRNA-124 and -137 oligonucleotides prevents hippocampal neural stem cell loss upon non-convulsive seizures. *Front Mol Neurosci* 12: 1–13
- Bonaguidi MA, Wheeler MA, Shapiro JS, Stadel RP, Sun GJ, Ming GL, Song H (2011) *In vivo* clonal analysis reveals self-renewing and multipotent adult neural stem cell characteristics. *Cell* 145: 1142–1155
- Braun SMG, Machado RAC, Jessberger S (2013) Temporal control of retroviral transgene expression in newborn cells in the adult brain. *Stem Cell Reports* 1: 114–122
- Clarke LE, Liddelow SA, Chakraborty C, Münch AE, Heiman M, Barres BA (2018) Normal aging induces A1-like astrocyte reactivity. *Proc Natl Acad Sci USA* 115: E1896–E1905
- Coufal NG, Garcia-Perez JL, Peng GE, Yeo GW, Mu Y, Lovci MT, Morell M, O'Shea KS, Moran JV, Gage FH (2009) L1 retrotransposition in human neural progenitor cells. *Nature* 460: 1127–1131
- Czech B, Munafò M, Ciabrelli F, Eastwood EL, Fabry MH, Kneuss E, Hannon GJ (2018) piRNA-guided genome defense: from biogenesis to silencing. *Annu Rev Genet* 52: 131–157
- De Luca L, Trino S, Laurenzana I, Simeon V, Calice G, Raimondo S, Podestà M, Santodirocco M, Di Mauro L, La Rocca F et al (2016) MiRNAs and piRNAs from bone marrow mesenchymal stem cell extracellular vesicles induce cell survival and inhibit cell differentiation of cord blood hematopoietic stem cells: a new insight in transplantation. *Oncotarget* 7: 6676–6692
- De Rie D, Abugessaisa I, Alam T, Arner E, Arner P, Ashoor H, Åström G, Babina M, Bertin N, Burroughs AM et al (2017) An integrated expression atlas of miRNAs and their promoters in human and mouse. *Nat Biotechnol* 35: 872–878
- Di Giacomo M, Comazzetto S, Saini H, DeFazio S, Carrieri C, Morgan M, Vasiliauskaite L, Benes V, Enright AJ, O'Carroll D (2013) Multiple epigenetic mechanisms and the piRNA pathway reinforce LINE1 silencing during adult spermatogenesis. *Mol Cell* 50: 601–608
- Diaspro A, Bianchini P (2020) Optical nanoscopy. *Riv Nuovo Cim* 43: 385–455
- Ding D, Liu J, Dong K, Midic U, Hess RA, Xie H, Demireva EY, Chen C (2017) PNLDC1 is essential for piRNA 3' end trimming and transposon silencing during spermatogenesis in mice. *Nat Commun* 8: 2–11
- Doetsch F, Caille I, Lim DA, Garcia-Verdugo JM, Alvarez-Buylla A (1999) Subventricular zone astrocytes are neural stem cells in the adult mammalian brain. *Cell* 97: 703–716
- Eisen MB, Spellman PT, Brown PO, Botstein D (1999) Cluster analysis and display of genome-wide expression patterns. *Proc Natl Acad Sci USA* 95: 12930–12933
- Encinas JM, Michurina TV, Peunova N, Park JH, Tordo J, Peterson DA, Fishell G, Koulakov A, Enikolopov G (2011) Division-coupled astrocytic differentiation and age-related depletion of neural stem cells in the adult hippocampus. *Cell Stem Cell* 8: 566–579
- Escartin C, Galea E, Lakatos A, O'Callaghan JP, Petzold GC, Serrano-Pozo A, Steinhäuser C, Volterra A, Carmignoto G, Agarwal A et al (2021) Reactive astrocyte nomenclature, definitions, and future directions. *Nat Neurosci* 24: 312–325
- Gainetdinov I, Colpan C, Arif A, Cecchini K, Zamore PD (2018) A single mechanism of biogenesis, initiated and directed by PIWI proteins, explains piRNA production in most animals. *Mol Cell* 71: 775–790
- Ghosheh Y, Seridi L, Ryu T, Takahashi H, Orlando V, Carninci P, Ravasi T (2016) Characterization of piRNAs across postnatal development in mouse brain. *Sci Rep* 6: 1–7
- Girard A, Sachidanandam R, Hannon GJ, Carmell MA (2006) A germline-specific class of small RNAs binds mammalian Piwi proteins. *Nature* 442: 199–202
- Huang DW, Sherman BT, Lempicki RA (2009) Systematic and integrative analysis of large gene lists using DAVID bioinformatics resources. *Nat Protoc* 4: 44–57
- Jain G, Stuendl A, Rao P, Berulava T, Pena Centeno T, Kaurani L, Burkhardt S, Delalle I, Kornhuber J, Hüll M et al (2019) A combined miRNA–piRNA signature to detect Alzheimer's disease. *Transl Psychiatry* 9: 250
- Jin WN, Shi K, He W, Sun JH, Van Kaer L, Shi FD, Liu Q (2021) Neuroblast senescence in the aged brain augments natural killer cell cytotoxicity leading to impaired neurogenesis and cognition. *Nat Neurosci* 24: 61–73
- Keam SP, Young PE, McCorkindale AL, Dang THY, Clancy JL, Humphreys DT, Preiss T, Hutvagner G, Martin DIK, Cropley JE et al (2014) The human Piwi protein Hiwi2 associates with tRNA-derived piRNAs in somatic cells. *Nucleic Acids Res* 42: 8984–8995
- Kirino Y, Mourelatos Z (2007) Mouse Piwi-interacting RNAs are 2'-O-methylated at their 3' termini. *Nat Struct Mol Biol* 14: 347–348
- Krishan A (1975) Rapid flow cytofluorometric analysis of mammalian cell cycle by propidium iodide staining. *J Cell Biol* 66: 188–193
- Langmead B, Salzberg SL (2012) Fast gapped-read alignment with Bowtie 2. *Nat Methods* 9: 357–359
- Lee JH, Schütte D, Wulf G, Füzesi L, Radzun HJ, Schweyer S, Engel W, Nayernia K (2006) Stem-cell protein Piwi2 is widely expressed in tumors and inhibits apoptosis through activation of Stat3/Bcl-XL pathway. *Hum Mol Genet* 15: 201–211
- Lee EJ, Banerjee S, Zhou H, Jammalamadaka A, Arcila M, Manjunath BS, Kosik KS (2011) Identification of piRNAs in the central nervous system. *RNA* 17: 1090–1099
- Leighton LJ, Wei W, Marshall PR, Ratnu VS, Li X, Zajackowski EL, Spadaro PA, Khandelwal N, Kumar A, Bredy TW (2019) Disrupting the hippocampal Piwi pathway enhances contextual fear memory in mice. *Neurobiol Learn Mem* 161: 202–209
- Liddelow SA, Guttenplan KA, Clarke LE, Bennett FC, Bohlen CJ, Schirmer L, Bennett ML, Münch AE, Chung W-S, Peterson TC et al (2017) Neurotoxic reactive astrocytes are induced by activated microglia. *Nature* 541: 481–487
- Liu GY, Sabatini DM (2020) mTOR at the nexus of nutrition, growth, ageing and disease. *Nat Rev Mol Cell Biol* 21: 183–203
- Love MI, Huber W, Anders S (2014) Moderated estimation of fold change and dispersion for RNA-seq data with DESeq2. *Genome Biol* 15: 1–21

- Madisen L, Zwingman TA, Sunkin SM, Oh SW, Zariwala HA, Gu H, Ng LL, Palmiter RD, Hawrylycz MJ, Jones AR et al (2010) A robust and high-throughput Cre reporting and characterization system for the whole mouse brain. *Nat Neurosci* 13: 133–140
- Martín-Suárez S, Valero J, Muro-García T, Encinas JM (2019) Phenotypical and functional heterogeneity of neural stem cells in the aged hippocampus. *Aging Cell* 18: 1–14
- Mignone JL, Kukekov V, Chiang AS, Steindler D, Enikolopov G (2004) Neural stem and progenitor cells in nestin-GFP transgenic mice. *J Comp Neurol* 469: 311–324
- Mills EW, Green R (2017) Ribosomopathies: there's strength in numbers. *Science* 358: 1–8
- Muotri AR, Chu VT, Marchetto MCN, Deng W, Moran JV, Gage FH (2005) Somatic mosaicism in neuronal precursor cells mediated by L1 retrotransposition. *Nature* 435: 903–910
- Nandi S, Chandramohan D, Fioriti L, Melnick AM, Hébert JM, Mason CE, Rajasethupathy P, Kandel ER (2016) Roles for small noncoding RNAs in silencing of retrotransposons in the mammalian brain. *Proc Natl Acad Sci USA* 113: 12697–12707
- Nolde MJ, Cheng EC, Guo S, Lin H (2013) Piwi genes are dispensable for normal hematopoiesis in mice. *PLoS One* 8: 1–8
- Ozata DM, Gainetdinov I, Zoch A, O'Carroll D, Zamore PD (2019) PIWI-interacting RNAs: small RNAs with big functions. *Nat Rev Genet* 20: 89–108
- Page NF, Gandal MJ, Estes ML, Cameron S, Butth J, Parhami S, Ramaswami G, Murray K, Amaral DG, Van de Water JA et al (2021) Alterations in retrotransposition, synaptic connectivity, and myelination implicated by transcriptomic changes following maternal immune activation in nonhuman primates. *Biol Psychiatry* 89: 896–910
- Patro R, Duggal G, Love MI, Irizarry RA, Kingsford C (2017) Salmon provides fast and bias-aware quantification of transcript expression. *Nat Methods* 14: 417–419
- Penning A, Tosoni G, Abiega O, Bielefeld P, Gasperini C, De Pietri Tonelli D, Fitzsimons CP, Salta E (2022) Adult neural stem cell regulation by small non-coding RNAs: physiological significance and pathological implications. *Front Cell Neurosci* 15: 1–20
- Perera BPU, Tsai ZTY, Colwell ML, Jones TR, Goodrich JM, Wang K, Sartor MA, Faulk C, Dolinoy DC (2019) Somatic expression of piRNA and associated machinery in the mouse identifies short, tissue-specific piRNA. *Epigenetics* 14: 504–521
- Pons-Espinal M, de Luca E, Marzi MJ, Beckervordersandforth R, Armirotti A, Nicassio F, Fabel K, Kempermann G, De Pietri Tonelli D (2017) Synergic functions of miRNAs determine neuronal fate of adult neural stem cells. *Stem Cell Reports* 8: 1046–1061
- Pons-Espinal M, Gasperini C, Marzi MJ, Braccia C, Armirotti A, Pöttsch A, Walker TL, Fabel K, Nicassio F, Kempermann G et al (2019) MiR-135a-5p is critical for exercise-induced adult neurogenesis. *Stem Cell Reports* 12: 1298–1312
- Quinlan AR, Hall IM (2010) BEDTools: a flexible suite of utilities for comparing genomic features. *Bioinformatics* 26: 841–842
- Robinson MD, Oshlack A (2010) A scaling normalization method for differential expression analysis of RNA-seq data. *Genome Biol* 11: R25
- Rojas-Ríos P, Simonelig M (2018) piRNAs and PIWI proteins: regulators of gene expression in development and stem cells. *Development* 145: 1–13
- Schindelin J, Arganda-Carreras I, Frise E, Kaynig V, Longair M, Pietzsch T, Preibisch S, Rueden C, Saalfeld S, Schmid B et al (2012) Fiji: an open-source platform for biological-image analysis. *Nat Methods* 9: 676–682
- Schouten M, Bielefeld P, Garcia-Corzo L, Passchier EMJ, Gradari S, Jungenitz T, Pons-Espinal M, Gebara E, Martín-Suárez S, Lucassen PJ et al (2020) Circadian glucocorticoid oscillations preserve a population of adult hippocampal neural stem cells in the aging brain. *Mol Psychiatry* 25: 1382–1405
- Sharma AK, Nelson MC, Brandt JE, Wessman M, Mahmud N, Weller KP, Hoffman R (2001) Human CD34⁺ stem cells express the hiwi gene, a human homologue of the Drosophila gene Piwi. *Blood* 97: 426–434
- Sierra A, Martín-Suárez S, Valcárcel-Martín R, Pascual-Brazo J, Aelvoet SA, Abiega O, Deudero JJ, Brewster AL, Bernales I, Anderson AE et al (2015) Neuronal hyperactivity accelerates depletion of neural stem cells and impairs hippocampal neurogenesis. *Cell Stem Cell* 16: 488–503
- Toda T, Parylak SL, Linker SB, Gage FH (2019) The role of adult hippocampal neurogenesis in brain health and disease. *Mol Psychiatry* 24: 67–87
- Torres AG, Reina O, Attolini CSO, De Poupiana LR (2019) Differential expression of human tRNA genes drives the abundance of tRNA-derived fragments. *Proc Natl Acad Sci USA* 116: 8451–8456
- Upton KR, Gerhardt DJ, Jesuadian JS, Richardson SR, Sánchez-Luque FJ, Bodea GO, Ewing AD, Salvador-Palomeque C, Van Der Knaap MS, Brennan PM et al (2015) Ubiquitous L1 mosaicism in hippocampal neurons. *Cell* 161: 228–239
- Vicidomini G, Bianchini P, Diaspro A (2018) STED super-resolved microscopy. *Nat Methods* 15: 173–182
- Viero G, Lunelli L, Passerini A, Bianchini P, Gilbert RJ, Bernabò P, Tebaldi T, Diaspro A, Pederzoli C, Quattrone A (2015) Three distinct ribosome assemblies modulated by translation are the building blocks of polysomes. *J Cell Biol* 208: 581–596
- Wakisaka KT (2019) The dawn of piRNA research in various neuronal disorders. *Front Biosci* 24: 1440–1451
- Walker TL, Kempermann G (2014) One mouse, two cultures: isolation and culture of adult neural stem cells from the two neurogenic zones of individual mice. *J Vis Exp* 84: 1–9
- Yu C-W (1992) The assessment of cellular proliferation by immunohistochemistry: a review of currently available methods and their applications. *Histochem J* 24: 121–131
- Zhang P, Si X, Skogerbø G, Wang J, Cui D, Li Y, Sun X, Liu L, Sun B, Chen R et al (2014) piRBase: a web resource assisting piRNA functional study. *Database* 2014: 1–7
- Zhao P, Yao M, Chang S, Gou L, Liu M, Qiu Z (2015) Novel function of PIWIL1 in neuronal polarization and migration via regulation of microtubule-associated proteins. *Mol Brain* 8: 1–12



License: This is an open access article under the terms of the [Creative Commons Attribution](https://creativecommons.org/licenses/by/4.0/) License, which permits use, distribution and reproduction in any medium, provided the original work is properly cited.

Expanded View Figures

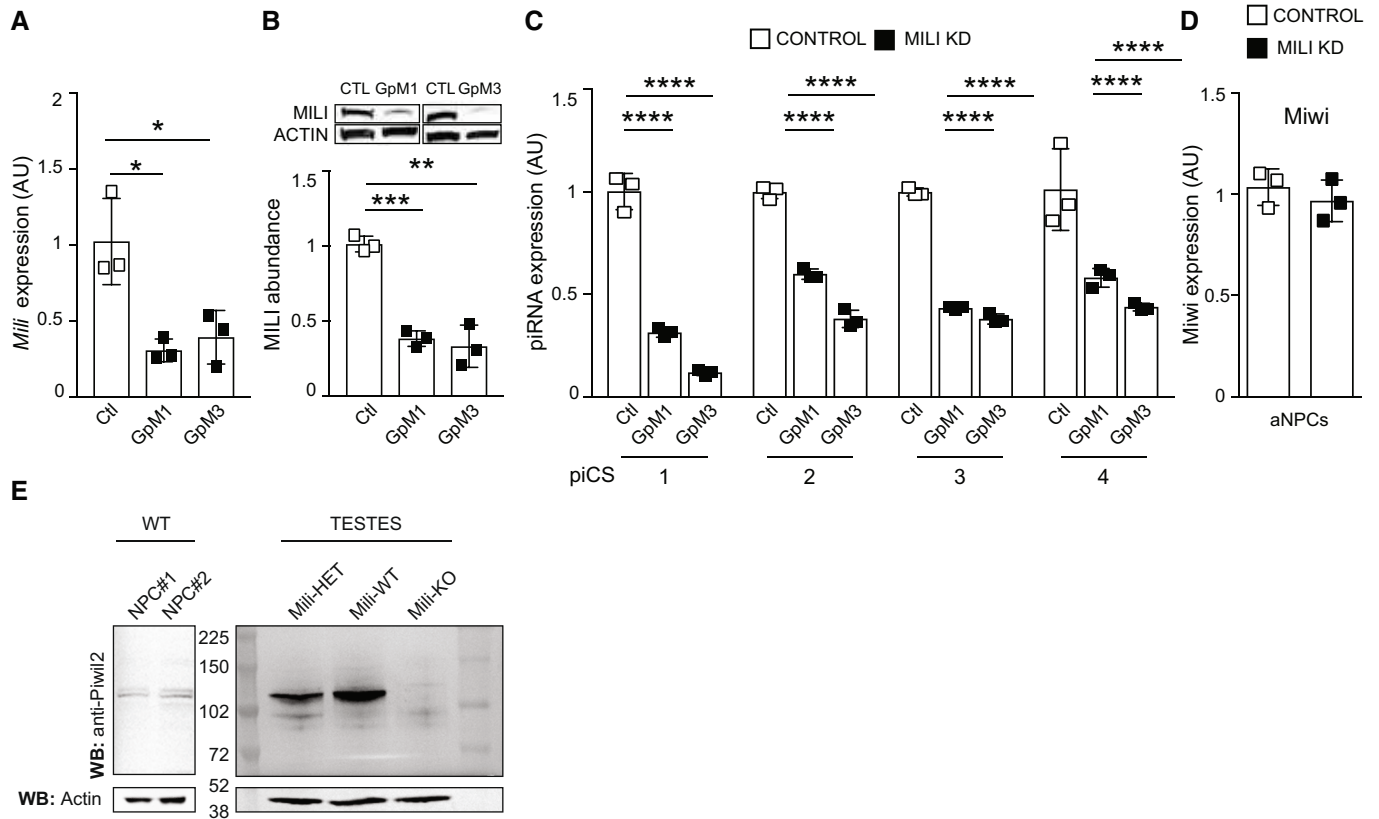


Figure EV1. Mihi KD depletes piRNAs and does not affect Miwi. Relative to Fig 2.

- A, B *Mihi* mRNA expression (A); western blot (B, inset) and quantification of *Mihi* protein abundance (B, bar graph) in lysates from aNPCs upon transfection with control GapmeR (Ctl) or two different GapmeRs (GpM1, GpM3) targeting *Mihi*.
- C Expression of transcripts of piRNA-cluster consensus sequences (piCS) in control and *Mihi* KD (two independent GapmeRs) aNPCs.
- D Relative expression of *Miwi* transcript in undifferentiated aNPCs transduced with viruses transcribing a Scrambled short hairpin (Control) and short hairpin against *Mihi* (*Mihi* KD).
- E Western blot of *Mihi* protein in lysates from aNPCs ($n = 2$ biological replicates) and from testes of mice wildtype (WT), heterozygous (HET) or knockout (KO) for the *Mihi* gene.

Data information: data are expressed as mean \pm SEM, $n = 3$ biological replicates (A–C). * $P < 0.05$, ** $P < 0.01$, *** $P < 0.001$, **** $P < 0.0001$, as assessed by the two-tailed Student's *t*-test (A, B) or One-way ANOVA, *post-hoc* Bonferroni (C).

Source data are available online for this figure.

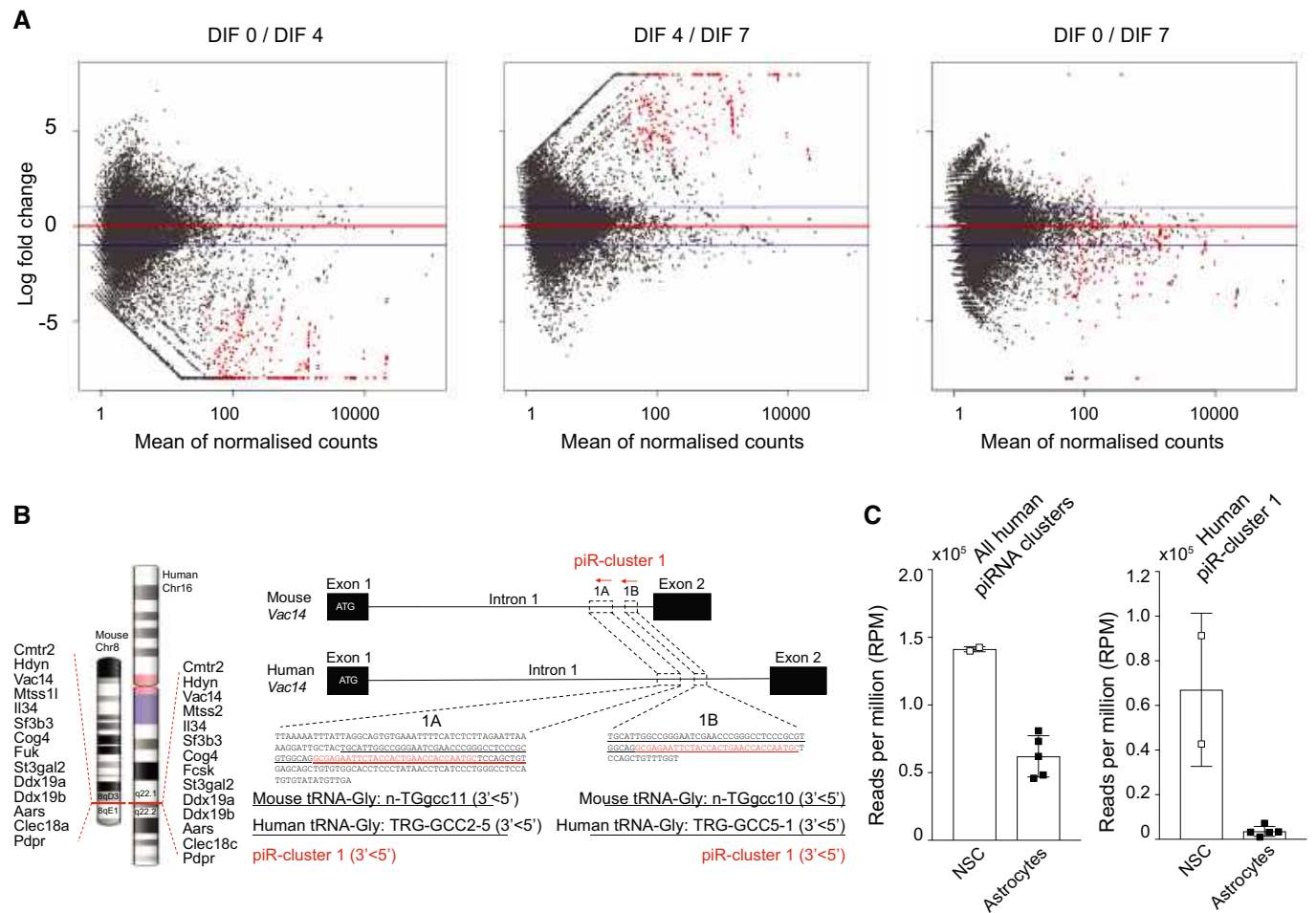


Figure EV2. Expression of piRNAs in mouse and human NSC and progeny. Relative to Fig 3.

A Pairwise comparison of 298 piRNA clusters differentially expressed in undifferentiated aNPCs (DIF0) or neuroblasts upon viral-induced neurogenesis (DIF4-7). $n = 2$ biological replicates.

B Chromosomal location of piR-cluster 1 in mouse and human; (Right) genomic location and sequences (underlined red text) of piR-cluster 1 corresponding to tRNAGly genes (underlined black text).

C Expression of piRNA clusters (left) and piR-cluster 1 (right) in human NSC and astrocytes. $n = 2$ biological replicates of human NSCs; $n = 5$ biological replicates of human astrocytes.

Data information: data in C are expressed as mean \pm SEM.

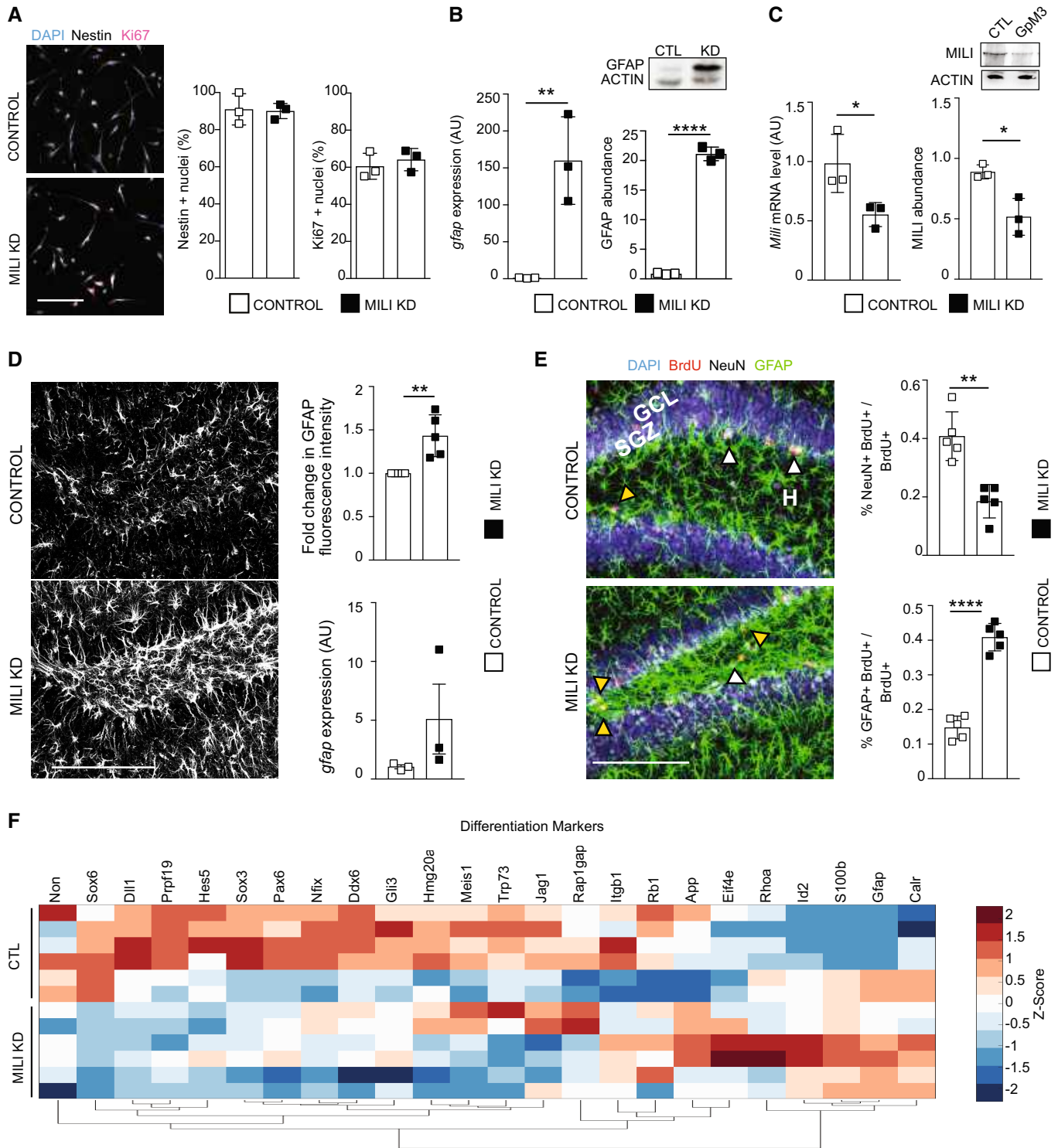


Figure EV3.

Figure EV3. Depletion of Mili and piRNAs does not alter stemness and proliferation and induces the expression of genes involved in astrogliogenesis. Related to Fig 4.

- A (left) Confocal microscopy images of undifferentiated aNPCs transduced *in vitro* with viruses transcribing a Scrambled (Control) and shMILI (Mili KD), immunostained with anti-Nestin (white), or anti-Ki67 (purple) antibodies and stained for nuclear DNA with DAPI (blue); (right) Percentage of Nestin or Ki67⁺ cells over total cells.
- B *Gfap* mRNA expression (left graph), western blot (inset), and quantification of Gfap protein abundance (right graph) in lysates from control and Mili KD neuroblasts at DIF7.
- C *Mili* mRNA expression (left graph), western blot (inset), and quantification of Mili protein abundance (right graph) in lysates from mouse hippocampi 48 h after the injection of scrambled (Control) or GapmeR3 against *Mili* (Mili KD).
- D Representative immunofluorescence micrograph of postnatal hippocampal sections immunostained for GFAP; (top right) quantification of GFAP fluorescence intensity level (top) in hippocampal section 30 dpi of GapmeR3 (Mili KD) compared with scrambled (Control). Expression of *Gfap* mRNA (bottom right) in the DG from mouse hippocampi 48 h after the injection of scrambled (Control) or GapmeR3 (Mili KD).
- E (left) Representative immunofluorescence micrograph of postnatal hippocampal sections immunostained for GFAP (green), BrdU (red), NeuN (white), and nuclear DNA (blue) at 30 dpi of scrambled (Control) or GapmeR3 against *Mili* (Mili KD); (right) percentages of NeuN⁺BrdU⁺ (white arrowheads), or GFAP⁺BrdU⁺ (yellow arrowheads) double-positive cells over total BrdU⁺ cells.
- F RNA seq. expression data of genes encoding for proteins involved in astrogliogenesis and regulation of neuronal fate in Mili KD neuroblasts at DIF7, compared with Scrambled control. Expression heatmap correlation plots were computed by the k-means clustering method. Scale bar indicates Z-scores.

Data information: data are expressed as mean \pm SEM, $n = 3$ (A–C, F) and $n = 5$ (D, E) biological replicates (in F each biological replicate was sequenced with two separate flow cells). * $P < 0.05$, ** $P < 0.01$, **** $P < 0.0001$, as assessed by the two-tailed Student's *t*-test. GCL, granular cell layer, SGZ, subgranular zone. The scale bars represent 50 μm (A) and 100 μm (D, E).

Source data are available online for this figure.

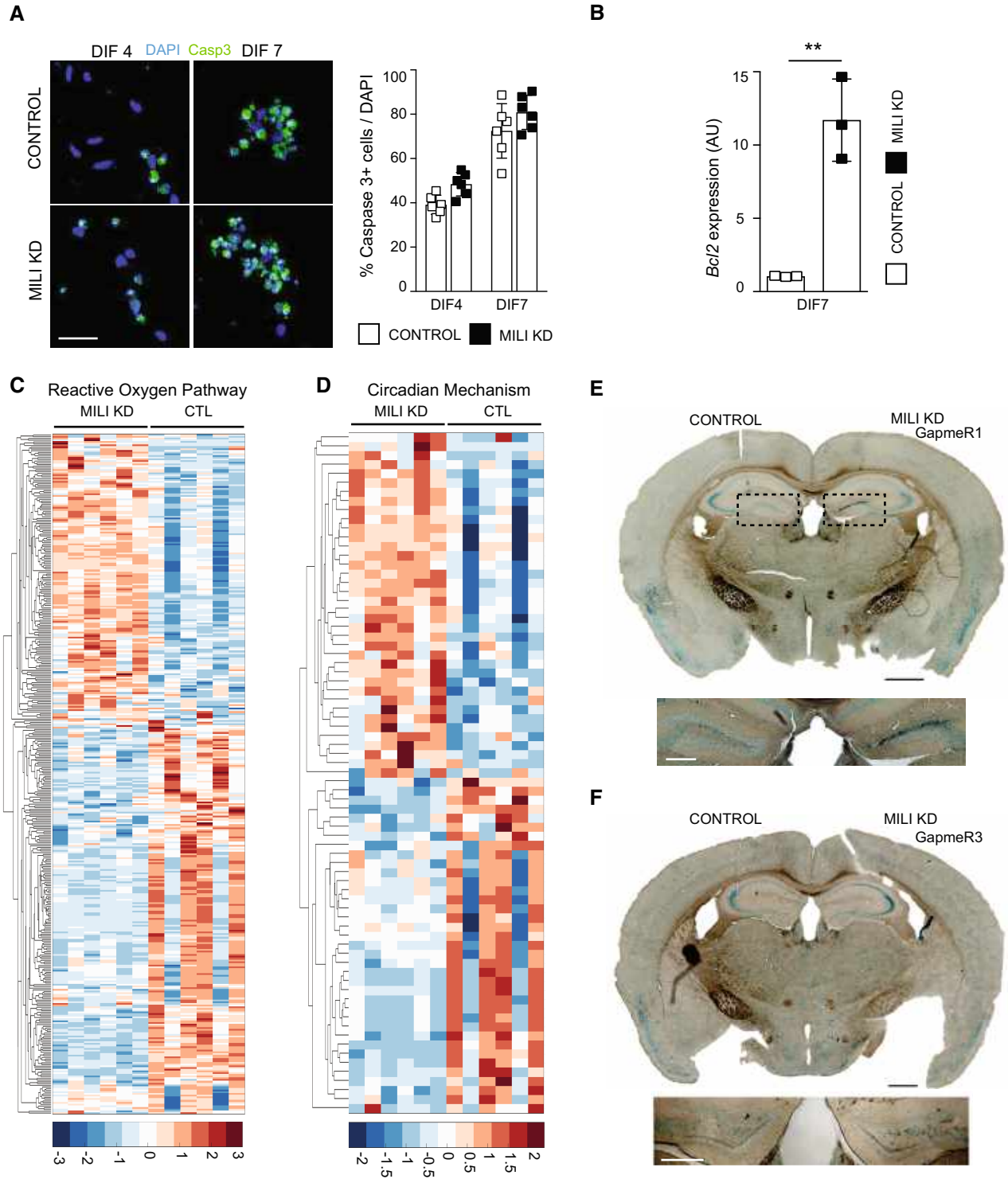


Figure EV4.

Figure EV4. Depletion of Mili and piRNAs does not lead to apoptosis and alters the expression of genes involved in inflammatory responses. Related to Fig 5.

- A Representative fluorescence micrographs of control or Mili KD neuroblasts 4 or 7 days after spontaneous differentiation (DIF4, 7), immunostained with anti-cleaved caspase-3 (green) and for nuclear DNA with DAPI (blue). (Right) Percentage of cleaved Caspase-3⁺ cells over total cells.
- B *Bcl2* mRNA expression level in control or Mili KD neuroblasts at DIF7.
- C, D Heatmap of differentially expressed transcripts in RNA seq from Mili KD neuroblasts, encoding proteins involved in ROS production (C) or circadian regulation (D). Target genes are listed in Dataset EV4. Expression heatmap correlation plots were computed by the k-means clustering method. Scale bar indicates Z-scores.
- E, F Representative light-microscopy images of the β -galactosidase staining in postnatal hippocampal sections, 30 dpi of scrambled (Control, left hemisphere) and Gapmer1 (E) or Gapmer3 (F) against *Mili* (Mili KD, right hemispheres). Dashed box in E indicates the areas shown in Fig 5. Bottom panels in (E, F) are higher magnification of the hippocampi shown in top panels.

Data information: data are expressed as mean \pm SEM, $n = 6$ (A) and $n = 3$ (B–D) biological replicates (in C and D each biological replicate was sequenced with two separate flow cells). ** $P < 0.01$, as assessed by the two-tailed Student's *t*-test. The scale bars represent 50 μm (A), 1 mm (E, F top) and 500 μm (E, F bottom).

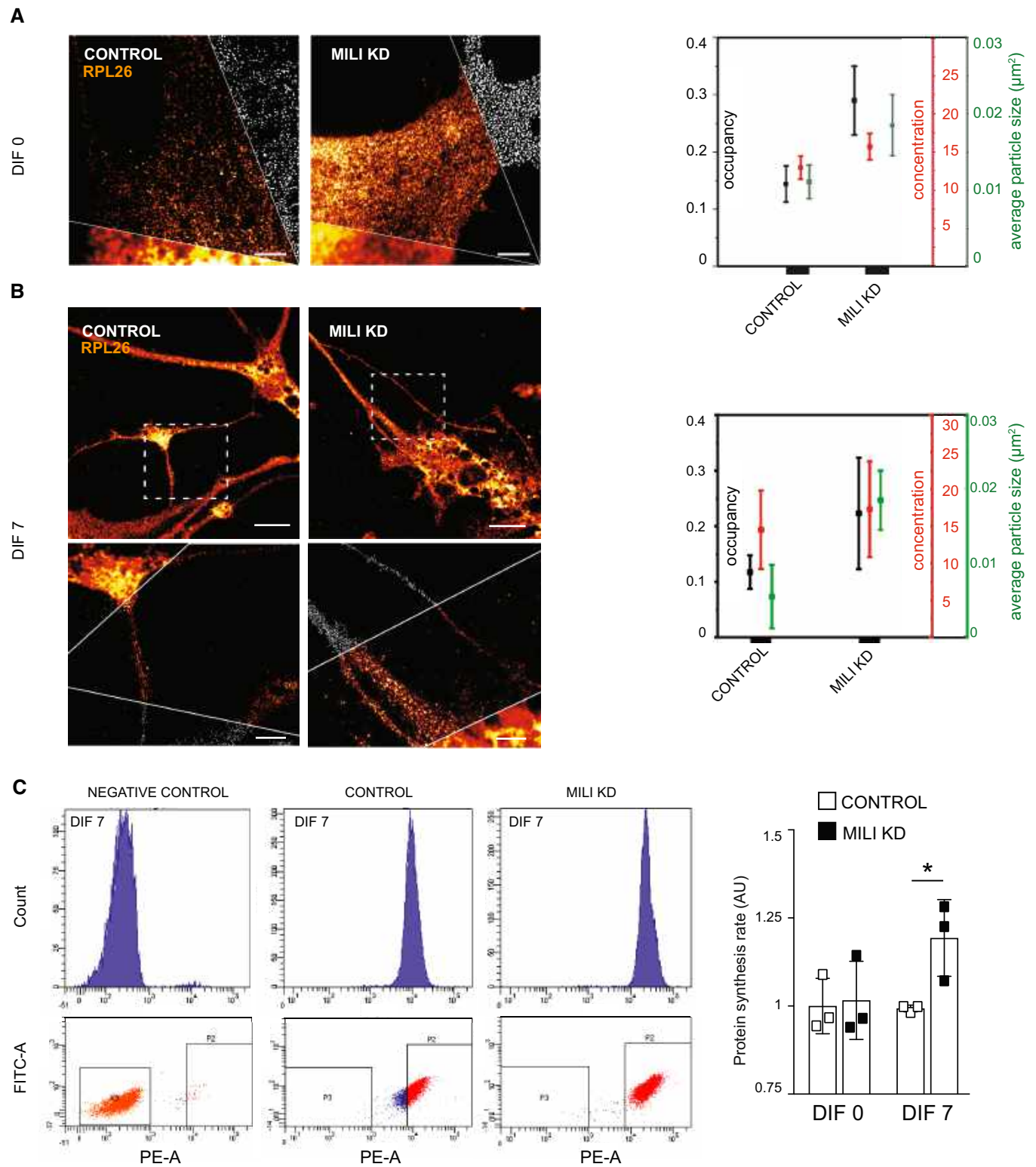


Figure EV5.

Figure EV5. Depletion of Mili and piRNAs enhances polysome assembly and results in higher protein synthesis upon differentiation.

- A, B Representative micrographs (Middle cut: g-STED nanoscopy; Bottom: Confocal; Top: analysis) of control and Mili KD undifferentiated aNPCs (DIF0) and neuroblasts (DIF7) immunostained for the ribosomal protein RPL26. (Right) Normalized distributions of the occupancy, concentration and average particle size of each polyribosome particle in the indicated cells.
- C Protein synthesis rate (right) as determined by OPP incorporation assay with flow cytometry (left) in control and Mili KD undifferentiated aNPCs (DIF0) and neuroblasts (DIF7).

Data information: data are expressed as mean \pm SEM, $n = 3$ biological replicates. $*P < 0.05$, as assessed by the two-tailed Student's t -test. The scale bars represent 2 μm (A) and 10 μm (B).